DOKUZ EYLÜL UNIVERSITY
GRADUATE SCHOOL OF NATURAL AND APPLIED SCIENCES

BACK ANALYSIS OF THE FOUNDATION OF A HIGH RISE BUILDING

by
Müslüm Uğur ÜLGEN

October, 2012
İZMİR

BACK ANALYSIS OF THE FOUNDATION OF A HIGH RISE BUILDING

A Thesis Submitted to the
Graduate School of Natural and Applied Sciences of Dokuz Eylül University
In Partial Fulfillment of the Requirements for the Degree of Master of Science
in
Civil Engineering, Geotechnical Engineering Program

by
Müslüm Uğur ÜLGEN

October, 2012
İZMİR

M.Sc THESIS EXAMINATION RESULT FORM

We have read the thesis entitled **"BACK ANALYSIS OF THE FOUNDATION OF A HIGH RISE BUILDING"** completed by **MÜSLÜM UĞUR ÜLGEN** under supervision of **ASSOC. PROF. DR. GÜRKAN ÖZDEN** and we certify that in our opinion it is fully adequate, in scope and in quality, as a thesis for the degree of Master of Science.

Gürkan Özden

Assoc. Prof. Dr. Gürkan ÖZDEN

Supervisor

Prof. Dr. Arif Şengün KAYALAR

(Jury Member)

Prof. Dr. Ramazan KARAKUZU

(Jury Member)

Prof.Dr. Mustafa SABUNCU

Director

Graduate School of Natural and Applied Sciences

ACKNOWLEDGMENTS

I would like to express my appreciation to my supervisor Assoc. Prof. Dr. Gürkan Özden for his outstanding supervision, contribution to my academic progress and perfect guidance throughout the research.

I would like to acknowledge the support provided by The Scientific and Technological Research Council of Turkey, TUBITAK, through my all graduation period.

My wholehearted appreciations go for Melis Yıldırım for her encouragement and adoring love and moral support.

Finally, I would like to thank my family for their understanding, encouragement, support and patience, making it possible for me to pursue the challenging work of my interest.

Müslüm Uğur ÜLGEN

BACK ANALYSIS OF THE FOUNDATION OF A HIGH RISE BUILDING

ABSTRACT

This study is about general properties of piled raft foundations, piled raft analysis methods and evaluation of such analysis methods using hypothetical examples and performing back analysis of foundation of an existed high rise building.

In the piled raft approach, different from conventional pile foundations, load carrying contribution of the raft is not ignored and this contribution is used effectively in the design of the foundation. Load sharing ratio of the piled raft can be obtained from revealing the complex interactions between piles, raft and soil. There are several simplified, approximate and advanced analysis methods in order to determine such interactions.

In this study, piled raft concept is explained in detail and analysis methods of piled rafts are introduced. Piled raft analysis of a hypothetical example and existed foundation of a high rise building are performed using such methods and obtained results compared each other and obtained settlement values from the situ.

According to the performed study, load carrying property of raft is clearly seen and it is observed that proposed analysis methods in the literature give satisfactory results when obtained settlement values from the situ is considered.

Keywords: Foundation design, piled raft, finite element method, load sharing

BİR YÜKSEK YAPI TEMELİNİN GERİYE DÖNÜK ANALİZİ

ÖZ

Bu çalışma, kazıklı radye temellerin genel özellikleri, kazıklı radye analiz yöntemleri ve söz konusu yöntemlerin varsayımsal örnekler kullanılarak ve mevcut bir yüksek yapı temelinin geriye dönük analizinin gerçekleştirilmesiyle değerlendirilmesi hakkındadır.

Kazıklı radye yaklaşımında, klasik kazıklı temel yaklaşımından farklı olarak, radyenin yük taşımaya olan katkısı ihmal edilmez ve bu katkı temel tasarımında etkin bir şekilde kullanılır. Kazıklı radyelerin yük paylaşım oranı, kazıklar, radye ve zemin arasındaki karmaşık ilişkinin ortaya çıkarılmasıyla elde edilebilir. Bu etkileşimlerin belirlenebilmesi amacıyla pek çok basitleştirilmiş, yaklaşık ve gelişmiş analiz yöntemleri mevcuttur.

Bu çalışmada, kazıklı radye kavramı detaylı bir şekilde açıklanmış ve kazıklı radye temellerin analiz yöntemleri tanıtılmıştır. Varsayımsal bir örnek ve mevcut bir yüksek yapının temeli için kazıklı radye analizleri bahsedilen yöntemler kullanılarak gerçekleştirilmiş ve elde edilen sonuçlar kendi içinde ve sahadan elde edilen oturma sonuçlarıyla karşılaştırılmıştır.

Yapılan çalışmalara göre, radyenin yük taşıma özelliği açık bir şekilde görülmüş ve sahadan elde edilen oturma verileri dikkate alındığında literatürde verilen analiz yöntemlerinin tatmin edici sonuçlar verdiği gözlemlenmiştir.

Anahtar Kelimeler: Temel tasarımı, kazıklı radye, sonlu elemanlar yöntemi, yük paylaşımı

CONTENTS

Page

Page

Page

CHAPTER ONE
INTRODUCTION

Foundations are structural members that are responsible for providing the contact between the soil and the structure. The main function of the foundations is to transmit the structural loads caused by structure's own weight, earthquakes, winds etc. to the soil media under required safety conditions. A proper foundation design for any structure has vital importance for providing structural integrity and sustainability of the structure against ambient effects.

There are two main criteria which control the design of the foundations. First of these is the "reliable bearing capacity" criterion and the other one is the "allowable settlement" criterion. In the design of the foundation both of these criteria must be satisfied obeying to the structural and geotechnical specifications.

The first step of the foundation design is selection of the foundation type. In the earlier approaches of the foundation design, it is generally convenient to start with the shallow foundation options. Shallow foundation options can be listed as spread footings, combined footings and raft foundations. Shallow foundations are generally desired to make an economic foundation design. Since they are significantly cost efficient and can be constructed easily. If bearing capacity and settlement criterion of the foundations are not fulfilled, design of the foundation must be revised. In this situation, deep foundation options should be studied. On the other hand, providing the safety of the foundation system against secondary effects such as liquefaction should also be investigated and possible ground improvement plans should be done.

Nowadays, there is a certain tendency of constructing high rise buildings due to population increase and change in residential trends. Especially in the crowded cities this situation may be noticed clearly. In addition, urbanization on sites which have insufficient engineering soil properties is encountered more frequently as a result of increasing residential demands.

The above mentioned factors avoid the use of shallow foundation options for high rise structures at the very beginning of the foundation design and deep foundation choice becomes an obligation in most cases.

The first foundation type that comes to mind when considering deep foundation options is pile foundation. Main philosophy of the pile foundation is transmitting the structural loads to soil layers which have appropriate engineering properties by passing through the insufficient soil layers. In the pile foundation approach, it is assumed that entire structural loads are carried by the piles. In other words, the load carrying contribution of the soil and pile cap (raft) is ignored in this approach. However, this situation does not represent the field behavior. In reality, raft carries a portion of the structural loads. Conventional pile foundation approach, however, results in highly conservative and non-economic designs.

In piled raft approach, load carrying contribution of the raft is taken into account and it is used effectively in the design of the foundation. The load sharing ratio between piles and raft is determined after the interplay among pile, soil and raft is investigated. The soil supporting the raft is quite effective on this interaction. Design philosophy of piled raft is directly based on the understanding of this interaction (Randolph, 1994). In order to determine the soil-structure interaction, simplified, approximate and advanced analysis methods were developed (Poulos, 2000). Efficiency of such methods was demonstrated by applying these methods on hypothetical examples and back analysis of instrumented foundations (Franke et al., 2000; Katzenbach et al., 2000; Poulos, 2000).

In the scope of this thesis, the concept of piled raft foundations is introduced comprehensively with design philosophies and application examples. Calculation abilities of the piled raft analysis methods which are available in the literature are compared and such analysis methods are applied on a hypothetical piled raft example and a real life piled raft application. A back analysis is performed using analysis results from different piled raft analysis methods and real settlement measurement. Thus, efficiency of those methods is determined.

In context of this thesis, Chapter 2 intends to provide detailed introduction of the piled raft concept with design philosophies, analysis methods and application examples. In Chapter 3, analysis techniques for piled rafts are applied on a hypothetical example and efficiency of the methods is shown. In Chapter 4, piled raft analysis of an existing high rise building is made using various analysis techniques and achieved results are compared with each other and measured settlement values of the building. Conclusions and recommendations are given in Chapter 5.

CHAPTER TWO
THE CONCEPT OF PILED RAFT FOUNDATION

2.1 Introduction

In this chapter, the conventional pile foundation approach is introduced briefly with the purpose of presenting main differences between conventional pile foundation and piled raft foundation approaches. Then, piled raft foundation concept is given comprehensively with the earlier studies related with piled raft and piled raft application examples. In addition, different design philosophies and analysis methods for piled raft concept are explained.

2.2 Conventional Pile Foundation Approach

Pile foundations are based on an idea that transmitting the structural loads to soil layers which show acceptable engineering attributes by passing through the soil layers that have insufficient engineering properties. According to conventional pile foundation approach, entire structural loads are carried by the piles and raft's load carrying function is ignored.

Pile foundation design using conventional approach focuses on single pile bearing capacity. In this approach, pile length, pile diameter and number of piles are major design parameters along with soil characteristics. First design stage is determining the single pile's axial load bearing capacity in this approach. Single pile's load capacity depends on pile properties (pile type, length, diameter etc.) and soil properties. In addition, calculated load capacity is generally reduced by a safety factor to obtain allowed capacity value. Allowable bearing capacity of a single pile can be expressed as follows:

$$Q_a = \frac{Q_p}{F} \tag{2.1}$$

where;
Q_a = Allowable bearing capacity of single pile
Q_p = Ultimate bearing capacity of single pile
F_s = Factor of safety (generally F_s =2.0-3.0)

The required number of piles for the foundation system is calculated by ignoring the contribution of the raft as mentioned before. Using this assumption, required number of piles can be calculated as below:

$$n = \frac{Q}{Q_a} \tag{2.2}$$

where;
n= Required number of pile
Q= Structural load
Q_a = Allowable bearing capacity of single pile

The first stage of the design is completed by determining the required number of piles and disposition plan of the foundation system is created considering foundation area and the number of piles. After that stage, pile group performance should be checked separately. In some circumstances, block behavior of pile group may limit the design. Different failure mechanisms are shown in the Figure 2.1.

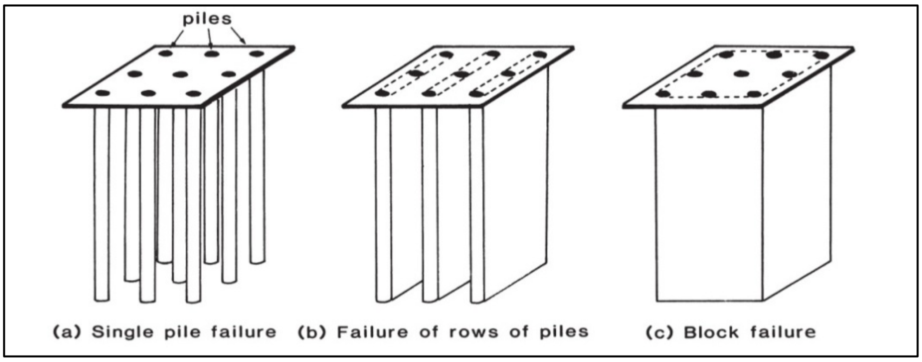

Figure 2.1 Different failure mechanisms of pile foundations (Fleming et al., 2009)

Overall factor of safety of a pile foundation system is re-calculated by considering total single pile and pile block bearing capacity as shown in Equation 2.3. Generally, it is expected that F is equal to 2 or higher.

$$F = \frac{Q}{\left(\sum_{i=1}^{n} Q_a(i) \,|\, Q_b\right)_{smaller}} \tag{2.3}$$

where;
n= Number of pile
Q= Structural load
Q_a = Allowable bearing capacity of single pile
Q_b = Pile block's bearing capacity

Design of the foundation system can be modified by changing pile length or pile diameter to obtain optimum alternative. For this purpose, iterative computer based spreadsheets can be used.

Design philosophy about the conventional pile foundation system as mentioned above is a design procedure where only vertical structural loads are taken into account. In real conditions, there are several factors which act on the foundation system and design must be revised by considering them. These factors can be denoted as follows:

- Negative skin friction
- Lateral loads due to non-uniform loading conditions
- Dynamic effects (inertial and kinematic)
- Pile group interaction

In addition to the bearing capacity, settlement is another design criterion of foundation systems. Foundation system which is designed obeying to bearing capacity criterion shall also satisfy the settlement criteria. In settlement analysis of a pile group, several recommended approaches in the literature may be followed (Fleming et al., 2009; Poulos & Davis, 1980; Tomlinson & Woodward, 2008).

As a conclusion, design philosophy of conventional pile foundation approach is based on ignoring raft's bearing contribution. This approach may cause over-design and non-economic solutions. In order to prevent this, the piled raft concept, which also considers the raft's bearing property, gaining popularity in recent years (Poulos, 2000).

2.3 The Piled Raft Approach

The piled raft approach is developed as a result of considering raft's bearing contribution against structural loads in the foundation system. Piled raft approach utilizes the actual load share between piles and the raft. Thus, real foundation behavior will be simulated in the analysis and design of pile foundations. Piled raft foundation concept allows designers to make more economic and reliable foundation designs without sacrificing the safety (Poulos, 2001). According to piled raft approach, raft contributes to load bearing depending on system properties. This concept has been mathematically expressed by Katzenbach et al. (2000) and given below with the addition of factor of safety:

$$R_{tot} = R_{raft} + \sum_{i=1}^{n} R_{pile}(i) \geq F_s \times S_{tot} \tag{2.4}$$

where;
R_{tot} = Total resistance Force
R_{raft} = Resistance force provided by raft
R_{pile}(i) = Resistance force provided by each pile
n= Number of piles
S_{tot} = Total structural force
F = Factor of safety

When Equation 2.4 is examined, it is clearly seen that total resistance force consists of forces provided by raft and piles. In addition, this resistance force combination must be higher than total structural force. In the piled raft analysis, one of the main goals is to determine the load sharing ratio between piles and raft. This ratio is simply formulated as shown in Equation 2.5:

$$\alpha_{pr} = \frac{\sum_{i=1}^{n} R_{pile}(i)}{R_{tot}} \tag{2.5}$$

where;
α_{pr} =Load sharing ratio of piled raft
R_{tot} = Total resistance force
$R_{pile}(i)$ = Resistance force provided by each pile
n= Number of pile

In the piled raft foundation approach the α_{pr} term varies between 0 and 1. The α_{pr}=0 case represents shallow foundation whereas, α_{pr} =1 indicates the conventional pile foundation. In addition, settlement of the foundation system decreases as α_{pr} increases. This relationship in the piled raft concept is shown in Figure 2.2.

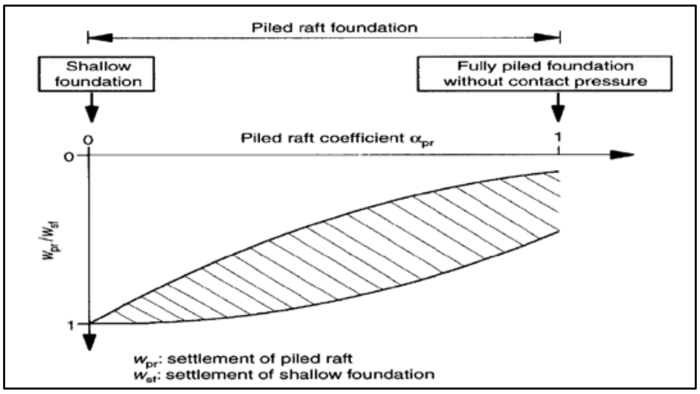

Figure 2.2 Variation of load sharing ratio in piled raft foundations (Katzenbach et al., 2000)

Determination of the α_{pr} value is a complex soil-structure interaction problem. In order to solve this problem, four major types of interactions must be investigated. These interactions are;

- Soil-Pile Interaction
- Pile-Pile Interaction

- Soil-Raft Interaction
- Pile-Raft Interaction

In Figure 2.3, a schematic representation of the soil-structure interaction effects for piled raft foundations is given:

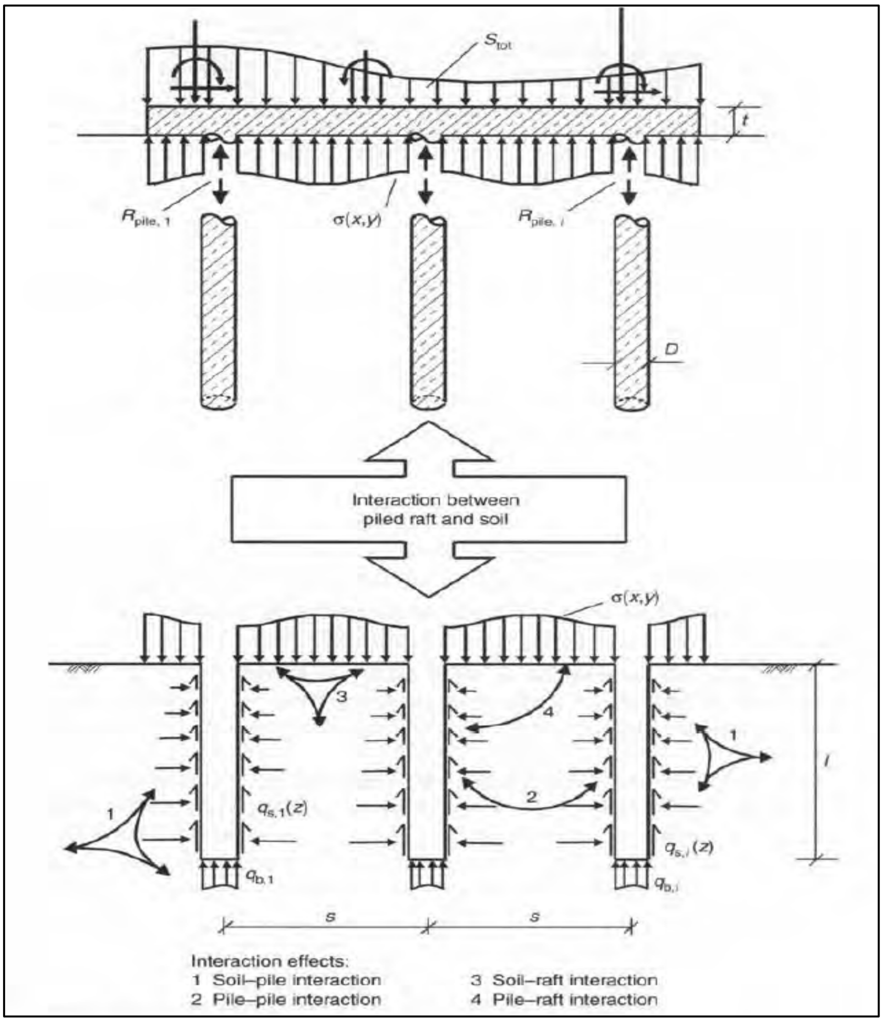

Figure 2.3 Soil-structure interaction effects for piled raft foundation (Katzenbach et al., 2000)

2.3.1 Required Soil Conditions for Piled Raft

According to piled raft approach, a significant portion of structural loads is carried by the raft via supporting soil layer beneath the raft. Thus, designers have the opportunity to make economic foundation design using this capacity. Therefore, in piled raft applications, soil layers must pose some engineering characteristics.

Appropriate soil profiles for piled raft applications are defined by Poulos, (2000) as "*soil profiles consisting of relatively stiff clays or dense sands*". In this case, the raft gives a huge contribution of bearing capacity and piles are settlement control agents and they work as "*settlement reducers*" (Love, 2003). This situation gives a chance of reaching economic designs.

On the other hand, construction sites which have "*soil profiles containing soft clays or loose sands near the surface*" is inappropriate to apply piled raft approach (Poulos, 2000). Insufficient soil conditions cause a reduction on raft's bearing contribution, thus, piles carry higher amount of the load. In this circumstance, required number of piles increases and foundation design tends to be a conventional pile foundation approach. In addition to soft or loose soil layers, soil layers which are sensitive to swelling and consolidation due to external effects also pose undesired soil conditions (Poulos, 2000). These unfavorable soil conditions may induce the cut-off contact between soil and raft or generation of negative skin friction. In this case, extra compression or tensile forces may be developed on the piles (Poulos, 1993). All of these negative effects prevent full functioning of the piled raft system properly. One of the different situations which is not suitable for piled raft foundation is huge stiffness differences between the adjacent layers. According to Gök (2007) and Katzenbach & Moorman (2001), piled raft application is not suitable if the stiffness ratio between two adjacent soil layers is 10 or greater. These researchers recommend not to use piled raft approach when the piled raft interaction factor, α_{pr}, is greater than 0.90. In a similar study which was performed by Katzenbach et al. (2000), stiffness differences between two layers were investigated on a parametric example -which has two different soil layers and stiffness ratio between these layers is 100- and negative effect of this phenomena on load-settlement behavior of piled raft foundation has been clearly stated. In addition to the above mentioned conditions, soil behavior against other external effects, for instance, liquefaction should be examined and required precautions must be taken.

In the circumstance of existing inappropriate soil conditions in the site, one of the possible solutions to apply piled raft approach is soil improvement. Inappropriate soil formations can be turned into appropriate soil layers to apply piled raft by performing soil improvement. A study which is related to piled raft application with ground improvement has been performed by Yamashita & Yamada (2009) and applicability of piled raft even in case of very inadequate soil conditions by performing ground improvement is reported. Besides improving soils conditions, soil improvement has a function of enhancing systems overall performance. Thus, more resolute system response can be obtained by performing soil improvement even in the soil profiles which have appropriate soil conditions. By making an optimization between soil improvement and piled raft approach, extra economy on foundation design can be achieved. In order to accomplish this task, an optimization model consisting of improved soil properties, foundation properties and cost functions should be established and results should be investigated from the viewpoint of cost savings.

2.3.2 Design Philosophies for Piled Rafts

Piled raft foundation approach gives a certain flexible design opportunity to the designers due to the fact that it considers the raft's bearing properties. In some circumstances, structural loads which are planned to be carried by the piles are reduced by the contribution of the raft and required number of piles is getting lower and lower (De Sanctis & Russo, 2008). On the other hand, in cases where the subsoil is satisfactory and capable of carrying entire structural loads by the raft only, piles can be used as "*settlement reducers*" to limit the overall and differential settlements (Broms, 1976; Burland et al. 1977; Gök, 2007; Love, 2003).

Different design philosophies for piled rafts are stated in the literature by considering soil, foundation and structure properties and each design strategy is focused on distribution of the bearing capacity between piles and raft or controlling the overall and differential settlements.

(Poulos, 2001a; Randolph, 1994) have listed these different design philosophies in terms of three cases:

1. In the "*conventional approach*", where piles are considered as primary load carrying structural members, raft's bearing contribution of the system increases the ultimate load capacity of the foundation.
2. In "*Creep piling*", piles work on approximately 70-80% of single pile's ultimate axial load capacity, a point where the creep behavior on the pile starts. Therefore, required numbers of piles are determined by targeting the transmitting stress to be lower than its preconsolidation pressure.
3. "*Differential settlement control*" is an approach in which the piles are used mainly to reduce differential and overall settlements rather than to improve bearing performance of the foundation system.

Poulos (2000) offers a "*more extreme version of creep piling*", where the piles work on their ultimate load capacity (factor of safety is 1) and only settlement reduction contribution is expected from the piles.

In the first two design philosophies, main aim is to provide the solidity of the foundation system by means of bearing capacity and not exceeding the total settlement limits. For this purpose, piles are usually placed in the foundation plan uniformly. On the other hand, in the third design philosophy, there is no bearing capacity problem and main design target is to minimize the differential settlements. Piles are located in strategic points in the foundation area (Gök, 2007).

Piled raft foundation's load-settlement is schematically represented by Poulos (2000) in Figure 2.4 considering different design philosophies:

According to Figure 2.4;

Curve 0 illustrates shallow foundation option (raft alone). In this situation settlements exceed the allowed settlement value under the design load.

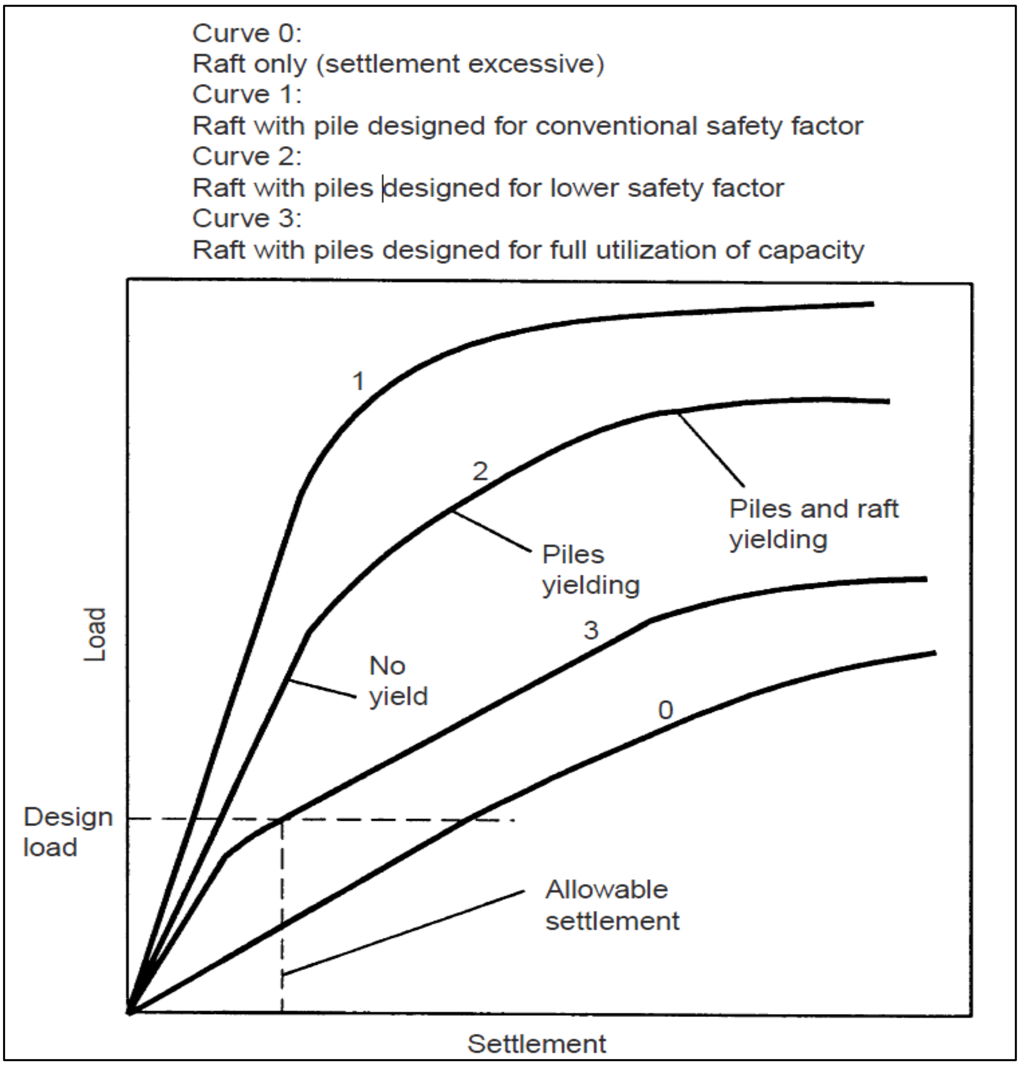

Figure 2.4 Load settlement behavior of piled rafts designed considering different design philosophies (Poulos, 2000)

Curve 1 represents the conventional pile foundation approach. In this case, load-settlement relationship is highly elastic and settlement of the foundation system is very low under the design load. Therefore, it is clearly seen that, conventional pile foundation approach may cause over-designs and non-economic foundation solutions.

Curve 2 shows the creep piling approach, and foundation design can be performed using less piles. In this situation, factor of safety of the piles are relatively lower than conventional approach ($F_{s,conventional}$=3 and $F_{s,creep\ piling}$=1.25) and more settlement is observed with respect to the conventional approach under the same load due to the fact that there are less piles in the creep pile approach. However, settlement of the overall foundation system at the design load is still elastic.

Curve 3 represents the foundation systems where piles are used as settlement reducers and piles are working at their ultimate load capacity. In other words, pile's capacity is fully mobilized. In this case, there are less number of piles rather than creep piling approach and factor of safety of piles is equal or slightly over than 1. At the design load, while some plastic settlements occur due to pile mobilization, overall settlement of the general system is in the allowed limits and overall factor of safety is generally higher than 2.5. So it can be said that the most optimum solution is represented by Curve 3. In the foundation design this load-settlement behaviour should be targeted if the soil conditions allow the designer to do so.

2.3.3 Design Procedures for Piled Rafts

2.3.3.1 Design Aspects for Piled Raft Foundations

Foundations are structural members which provide the integrity of superstructure against internal and external effects. In order to implement this issue, foundations are designed by considering some geotechnical and structural engineering aspects. These aspects can be listed as below (Poulos, 2000);

- Ultimate geotechnical capacity under vertical, lateral and moment loading
- Overall settlement and axial stiffness
- Differential settlements and angular rotations
- Lateral displacements and stiffnesses
- Structural design for both raft and piles

Design aspects for designing the piled raft foundations as listed above are investigated in the different stages of the design.

2.3.3.2 Design Stages of Piled Raft Foundations

In civil engineering applications, generally accepted design procedure is progressing from the simple to the advanced. In a similar way, three major design steps are introduced for designing piled raft foundations (Poulos, 2001b). These steps are;

- *"Preliminary stage"* to evaluate the suitability of using piled raft, appropriate design philosophy and determine the basic foundation system properties, for instance, pile properties, required number of piles.
- *"Second stage"* to investigate the location of the piles in the foundation plan considering non-uniform structural load transfer mechanism which is ignored in the preliminary stage and represents a more realistic situation.
- *"Final detailed design stage"* to adjust the optimum foundation design parameters like number of piles, exact pile locations and calculate precise values of settlements, bending moments, shear forces in the raft and the pile loads and moments for structural design.

Preliminary and second stage calculations are based on simple hand calculations or basic conventional simplified methods. On the other hand, final detailed design stage calculations require solution of complex soil-structure interactions and generally computerized numerical solution schemes are used in this stage. In some complex cases, the effect of the superstructure on the soil-structure interaction should be considered in this part of the design (Poulos, 2001b).

2.3.3.2.1 Preliminary Design Stage. In this stage, first of all, conventional raft foundation option (without piles) is considered and bearing capacity, overall and differential settlements are calculated along with raft's internal forces approximately using simplified conventional methods. After this step, a suitable design philosophy for piled raft is selected depending on raft's bearing properties. If raft's bearing capacity is not adequate, conventional design philosophy –which was introduced in Section 2.3.2- is selected. In this situation, raft's function is to reduce the required number of piles with a small amount. On the other hand, if the raft has acceptable bearing capacity, however, overall and differential settlement limits are exceeded, validating “creep piling” or “piles as settlement reducers” approaches.

One of the goals in the preliminary design is to determine ultimate vertical and lateral geotechnical capacity of piled raft. In this design stage, conventional vertical and lateral load computations can be used while finding ultimate capacity of the system.

The ultimate moment capacity of the piled raft should also be determined approximately in this stage of the design. By determining ultimate moment capacity, lesser value of the ultimate moment capacity of raft (M_{ur}) and the individual piles (M_{up}) and the ultimate moment capacity of a block containing the piles, raft and the soil (M_{ub}) is considered. The ultimate moment capacity of the raft can be calculated as shown below (Poulos, 2000):

$$M_{ur} = \frac{27}{4}\frac{V}{V_u}\left[1-\left(\frac{V}{V_u}\right)^{1/2}\right]\left[\frac{p_{ur}BL^2}{8}\right] \tag{2.6}$$

where;
V =Applied vertical load
V_u =Ultimate cenctric load on raft when no moment is applied
p_{ur} =Ultimate bearing capacity below raft
B =Width of raft (in y-direction)
L =Length of raft (in x-direction)

Contribution of the piles on the ultimate moment capacity is estimated using below given equation (Poulos, 2000):

$$M_{up} \cong \sum_{i=1}^{n_p} p_{uui}\left|x_i\right| \tag{2.7}$$

where;
p_{uui} =Ultimate uplift capacity of typical pile i
$|x_i|$ = Absolute distance of pile i from center of gravity of group
n_p =Number of piles

Ultimate moment capacity of soil block (M_{ub}) can be calculated as shown below (Poulos, 2000):

$$M_{ub} = \alpha_B \overline{p}_u B_B D_B^{\ 2} \tag{2.8}$$

where;
B_B =Width of block perpendicular to direction of loading
D_B =Depth of block
$\overline{p}_u$ =Average ultimate lateral resistance of soil along block
α_B =Factor depending on distribution of ultimate lateral pressure with depth (0.20-0.25)

Moment capacity of the system (M_{sys}) can be defined as shown below in Equation 2.9:

$$M_{sys} = \left[\left(M_{ur} + M_{up} \right) | \, M_{ub} \right]_{smaller} \tag{2.9}$$

In the preliminary design stage, determination of the load-settlement behaviour of the piled raft is one of the main goals. Different approaches to determine this load-settlement behaviour are available in the literature. In order to state the load-settlement behaviour of the piled raft in detail, this issue will be handled in the subsection titled as “analysis of the piled raft foundations”.

One of the design parameters required to be determined in the preliminary design stage is the pile loads. In a foundation system piles can be exposed to additional compressive or tensile forces due to eccentric or moment loading. In this stage such additional forces are calculated. There are several approaches to calculate pile loads in the literature. Poulos (2000) offered a simplified calculation method for computing pile loads assuming that the raft is rigid, pile heads are pinned to the raft and piles are vertical. The axial force on each pile (P_i) which carries a portion (β_p) the vertical load can be calculated as follows:

$$P_i = \frac{V\beta_p}{n_p} + \frac{M_x^{*} x_i}{I_y} + \frac{M_y^{*} y_i}{I_x} \qquad (2.10)$$

with

$$M_x^{*} = \frac{M_x - \dfrac{M_y I_{xy}}{I_x}}{1 - \dfrac{I_{xy}^{2}}{I_x I_y}} \quad \text{and} \quad M_y^{*} = \frac{M_y - \dfrac{M_x I_{xy}}{I_y}}{1 - \dfrac{I_{xy}^{2}}{I_x I_y}} \qquad (2.11)$$

where;

V =Total vertical load acting at centroid of foundation

n_p =Number of pile in group

M_x, M_y =Moments about centroid of pile group in direction of x and y axes respectively

β_p =Proportion of load carried by piles

I_x, I_y =Moment of inertia of pile group with respect to x and y axes respectively

I_{xy} =Product of inertia of pile group about centroid

x_i, y_i =Distance of pile i from y and x axes respectively

M_x^{*}, M_y^{*} =Effective moments in x and y directions respectively, taking symmetry of pile layout into account

In symmetric pile groups I_{xy}=0 and M_x^{*} and M_y^{*} becomes equal to M_x and M_y respectively. In this situation Equation (2.11) simplifies as below:

$$P_i = \frac{V\beta_p}{n_p} \pm \frac{M_x x_i}{\sum_{i=1}^{n_p} x_i^{2}} \pm \frac{M_y y_i}{\sum_{i=1}^{n_p} y_i^{2}} \qquad (2.12)$$

2.3.3.2.2 Second Design Stage. In the preliminary design stage, calculations performed under the assumption of uniform loading conditions especially in load-settlement computations and number of required piles and pile configuration are obtained under these conditions. However, if the application examples are investigated, it can be clearly seen that structural loads are transmitted to the raft by columns and shear walls. This situation causes generation of extra bending moments and shear forces in the raft. Contact pressure and settlements below the raft around the points which have high stress level on the raft (column points) take place. Such extra internal effects in the raft cannot be determined under the assumption of equivalent uniform loading. As a result of these extra internal effects, some modifications on the pile configuration may be needed (adding piles below the highly stressed locations on the raft etc.).

In order to determine extra internal effects due to localized non-uniform loading on the raft Poulos (2001b) has introduced a simplified method which is based on a model consisting of the raft and a single column. In this concept, raft is defined by elasticity modulus, Poisson's ratio, thickness and characteristic length which is a function of both raft and soil properties. Column loads are defined by its magnitude and the distance from the edge of the raft. This concept is given schematically in Figure 2.5:

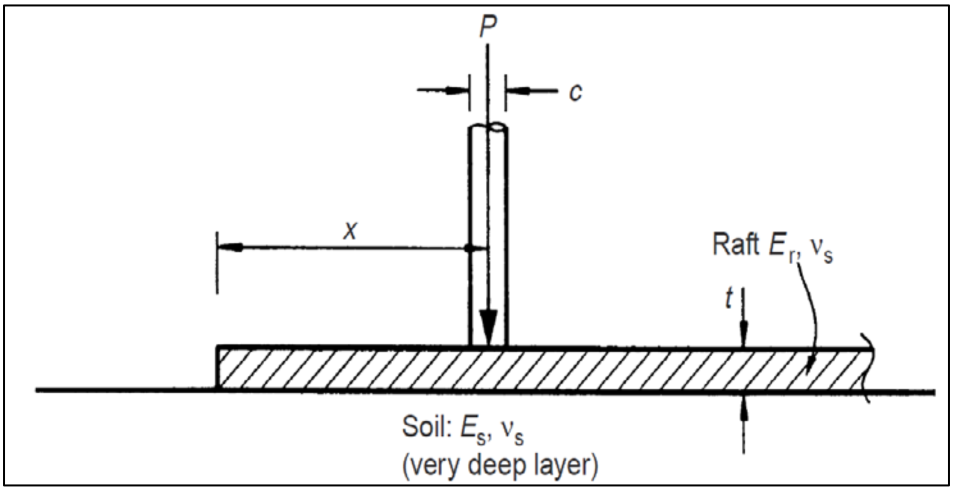

Figure 2. 5 The concept of column load on the raft (Poulos, 2001b)

In Figure 2.5 a column which transmits the load P to the raft is shown. In this concept, in order to provide raft's structural integrity, some conditions should be satisfied. Poulos (2001b) defined these conditions in four main cases as listed below:

- Maximum bending moment condition
- Maximum shear force condition
- Maximum contact pressure condition
- Maximum local settlement condition

In order to satisfy the conditions which were mentioned before, critical column load should be determined. If applied column load is higher than critical column load, raft should be supported by piles at that point. Procedures needed to calculate critical column load some simplified elastic solutions are given in the afore mentioned reference. The characteristic length of the raft, a, which will be used in the calculations is defined as below:

$$a = t\left(\frac{E_r\left(1-\nu_s{}^2\right)}{6E_s\left(1-\nu_r{}^2\right)}\right)^{1/3} \tag{2.13}$$

where;
a =Charecteristic length of the raft
t =Raft thickness
E_r =Elasticity modulus of the raft
E_s =Elasticity modulus of the soil
ν_r =Poisson's ratio of the raft
ν_s =Poisson's ratio of the soil

The maximum bending moment M_x and M_y for the raft beneath the column load can be calculated by Equation 2.14:

$$M_x = A_x P$$
$$M_y = B_y P \tag{2.14}$$

with

$$A_x = A - 0.0928 \ln(c/a)$$
$$B_y = B - 0.0928 \ln(c/a) \tag{2.15}$$

where;

A, B = Moment factors as a function of x/a (Figure 2.6)

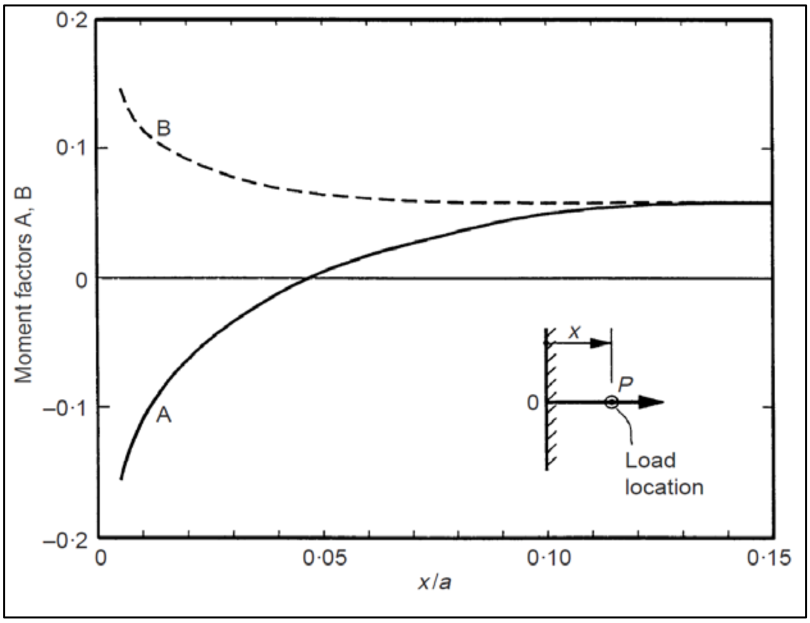

Figure 2.6 Moment factors A and B for circular column (Poulos, 2001b)

The critical column load, P_{c1}, is given as a function of moment in Equation 2.16:

$$P_{c1} = \frac{M_d}{(A_x \mid B_y)_{max}} \tag{2.16}$$

where;

M_d =Design moment capacity of raft

The maximum shear force (V_{max}) due to column load is calculated as in Equation 2.17:

$$V_{\max} = \frac{\left(P - q\pi c^2\right)c_q}{2\pi c} \tag{2.17}$$

where;
q =Contact pressure below the raft
c =Column radius
c_q =Shear factor (Figure 2.7)

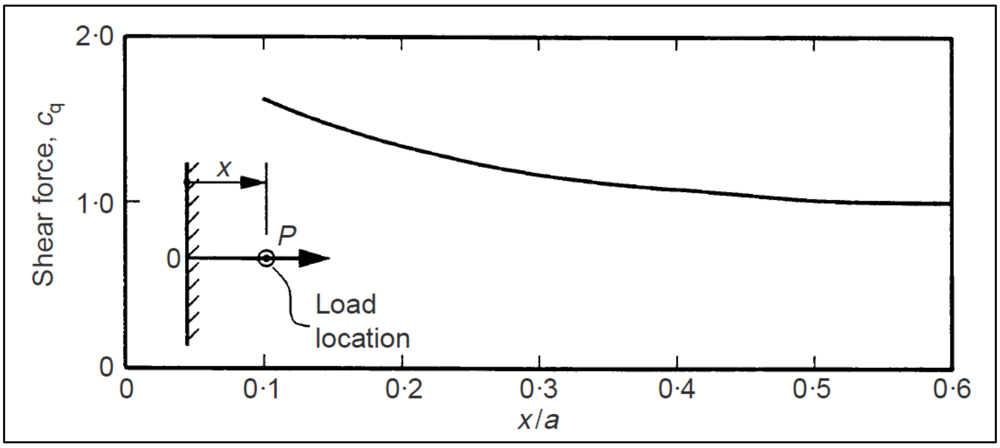

Figure 2.7 Shear factor, c_q, for circular column (Poulos, 2001b)

The column load which satisfies the maximum shear force conditions, P_{c2}, is defined as below:

$$P_{c2} = \frac{V_d 2\pi c}{c_q} + q_d \pi c^2 \tag{2.18}$$

where;
V_d =Design shear force capacity of raft
q_d =Design allowable bearing pressure below raft

The maximum contact pressure (q_{max}) as a result of column load can be computed as introduced below:

$$q_{\max} = \frac{\bar{q}P}{a^2} \tag{2.19}$$

where;

$\bar{q}$ =Contact pressure factor (Figure 2.8)

a =Characteristic length of raft

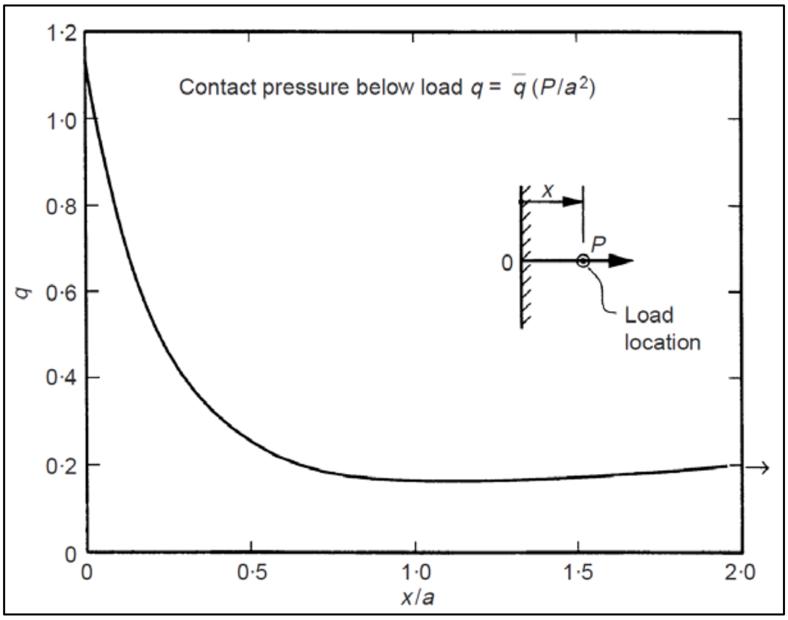

Figure 2.8 Contact pressure factor, q, (Poulos, 2001b)

Allowable column load without exceeding the maximum contact pressure, P_{c3}, is defined as follows:

$$P_{c3} = \frac{q_u a^2}{F_s \bar{q}} \tag{2.20}$$

where;

q_u =Ultimate bearing capacity of soil below the raft

F_s =Factor of safety for contact pressure

The maximum local settlement (S) below a column under the concentrated column load P is calculated as shown below:

$$S = \frac{\omega(1-\nu_s^{\ 2})P}{E_s a} \qquad (2.21)$$

where;

ω =Settlement factor (Figure 2.9)

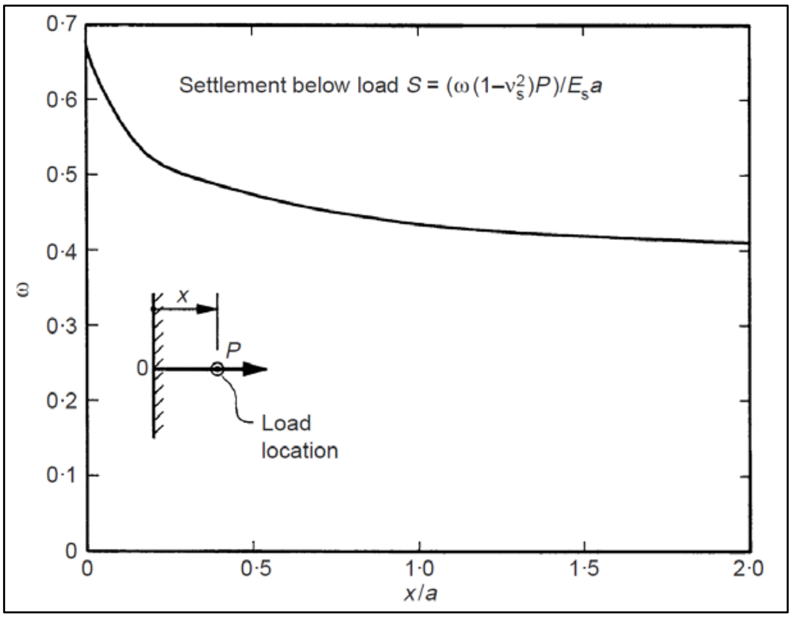

Figure 2.9 Settlement factor, ω, (Poulos, 2001b)

Maximum column load to satisfy maximum local settlement condition, P_{c4}, can be estimated as given below:

$$P_{c4} = \frac{S_a E_s a}{\omega(1-\nu_s^{\ 2})} \qquad (2.22)$$

where;

S_a =Allowable local settlement

Evaluation of the effect of the column load can be performed after the determination of the critical column loads for four conditions which were introduced previously. If the design column load (P_c) is higher than the minimum value of the calculated critical column loads, a pile should be added in the foundation plan to support the raft at the point of interest. This situation is presented in Equation 2.23 as shown below:

$$P_c > P_{critical} \tag{2.23}$$

where;
P_c = Design column load
$P_{critical}$ = Minimum value of P_{c1}, P_{c2}, P_{c3} and P_{c4}

If the critical column load is obtained under the moment, shear or contact pressure cases, ultimate axial load capacity of added pile should provide the capacity corresponding to difference between P_c and $P_{critical}$ values. In addition, researchers have stated that, 90% of ultimate axial load capacity of pile should be used for the piles in the piled raft (Poulos, 2001b; Burland, 1995). In this case, the ultimate load capacity of added pile (P_{ud}) can be calculated as follows:

$$P_{ud} = \frac{1}{0.90} F_p (P_c - P_{critical}) \tag{2.24}$$

where;
F_p = Factor of safety for single pile's ultimate axial load capacity

If the critical condition is stated as the settlement, an additional pile is used as local stiffness increaser. Desired total stiffness the including raft and the pile at column point is calculated using following simple formula:

$$K_{cd} = \frac{P_c}{S_a} \tag{2.25}$$

where;
K_{cd} = Desired stiffness below the column
S_a =Acceptable maximum local settlement

Required pile stiffness to satisfy the calculated K_{cd} stiffness below the column point is determined as a function of depending on raft stiffness and piled raft interaction factor. This value can be calculated by solving the equation as shown below:

$$K_p^{\ 2} + K_p \left[K_r \left(1 - 2\alpha_{cp} \right) - K_{cd} \right] + \alpha_{cp}^{\ 2} K_r K_{cd} = 0 \tag{2.26}$$

where;
K_p =Required pile stiffness
K_r =Raft stiffness
α_{cp} =Piled raft interaction factor

The manner how K_r and α_{cp} values are obtained will be given in detail in the next sections.

2.3.3.2.3 Detailed Design Stage. In this stage of the design, complex analyses are performed to achieve on optimum design for the foundation system. For this purpose, advanced calculation methods are used. Following these calculations, some detailed information, like optimum number and placing of piles, precise values of raft bending moments, shear forces, contact pressures, and detailed distribution of overall and differential settlements are obtained.

2.3.3.3 Recommendations for Optimum Design of Piled Rafts

Foundations are designed to transmit the structural loads to the soil. There are two design criteria which control the foundation design. These criteria are bearing capacity and settlement. From an engineering point of view, a foundation design must satisfy the design criteria with a reasonable economy. Figure 2.10 illustrates the relationship between foundation response and the cost:

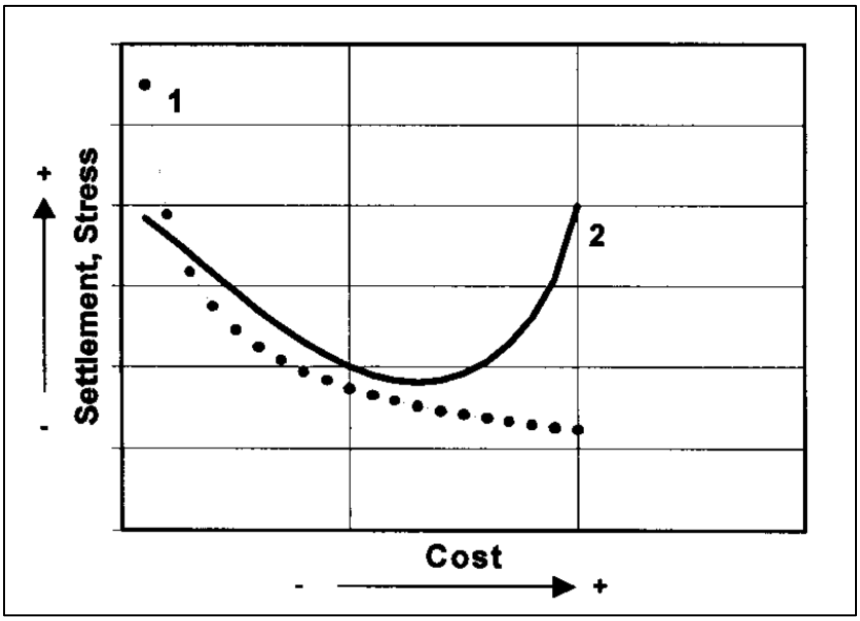

Figure 2.10 Foundation performance versus cost (De Sanctis et al., 2002)

Under the general conditions of the foundation design, response of the foundation system tends to be improved with increasing cost required operations just like increasing the number and length of pile and so on (Curve 1 in Figure 2.10). On the other hand, in some circumstances, this may lead to decrease the performance of the system (Curve 2). In conclusion, obtaining the optimum balance between system response and cost is very important.

In order to obtain optimum design properties of piled rafts, numerous different studies have been performed. De Sanctis et al. (2002) classified the piled rafts as "small" and "large" piled rafts. For "small piled rafts" ($5m<B_{raft}<10m$ and $B_{raft}/L_{pile}<1$) main design consideration is the bearing capacity and piles are used for increasing the factor of the safety against the vertical loads. Since the flexural stiffness of the “small piled rafts” is relatively high, there is no differential settlement problem. In contrast to “small piled rafts”, differential settlement is one of the critical aspects and piles are used for controlling overall and differential settlements in the “large piled rafts”. This researchers have performed a parametric study on optimum design of the piled rafts and they have obtained the relationship between the load carried by the raft (Q_r/Q) and average settlement reduction (w/w_r) as a function of (L/B) and (A_g/A) for “small piled rafts” (Figures 2.11 and 2.12).

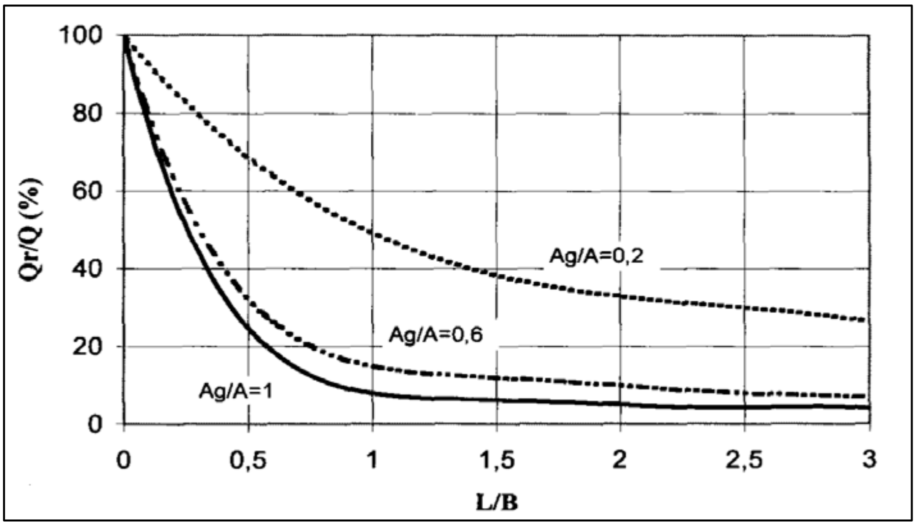

Figure 2.11 Load sharing between piled and raft for “small piled rafts” (De Sanctis et al., 2002)

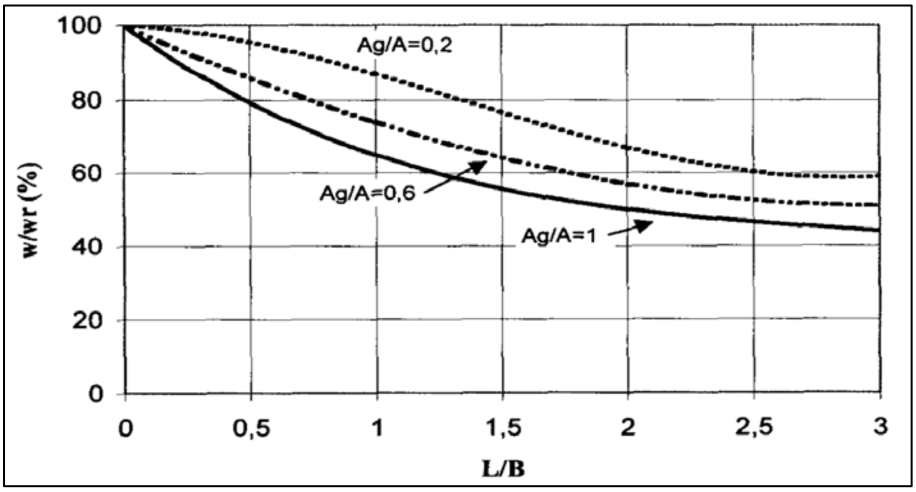

Figure 2.12 Average settlement reduction for “small piled rafts” (De Sanctis et al., 2002)

In Figure 2.11 and 2.12, (Q_r/Q) represents the proportion of the load carried by the raft, (w/w_r) indicates the settlement of piled raft foundation compared to raft only configuration, (L/B) shows the proportion of pile length and raft width, (A_g/A) identifies the ratio between the pile group area and raft area. For “large piled rafts” similar behavior has been reported, as well.

De Sanctis et al. (2002) have suggested some optimum design approaches for piled rafts based on their study:

- Addition of the piles generally improves the foundation response, but after a certain point, increasing the number of the piles does not provide extra performance.
- Longer piles are more effective in settlement reducing and using less number of longer piles is more convenient rather than using a lot of shorter piles.
- Optimum value for (A_g/A) varies between 0.25-0.40 independently of pile length.

Other researchers such as Horikoshi & Randolph (1998) performed a similar study on optimum design of piled raft foundations. They have considered soil strength properties increasing with depth in the centrifuge model tests and also they conducted parametric study. As a result of the study, some optimum design recommendations were proposed as follows:

- Piles should be placed in the 16-25% of the central region of the raft when the piles are used as “settlement reducers”.
- The axial stiffness of the pile group (or equivalent pier) and the raft alone shall be close to each other.
- The pile capacity should be in a range of 40-70% of the ultimate capacity of single pile depending on the ratio between the area of the pile group and the raft area and Poisson’s ratio of the soil.
- To eliminate the differential settlements, the ratio of the pile capacity mobilization should not to exceed 0.80.

These recommendations for optimum piled raft design are generated for general conditions and they should be used for as the first approach in foundation design. In case of special situations, usage of these recommendations may cause some misleading results. For instance; it was reported that, these recommendations may not be suitable for the situation of concentrated loading especially near the raft, edge (Poulos, 2000).

2.3.4 Analysis Techniques for Piled Rafts

As it was explained in previous sections, according to piled raft foundation approach, the raft carries a defined proportion of the structural loads which depend on its stiffness and interaction between soil and piles. In order to define the raft’s contribution on the bearing capacity, a complex soil-structure interaction problem should be solved. Several solution techniques to handle this problem were proposed by some researchers. It is possible to group these analysis techniques in three groups:

- Simplified analysis techniques
- Approximate analysis techniques
- Advanced analysis techniques

2.3.4.1 Simplified Analysis Techniques

Simplified analysis techniques consist of basic approaches and semi-empirical formulations. However, the soil-raft-pile interaction is considered in these types of analysis methods. In these methods, major analysis outputs are the load sharing between piles and raft and the load settlement behaviour of the piled raft.

2.3.4.1.1 Poulos & Davis Method. This simplified analysis method is a base point of most of the analysis approaches for piled rafts. In this method, load-settlement behavior of the piled raft system has been idealized as a tri-linear line. Depending on the load level acting on the foundation system, the load is carried by piles or raft. The idealized load-settlement behavior of the piled rafts according to this approach is given in the Figure 2.13. According to Figure 2.13, P_1 represents the point where the pile capacity is fully mobilized. Up to point P_1, structural loads are carried by raft and piles. Settlement of the system is related to the combined stiffness of piles and raft. If applied load to the foundation is in first part of the graph, settlement can be calculated using interaction factors and charts which were developed by Poulos & Davis (1980) and Gök (2007). Beyond point P_1, the load which is the difference between applied load and P_1 is carried by the only raft since pile capacity is fully mobilized. In this situation, settlement of the foundation system is calculated by in two stages. First settlement component can be calculated as mentioned before. Second settlement component is calculated using only raft's stiffness. In Figure 2.13, the point P_u symbolizes the ultimate capacity of the piled raft system. In order to avoid excessive settlement and plastic behaviour of the foundation system, it is targeted that structural loads are less than or equal to P_1.

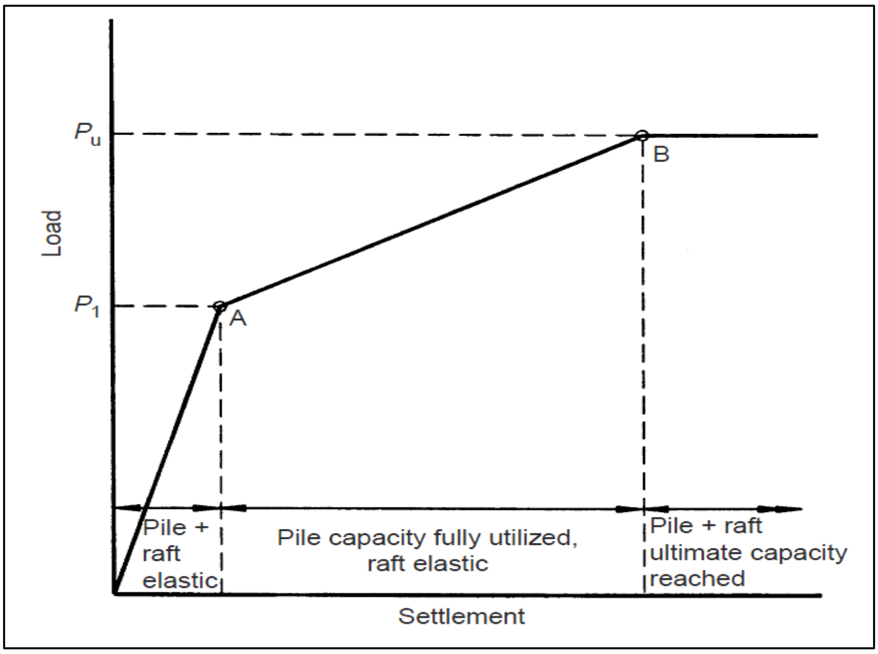

Figure 2.13 Idealized load-settlement behavior of piled rafts (Poulos, 2001)

2.3.4.1.2 Randolph Method. A different piled raft analysis approach was suggested by Randolph (1994). This analysis method was developed by considering the behavior of a unit element which consists of pile, pile cap and surrounding soil

(Gök, 2007). In this method, settlement of the piles and raft was shown in the matrix form in Equation 2.27 as given below:

$$\begin{Bmatrix} w_p \\ w_r \end{Bmatrix} = \begin{bmatrix} \dfrac{1}{k_p} & \dfrac{\alpha_{pr}}{k_r} \\ \dfrac{\alpha_{rp}}{k_p} & \dfrac{1}{k_r} \end{bmatrix} \begin{Bmatrix} P_p \\ P_r \end{Bmatrix} \tag{2.27}$$

where;
w_p, w_r =Settlement of piles and raft, respectively
k_p, k_r =Stiffness of piles and raft
α_{pr}, α_{rp} =Interaction factors between pile and raft
P_p, P_r =Loads which are carried by piles and raft

For the mathematical suitability in the matrix calculations, the following relationship between the interaction factors, α_{pr} and α_{rp}, must be satisfied:

$$\alpha_{pr} = \alpha_{rp} \frac{k_r}{k_p} \tag{2.28}$$

For the provision of the physical integrity of the foundation system, the overall settlements of the piles and raft must be equal. The overall stiffness of the system (k_{pr}) can be obtained as shown below:

$$k_{pr} = \frac{k_p + (1 - 2\alpha_{rp}) k_r}{1 - \alpha_{rp}{}^2 \left(\dfrac{k_r}{k_p} \right)} \tag{2.29}$$

Using a similar approach, the load which is carried by piles and raft is calculated as given below:

$$\frac{P_r}{P_r + P_p} = \frac{\left(1-\alpha_{rp}\right)k_r}{k_p + \left(1-2\alpha_{rp}\right)k_r} \tag{2.30}$$

The interaction factor between piles and raft can be calculated analytically by considering single pile and circular pile cap approach as presented in Equation 2.31:

$$\alpha_{rp} \cong 1 - \frac{\ln\left(\frac{r_c}{r_0}\right)}{\zeta} \tag{2.31}$$

where;

r_c =Radius of circular pile cap for single pile

(Raft area / Number of piles for pile groups (Poulos, 2001))

r_0 =Pile radius

l =Pile length

ν =Poisson's ratio of soil

$\zeta \cong \ln(r_m / r_0)$

r_m =Maximum radius of influence

$r_m = \left\{0.25 + \xi\left[2.5\rho(1-\nu) - 0.25\right]\right\} l$

$\xi = G_l / G_b$

$\rho = G_{avg} / G_l$

G_l =Shear modulus of soil at depth of l

G_b =Shear modulus of soil at depth of pile base

G_{avg} =Average shear modulus of soil along the pile

It was reported that the α_{rp} value, converges the value of the 0.8 independently from the foundation properties like pile spacing etc. in the situation of large pile groups and high stiffness differences between piles and soils which represents the usual piled raft application (Clancy & Randolph, 1993; Randolph, 1994). The variation of the interaction factor of different sized pile groups is shown in Figure 2.14:

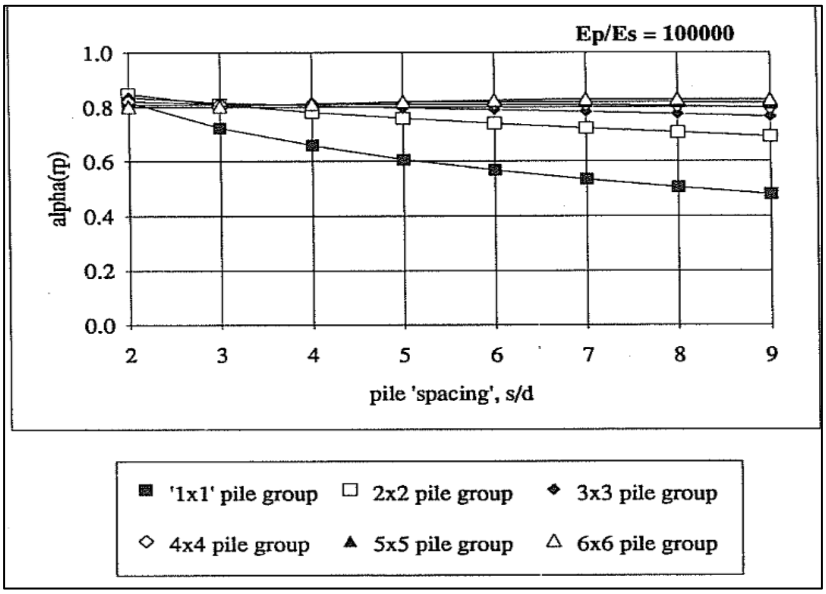

Figure 2.14 Variation of the interaction factor (Randolph, 1994)

The overall stiffness of piled raft is calculated by substituting α_{rp}=0.8 in Equation 2.29:

$$k_{pr} = \frac{1-0.6\left(\dfrac{k_r}{k_p}\right)}{1-0.64\left(\dfrac{k_r}{k_p}\right)} k_p \tag{2.32}$$

In a similar way, load sharing ratio between raft and piles can be computed as given below:

$$\frac{P_r}{P_p} = \frac{0.2}{1-0.8\left(\dfrac{k_r}{k_p}\right)} \frac{k_r}{k_p} \tag{2.33}$$

After the determination of the load sharing ratio between piles and raft settlement of the system can be calculated. For this purpose following Equation can be used.

$$S = \frac{P}{k_{pr}} \tag{2.34}$$

where;
S = Settlement of the system
P = Applied load on system
k_{pr} = Axial stiffness of the piled raft

2.3.4.1.3 Poulos-Davis-Randolph Method. This method is a combination of the previously presented two methods. Randolph's technique is used for determining of the load sharing ratio between piles and raft. Load-settlement behavior of the system is calculated using Poulos & Davis approach. In this method, at which the point that pile capacity is fully mobilized (P_1) is determined the below given equation (Poulos, 2001b):

$$P_1 = \frac{P_{up}}{1 - X} \tag{2.35}$$

with

$$\frac{P_r}{P_p} = X \tag{2.36}$$

where;
P_r, P_p =Load carried by raft and piles (from Eq. 2.30 or 2.33)
X =Load sharing ratio
P_{up} =Ultimate load capacity of the pile group

After the determination of P_1 point, the settlement of the foundation system can be calculated as shown below:

Up to Point P_1;

$$S = \frac{P}{k_{pr}} \tag{2.37}$$

Beyond the Point P_1;

$$S = \frac{P_1}{k_{pr}} + \frac{\left(P - P_1\right)}{k_r} \tag{2.38}$$

where;
S =Settlement of the piled raft
P =Applied axial load
k_{pr}, k_r = Stiffness of piled raft and raft only (from Eq. 2.32)

2.3.4.1.4 Modified version of Poulos-Davis-Randolph Method. A modified version of the previously mentioned simplified method was proposed by Poulos (2000). In this method, in order to simulate more realistic behavior of the piled raft system, a hyperbolic load settlement curve is utilized instead of a model which consists of three linear segments. In addition, in this method, stiffness of the piles, raft and piled raft vary depending on the level of the load applied on the foundation. Figure 2.15 shows the hyperbolic load-settlement behavior of the piled raft. In this figure, the parameter of V_u represents the ultimate load capacity of the piled raft, V_{pu} and V_{ru} show the ultimate axial load capacity of the only piles and only raft, respectively. The point V_A denotes the load level beyond which the response of the piled raft system gets non-linear. Finally, the S_A value indicates the allowable settlement limit of the piled raft. In the design stage, it is aimed not to exceed the point V_A in order to avoid plastic behavior of foundation and excessive overall and differential settlements.

The load V_A can be calculated in the same manner with using Equation 2.39. Using a different notation, the load V_A is obtained by:

$$V_A = \frac{V_{pu}}{\beta_p} \tag{2.39}$$

where;

V_{pu} =Ultimate load capacity of pile group

β_p =Proportion of the load carried by the piles

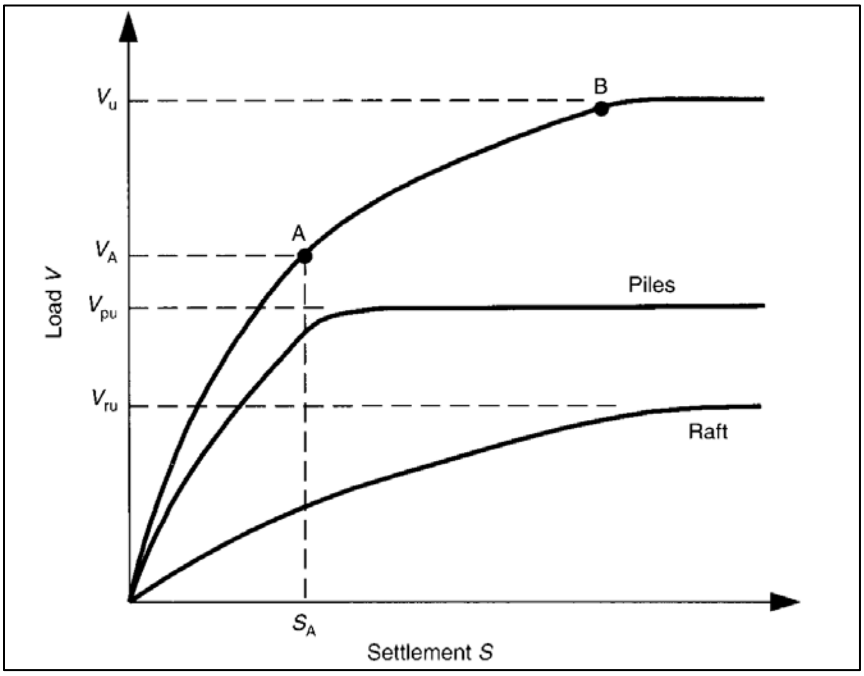

Figure 2.15 Hyperbolic load-settlement behavior of piled raft in the Modified Poulos-Davis-Randolph method (Poulos, 2000)

Stiffness of the piled raft can be calculated as shown in Equation 2.40:

$$K_{pr} = XK_p \tag{2.40}$$

with

$$X \cong \frac{1-0.6(K_r / K_p)}{1-0.64(K_r / K_p)} \tag{2.41}$$

where;

K_r, K_p =Secant stiffness of the raft and pile group, respectively

The proportion of the load carried by the piles (β_p) can be calculated as given below:

$$\beta_p = \frac{1}{1+a} \tag{2.42}$$

with

$$a = \frac{0.2}{1-0.8(K_r / K_p)}\left(\frac{K_r}{K_p}\right) \tag{2.43}$$

The secant stiffnesses of the pile group and the raft alone are determined as presented by Equations 2.44 and 2.45:

$$K_p = K_{pi}\left(1 - R_{fp}\frac{V_p}{V_{pu}}\right) \tag{2.44}$$

$$K_r = K_{ri}\left(1 - R_{fr}\frac{V_r}{V_{ru}}\right) \tag{2.45}$$

where;

K_r, K_p =Secant stiffnesses of the raft and the pile group, respectively

K_{pi}, K_{ri} = Initial stiffnesses of the pile group and the raft

R_{fp}, R_{fr} =Hyperbolic factor for the pile group and the raft

V_p, V_r =Load carried by the piles and the raft

V_{pu}, V_{ru} =Ultimate capacity of the pile group and the raft

It is recommended to assign 0.50 and 0.75 to R_{fp} and R_{fr}, respectively (Poulos, 2000).

The load carried by the piles and the raft under the applied load V is expressed as:

$$V_p = \beta_p V \leq V_{pu} \tag{2.46}$$

$$V_r = V - V_p \tag{2.47}$$

Settlement of the piled raft system can be calculated as shown below for two different conditions:

Up to Point V_A;

$$S = \frac{V}{XK_{pi}\left(1 - \frac{R_{fp}\beta_p V}{V_{pu}}\right)} \tag{2.48}$$

Beyond Point V_A;

$$S = \frac{V_A}{XK_{pi}(1 - R_{fp})} + \frac{V - V_A}{K_{ri}\left[1 - R_{fr}\frac{(V - V_{pu})}{V_{ru}}\right]} \tag{2.49}$$

One of the difficulties that could be encountered while using this method is variation of the secant stiffness and load sharing ratio at various load levels. In order to cope with this, calculations are first performed for an assumed β_p value. Then, computed actual β_p value is compared with the initial one. Calculations continue until the difference between consecutive β_p values fall below a previously decided convergence criterion.

2.3.4.1.5 Burland's Approach. A Simplified piled raft analysis technique, especially based on the "settlement reducers" concept, was recommended by Burland (1995) and Poulos (2001a). According to this approach, first of all, the load settlement behavior of the raft solely is determined using a suitable method. This type of load-settlement relationship is given in Figure 2.16:

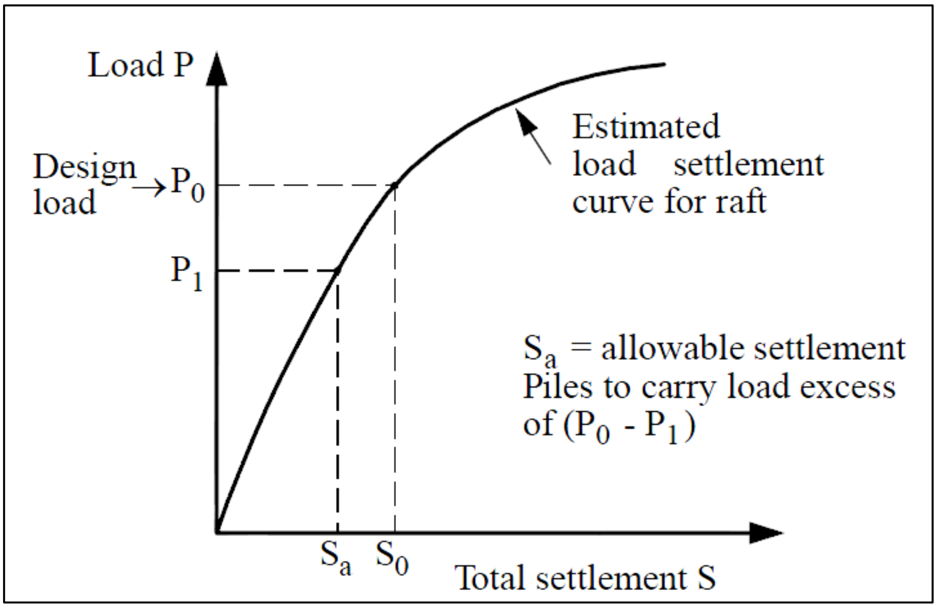

Figure 2.16 Load-settlement relationship for raft only in the Burland approach (Poulos, 2001a)

After obtaining of the load-settlement relationship for raft only, total settlement, S_0, corresponding to the design load, P_0, and the maximum load, P_1, which can be encountered under the allowable settlement limit, S_a, is determined. The difference between P_0 and P_1 is considered to be carried by the piles. On the other hand, in this approach, it is stated that, only 90% of pile capacity is mobilized and this issue should be considered in the design. Under these circumstances, the required number of piles can be calculated as shown below:

$$n = \frac{P_0 - P_1}{0.90 Q_u} \tag{2.50}$$

where;

n =Required number of piles

Q_u =Ultimate axial load capacity of single pile

Once the required number of piles is determined, a suitable layout for piles is selected and pile group properties are defined. Actual settlement of the piled raft can be determined using previous methods after this step in this approach.

2.3.4.1.6 Incremental Load Step Approach. A simple yet not requiring to use complex interaction factors was developed by Gök (2007). According to this method, piled raft system is considered in terms of two different systems, piles and raft individually, and load-settlement behaviour of these two different systems is calculated step by step with increments up to the design load. Due to compatibility assumption, the overall settlement of pile group and raft must be the same. In this method, the equal settlement obtained. Figure 2.17 expresses this approach:

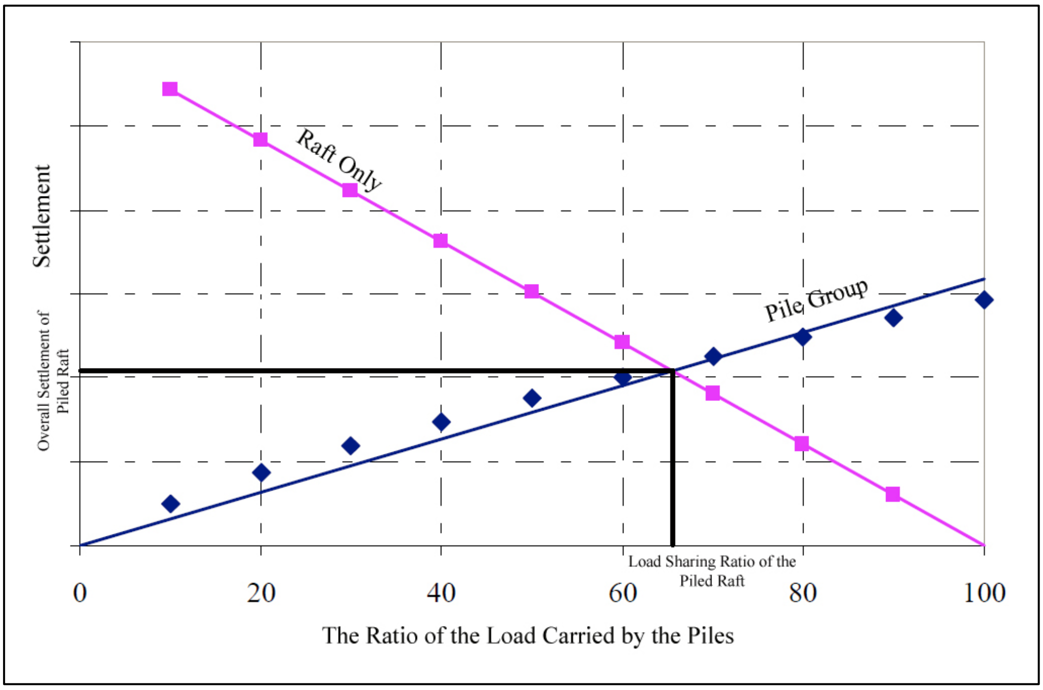

Figure 2.17 Determination of the overall settlement and load sharing ratio using incremental load step approach (after Gök, 2007)

When Figure 2.17 is examined, pile group's and raft's individual load-settlement behaviour is seen. According to physical continuity principle, overall system properties are acquired at the intersection of these two lines. In order to perform this technique, a satisfactory pile and raft settlement approach should be used. To calculate the pile group's settlement "the equivalent raft" method can be used

(Tomlinson & Woodward, 2009). On the other hand, several elastic analysis formulations are available for the evaluation of the raft's settlement in the literature.

2.3.4.2 Approximate Analysis Techniques

Approximate analysis techniques stay somewhere between the simplified and advanced methods. They require use of computers however the computational power that is needed is not as high as the advanced methods where 3D numerical discretization of the boundary value problem is made. In approximate methods, on the other hand the foundation-soil relationship is established by means of foundation soil springs which reduce the size of the problem significantly.

Approximate analysis techniques may considered in two major branches. One of this is the "strip-on-springs approach" (Poulos, 2000). In this technique, a pre-defined section of the raft is idealized as a strip and piles are modeled as springs or equivalent stiffnesses. Figure 2.18 shows the strip-on-springs model with details about pile and contact pressure assumptions.

Strip-on-springs approach considers the pile-raft, raft-pile, raft-raft, pile-pile interactions and analysis results from this approach are in good agreement with results obtained from complex analysis techniques. On the other hand, there are some disadvantages of using strip-on-spring approach, for instance, torsional raft moments cannot be calculated in this method (Poulos, 2000).

One of the other approximate methods is "plate-on-spring" approach (Poulos, 2000). In this technique, whole raft is modeled as a plate and piles are idealized as springs. This method gives the results which are in a good agreement on average settlements and load sharing ratio, but maximum bending moments and differential settlements are obtained higher than the results obtained from other methods (Poulos, 2000). In order to develop this approach, some modifications were made by researchers Clancy & Randolph (1993) and Franke et al. (1994).

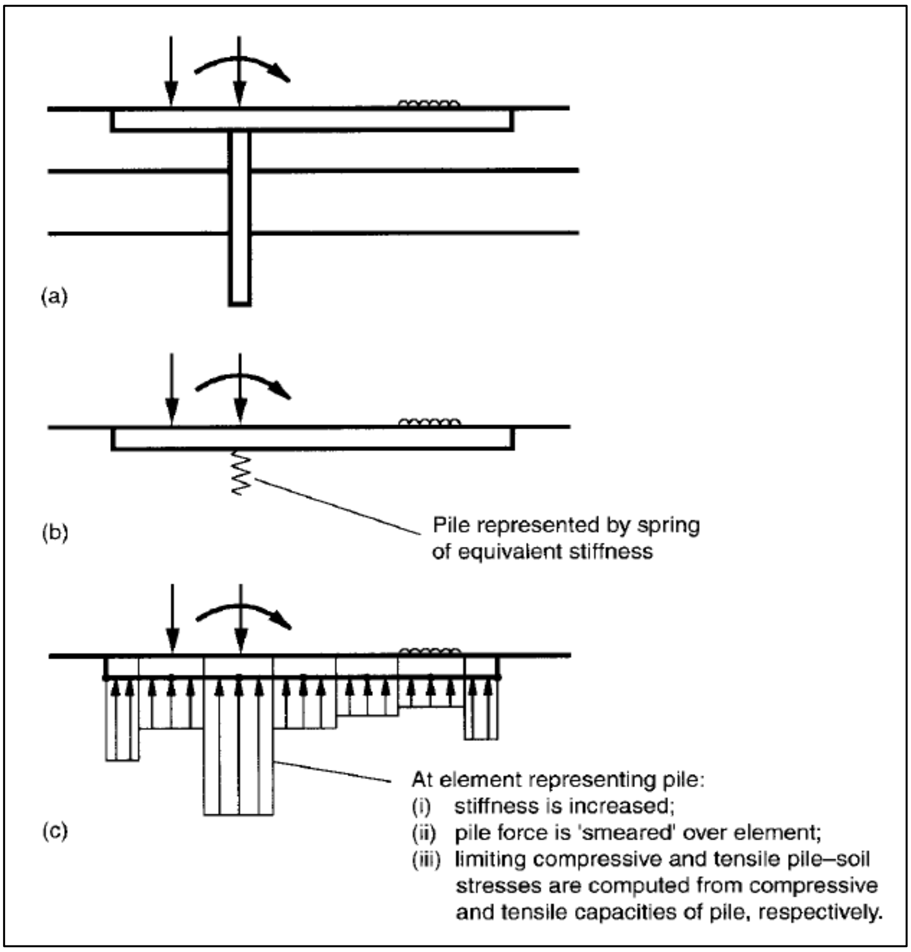

Figure 2.18 Schematic representation strip-on-spring approach. a) Pile and raft in real condition. b) Spring idealization for pile. c) Contact pressure distribution assumptions below the raft (Poulos, 2000)

2.3.4.3 Advanced Analysis Techniques

The simplified methods that were explained so far are generally utilized to find out load share between the pile and the raft. Such methods are also employed to calculate the overall settlement of the system. The load that each pile is subjected to, however, cannot be computed using simplified methods. Numerical analysis techniques are called for this purpose. Such methods are named as Advanced Analysis Techniques in this section of thesis.

One of the earliest methods, in this respect is the Boundary Element Method (BEM) (Butterfield & Banerjee, 1971; Griffiths et al., 1991; Kuwabara, 1989). The application of the Finite Element Method (FEM), on the other hand, commenced with simplified 2D (Desai et al., 1974; Prakoso & Kulhawy, 2001; Pressley & Poulos, 1986) and progressed, with the advancement of computer and software technology towards 3D applications (Liang et al., 2003; Ottaviani, 1975; Reul & Randolph, 2003). There are also hybrid methods that combine the boundary element and finite element methods (Clancy & Randolph, 1993; Franke et al., 1994; Hain & Lee, 1978; Ta & Small, 1996) (Gök, 2007).

Boundary Element Method (BEM) depends on integration of appropriate functions along the depth of interest. For instance, Mindlin Equations (1936) are frequently applied to obtain response of raft and pile elements that are discretized into smaller parts. A recent study introducing this technique was realized by Gök (2007).

2D Finite Element Methods were developed in the purpose of performing calculations in a shorter analysis time. For that reason, these analysis techniques have some simplifying assumptions. Such analysis methods are based on use of plain strain or axisymmetric model.

3D Finite Element Method is capable of analyzing the soil-structure interaction in a more realistic manner. However, required computational capacity is relatively higher due to large number of degree of freedoms inherent in the model.

It appears that the BEM requires less computing time and computational resources among the above mentioned numerical analysis methods. Applicability of this method is restricted since complex shaped foundations types are not easily handled and the method itself is not so suitable for programming. For that reason, finite element method is getting more popular to analyze piled raft foundations. In addition, increasing computer technology shortens analysis time for 3D Finite Element Method calculations is and Finite Element Method is becoming as "industrial standard" for piled raft and several other geotechnical applications (Özden, private communication, June 2012). The increasing number of commercial computer codes that employ FEM supports this fact.

A comparison of several available analysis methods including the simplified, approximate and the advanced was made by Poulos (2000) as shown in the Table with some addition.

Table 2.1 Capabilities of different analysis methods for piled raft foundations (after Poulos, 2000)

The Method Based On	Reference	Response Characteristics					Problem Modeling			
		Total Settlement	Diff. Settlement	Pile Load	Raft Bending Moment	Raft Torsional Moment	Non-Linear Soil Behavior	Non-Linear Pile Behavior	Non-Uniform Soil Profile	Raft Flexibility
Simplified	(Poulos&Davis, 1980)	x						x		
	(Randolph, 1994)	x		x					x	
	(Poulos, 2000)	x		x			x	x	x	
Approximate (Strip on Springs)	(Poulos, 1991)	x	x	x	x		x	x	x	x
	(Brown&Wiesner, 1975)	x	x	x	x					x
Approximate (Plate on Springs)	(Clancy&Randolph, 1993)	x	x	x	x	x			x	x
	(Poulos, 1994)	x	x	x	x	x	x	x	x	x
Advanced (BEM)	(Kuwabara, 1989)	x		x						
Advanced (Hybrid)	(Hain&Lee, 1978)	x	x	x	x	x		x		x
	(Franke et al., 1994)	x	x	x	x	x	x	x		x
	(Sinha, 1997)	x	x	x	x	x	x	x		x
Advanced (2D FEM)	(Hooper, 1973)	x	x	x	x		x	x	x	x
	(Hewitt&Gue, 1994)	x	x	x	x				x	x
Advanced (3D FEM)	(Lee, 1993)	x	x	x	x	x				x
	(Ta&Small, 1996)	x	x	x	x	x			x	x
	(Brinkgreve et al., 2011)	x	x	x	x	x	x	x	x	x

Note: “x” shows the calculation ability

2.3.5 Application Examples for Piled Raft Foundations

The piled raft foundation approach has been applied in the design of the foundations with an increasing manner starting 1970-1980's. Some piled raft applications which performed in different types of soil conditions are available in the literature. These application examples are a good reference to designers for the applicability of piled raft concept. In addition, such case histories show different design philosophies depending on different soil and superstructure conditions. In this section of the thesis, some piled raft application examples which are also available in the literature will be briefly introduced.

2.3.5.1 Messe-Torhaus Building (Katzenbach et al., 2000)

Messe-Torhaus Building is one of the first applications of the piled raft concept. It was constructed in Frankfurt/Germany between 1983 and 1985. This building was actually designed by considering German codes covered the conventional pile foundation approach. However, load sharing function of the raft was observed by the help of performing good instrumentation and measurement operations.

Messe-Torhaus Building was constructed on Frankfurt Clay which is a well-known and well-documented soil profile. General soil profile in the Frankfurt City is shown in the Figure 2.19.

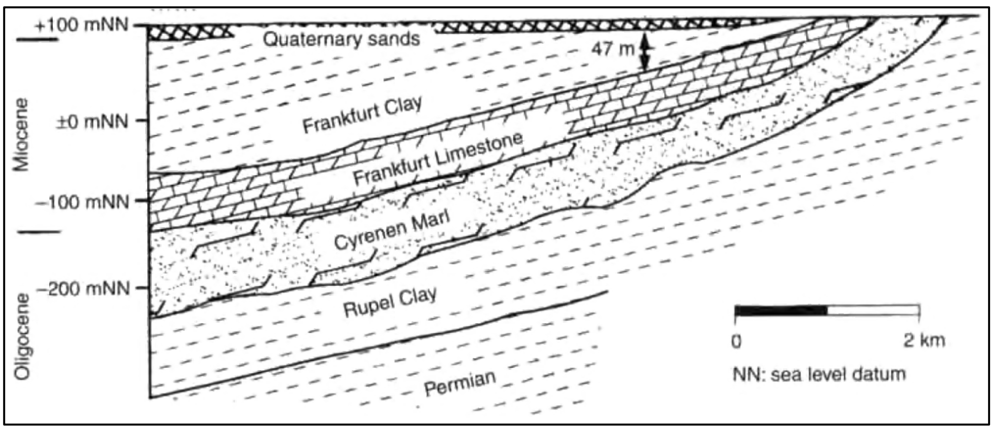

Figure 2.19 General soil profile in Frankfurt area (Katzenbach et al., 2000)

There are numerous studies about the Frankfurt Clay (El-Mossallamy, 2002; Franke et al., 2000; Katzenbach et al., 2000), and due to this reason general geotechnical engineering properties of the Frankfurt Clay is well-known. These properties are given in the Table 2.2. In addition, variation of the undrained shear strength (c_u) with depth and modulus of elasticity (drained) properties of the Frankfurt Clay are represented in Figure 2.20 and Table 2.3, respectively.

Table 2.2 General geotechnical engineering properties of Frankfurt Clay (Franke et al., 2000)

Property	Min.	Max.	Average
Liquid Limit, w_L (%)	50.0	110.0	70.0
Plasticity Index, I_p (%)	32.0	81.0	45.0
Natural Water Content, w_n (%)	16.0	45.0	32.0
Consistency Index, I_c	0.76	1.03	0.90
Wet Unit Weight, γ (kN/m^3)	16.5	20.5	18.5
Degree of Saturation, S_r	0.80	1.0	0.94
Activity, I_A	0.70	1.30	1.0
Drained Cohesion, c′ (kN/m^2)	10.0	65.0	20.0
Angle of Internal Friction, φ′ (degrees)	10.0	25.0	20.0
Clay Content (dia. <0.002 mm.) (%)	35.0	60.0	47.0

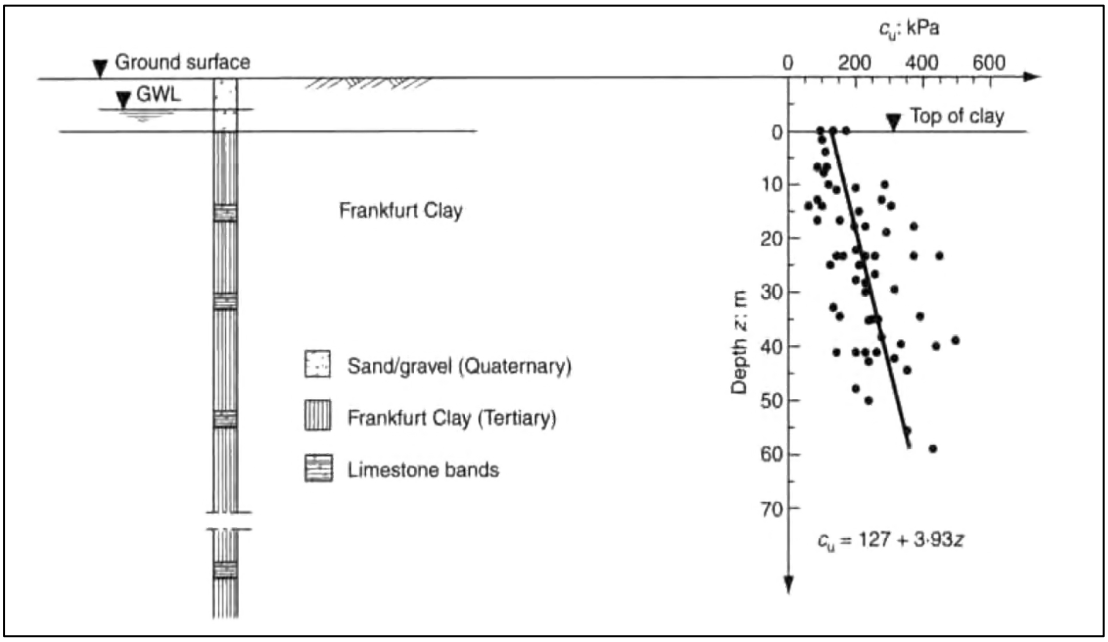

Figure 2.20 Variation of the c_u value of Frankfurt Clay with depth (Franke et al., 2000)

Table 2.3 Modulus of elasticity (drained) values for Frankfurt Clay (Franke et al., 2000)

Type of Loading	E_s' (MPa)
Unloading	$E_s' = 120.0$
Reloading	$E_s' = 70.0$
Primary Loading	$E_s' = 7.0 + 2.45*z$
	z: Depth in meters from the surface

Messe-Torhaus is a 30 storey building with a height 130 m. Foundation system of Messe-Torhaus consists of two separate rafts because of sewage culverts passing through the foundation area (Franke et al., 2000). Weight of the structure is 400 MN (total) and total foundation area is 24.5 m x 43 m. Due to the separation of the rafts, each raft has 24.5 m x 17.5 m area. In order to minimize harmful settlement effects to adjacent structures, settlement of the two separate rafts should have been limited. For that reason, 42 piles were placed under each raft with a layout of 6x7. Elevation, section and plan views of Messe-Torhaus Building are shown in Figure 2.21.

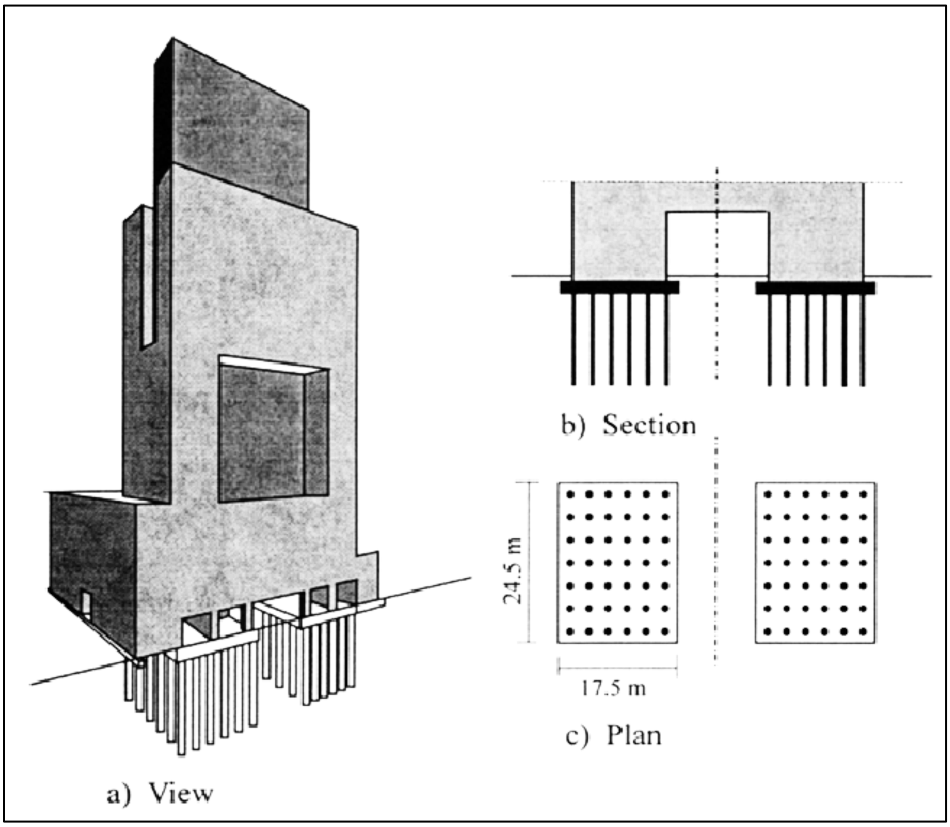

Figure 2.21 a) Elevation b) Section c) Plan view of Messe-Torhaus Building (El Mossallamy, 2002)

General structural and foundation properties of Messe-Torhaus Building are summarized in Table 2.4.

Table 2.4 General properties of Messe-Torhaus Building (Katzenbach et al., 2000)

Property	Value
Maximum Structural Height (m)	130
Number of Floors	30
Number of Basement Floors	0
Foundation Area (m^2)	2 x 430=860
Foundation Level below Ground Surface (m)	-3.0
Raft Thickness (m)	2.5
Number of Piles	2 * 42
Pile Length, L (m)	20
Average Pile Spacing, s (m)	3.0 – 3.5 * D
Pile Diameter, D (m)	0.90
Eccentricity of Building Load, e (m)	0.80
Slenderness Ratio (Height/Width)	5.4
Total Load (G+Q) (MN)	2 * 200=400

Measurements were performed during and after the construction of the Messe-Torhaus Building via instrumented piles. These measurement results are shown in Table 2.5.

Table 2.5 Measurement results for Messe-Torhaus Building (Katzenbach et al., 2000)

Result	Value
Observed Piled Raft Coefficient, α_{pr}	0.80
Observed Pile Loads (MN)	1.7-6.9
Observed Maximum Settlement, w (mm)	150

According to Table 2.5, it is seen that, 80% of the structural load was carried by the piles. Observed pile loads vary 1.7 to 6.9 MN center piles to corner piles (Katzenbach et al., 2000). Variations of the resistance forces of the raft and the piles piled raft interaction factor and observed settlement with time following the construction are illustrated in Figure 2.22:

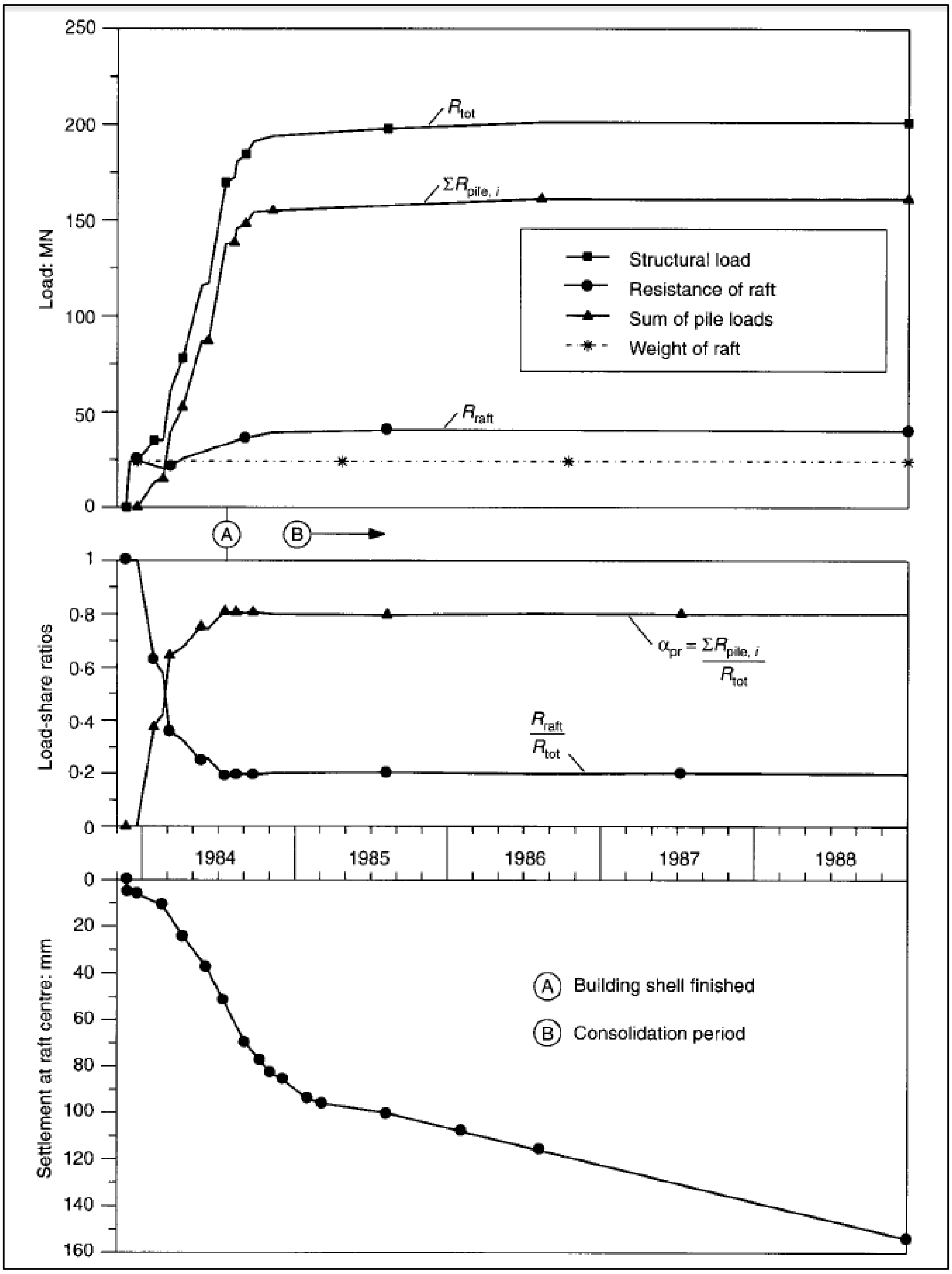

Figure 2.22 Variation of pile and raft resistance, load sharing ratio and settlement with time after construction (Katzenbach et al., 2000)

In summary, raft's load carrying function is clearly observed, although Messe-Torhaus Building was designed by considering conventional pile foundation approach. The amount of resistance which is obtained from raft increases the factor of safety of the overall system. Thus, it can be said that, foundation design of Messe-

Torhaus Building matches the first design philosophy (conventional approach) which was introduced in earlier sections. Finally, Messe-Torhaus Building is one of the first piled raft application and it has been a good reference for next buildings.

2.3.5.2 Westend Tower Building (Franke et al., 2000)

One of the well-measured and well-documented piled raft application examples is Westend Tower Building which was constructed in financial building district of Frankfurt/Germany in 1993. Building consists of office tower and side building. Height of the office tower is 208 meters with 53 storeys. Foundation of the office tower and side building was separated by a settlement joint in order to avoid high raft bending moments at contour line of the office tower. In this example, only foundation of the office tower will be investigated. Plan and elevation view of Westend Tower are given in Figure 2.23:

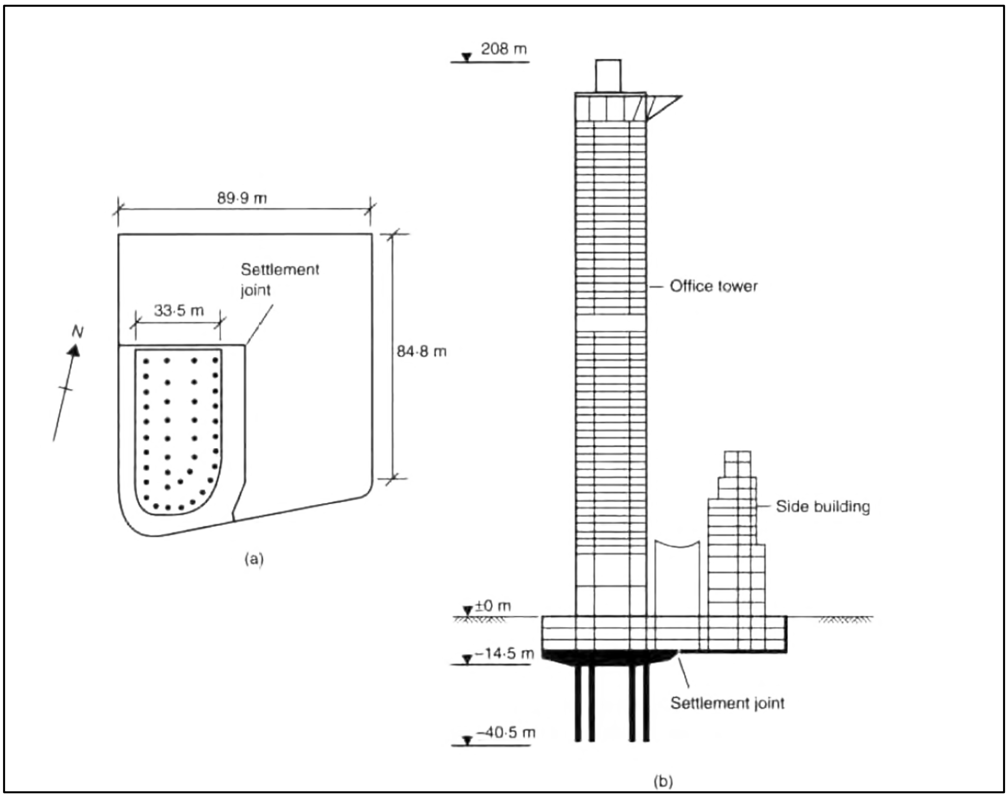

Figure 2.23 Plan (a) and elevation (b) view of Westend Tower Building (Katzenbach et al., 2000)

The Westend Tower Building was also constructed on Frankfurt Clay. Although the actual soil properties below the construction site are not available in the literature, general engineering properties of Frankfurt Clay does not change from site to site (Poulos, 2000). For that reason, soil properties under the Westend Tower Building can be considered just as the Messe-Torhaus case.

The Westend Tower Building has a weight of approximately 1420 MN. It has three basement floors and foundation level of the building is 14.0 meters below the ground surface. Groundwater level is about 9.5 meters above the foundation level. The plan area of the foundation is approximately 3000 m^2. Due to excessive foundation contact pressure, settlement, existing limitations on the foundation depth and high slenderness ratio of the structure (H/B=4.7), piled raft option was preferred by the designers (Franke et al., 2000). Thickness of the raft is 4.65 meters at the center of the raft and 3.0 meters at the edge. There are 40 piles with diameter of 1.3 meters and length of 30 meters placed at the strategic points in the foundation plan. General structural and foundation properties of the Westend Tower Building is given in Table 2.6

Table 2.6 General properties of the Westend Tower Building (Katzenbach et al., 2000)

Property	Value
Maximum Structural Height (m)	208
Number of Floors	53
Number of Basement Floors	3
Foundation Area (m^2)	3000
Foundation Level below Ground Surface (m)	-14
Thickness of Raft (m)	3.0 - 4.5
Number of Piles	40
Pile Length, l (m)	30
Average Pile Spacing, S/D	3.8 - 6.0
Pile Diameter, D (m)	1.30
Eccentricity of Building Load, e (m)	0
Slenderness Ratio (Height/Width)	4.7
Total Load (G+Q) (MN)	1420
Buoyancy Uplift Force (MN)	280

After the performed measurements, following values were obtained for piled raft foundation of the Westend Tower Building (Table 2.7 and Figure 2.24):

Table 2.7 Measurement results for Westend Tower Building (Katzenbach et al., 2000)

Result	Value
Observed Piled Raft Coefficient, α_{pr}	0.50
Observed Pile Loads (MN)	9.2 – 14.9
Observed Maximum Settlement, w (mm)	110

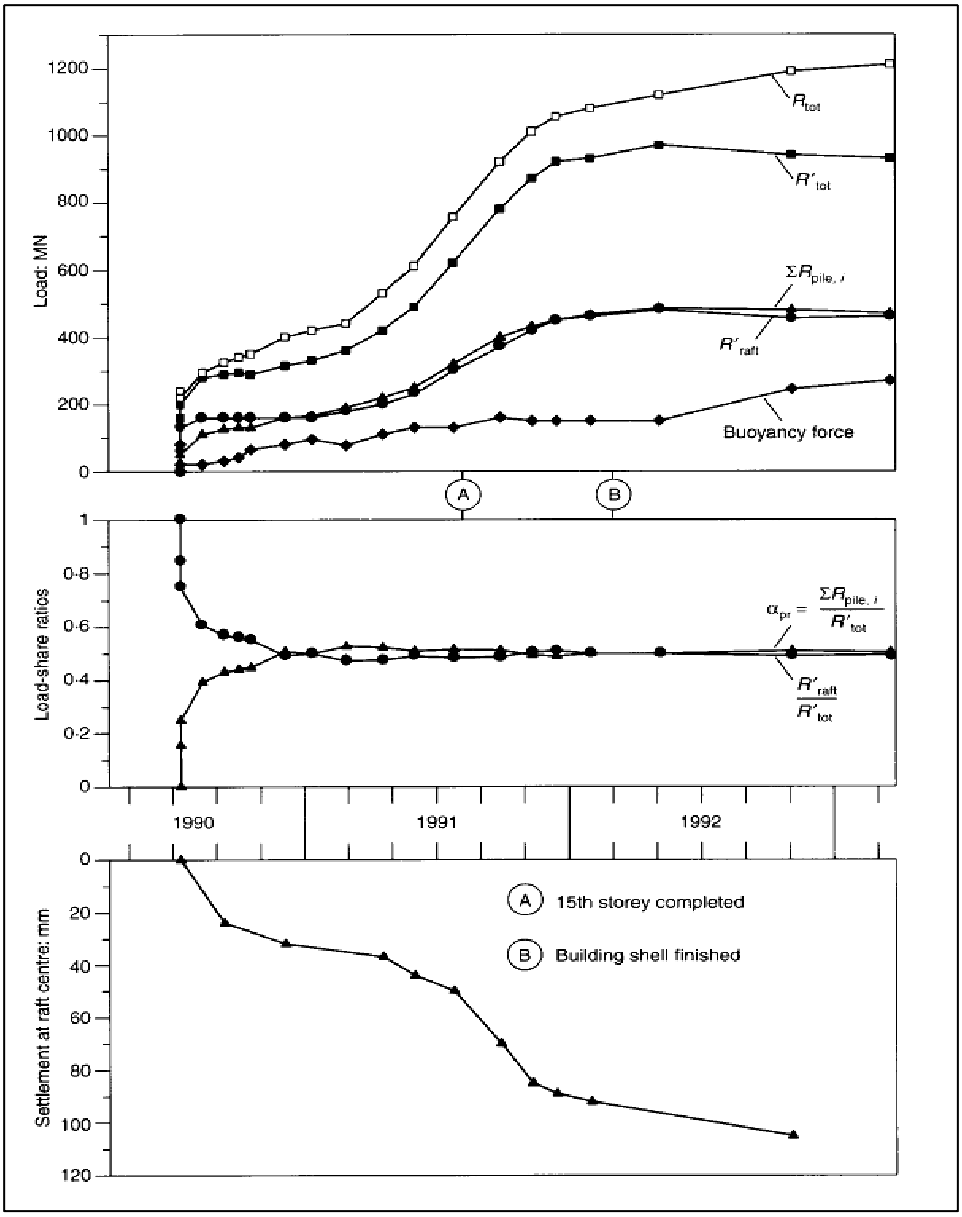

Figure 2.24 Variation of pile and raft resistance, load sharing ratio and settlement with time after Construction (Katzenbach et al., 2000)

According to Table 2.7 and Figure 2.24, 50% of structural load is carried by the raft and pile loads are in a range of 9.2 and 14.9 MN depending on pile's location. Observed maximum settlement is about 110 mm.

A study performed by Poulos (2000), he investigated the Westend Tower Building using different analysis techniques and obtained results were compared by each other and measurement data. Used analysis techniques are: 3D Finite Element Method (Ta & Small, 1996), approximate "plate on springs" method named as "GARP" (Poulos, 1994), approximate "strip on springs" method named as "GASP" (Poulos, 1991), two different simplified methods which were already introduced in the previous sections (Poulos & Davis, 1980) and (Randolph, 1994), Poulos also used two different hybrid methods by Sinha (1997) and Franke et al. (1994). Obtained results are shown in the Figure 2.25:

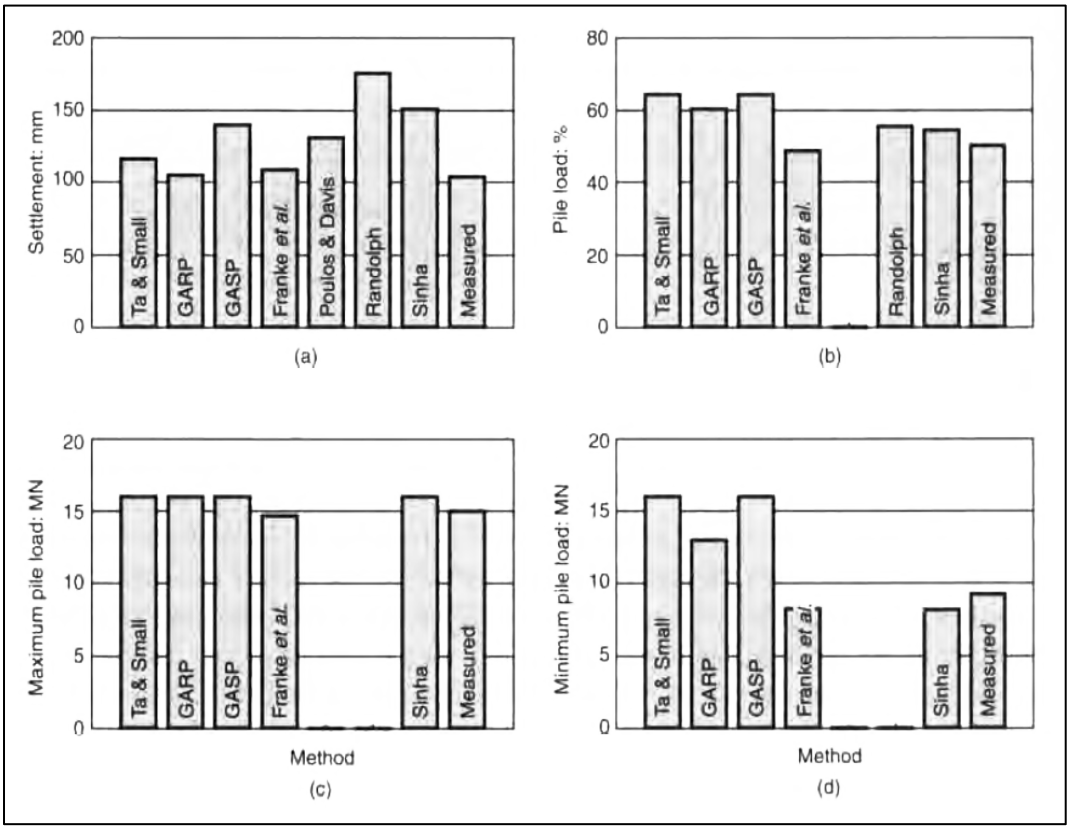

Figure 2.25 Comparison of different analysis techniques results for the Westend Tower Building: a) Settlement, b) Load carrying ratio, c) Maximum pile load, d) Minimum pile load (Poulos, 2000)

When Figure 2.25 is examined, it can be said that different analysis techniques are generally in good agreement with each other as well as with observed values. Only there is a deviation from measured results for the minimum pile loads.

Load carrying function of the raft is clearly seen again in this application example. Proportion of the load carried by the raft is relatively high in this case study and this situation indicates that, the pile capacity is nearly fully mobilized. This situation can be seen in the Figure 2.26:

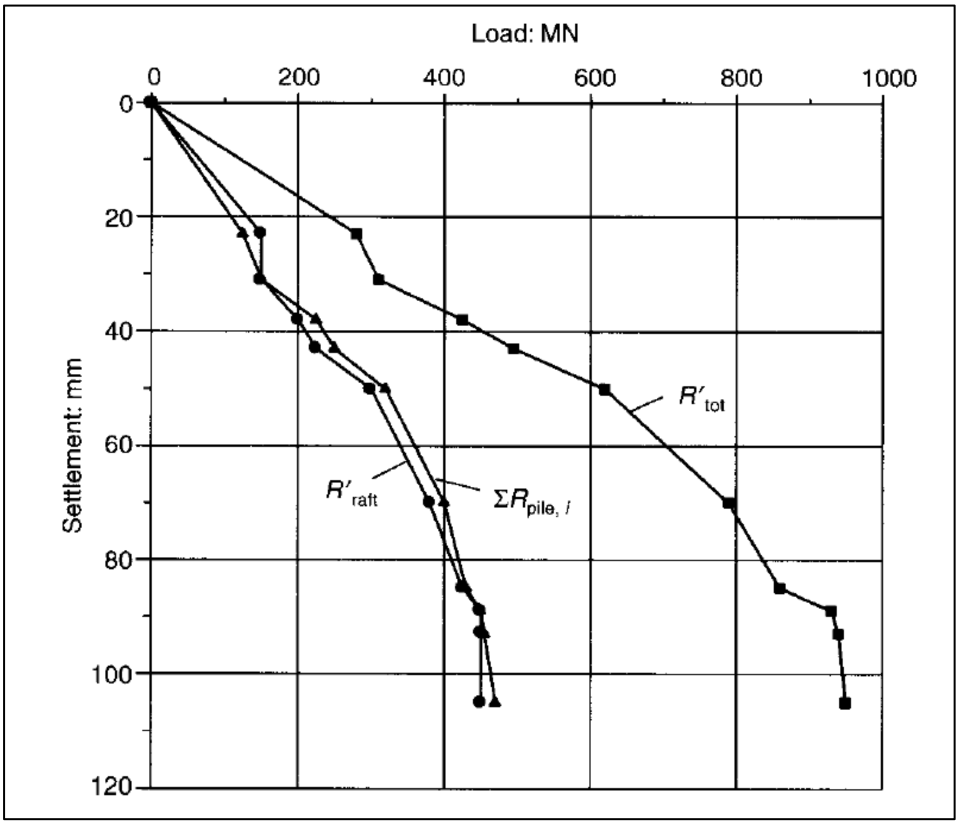

Figure 2.26 Observed load-settlement behaviour of raft, piles and total foundation system of Westend Tower Building (Katzenbach et al., 2000)

In Figure 2.26, if $\Sigma R_{pile,i}$ curve is investigated it is seen that slope of the curve is getting lower and lower by increasing load and slope is almost zero at the design load. So, piles are fully mobilized and it can be said that the foundation design of the Westend Tower Building is similar to “piles are settlement reducers” approach. This situation was also reported by Poulos (2000).

In addition, in this application example, the main settlement reducing function of piled raft foundation was also observed by performing complex geotechnical measurements. Franke et al. (2000) has defined the concept of "*normalized stress*" which can be defined as the ratio between vertical stress increase and vertical effective stress in the initial state and "*normalized stress*" contours were generated for piled raft and only raft options (Figure 2.27).

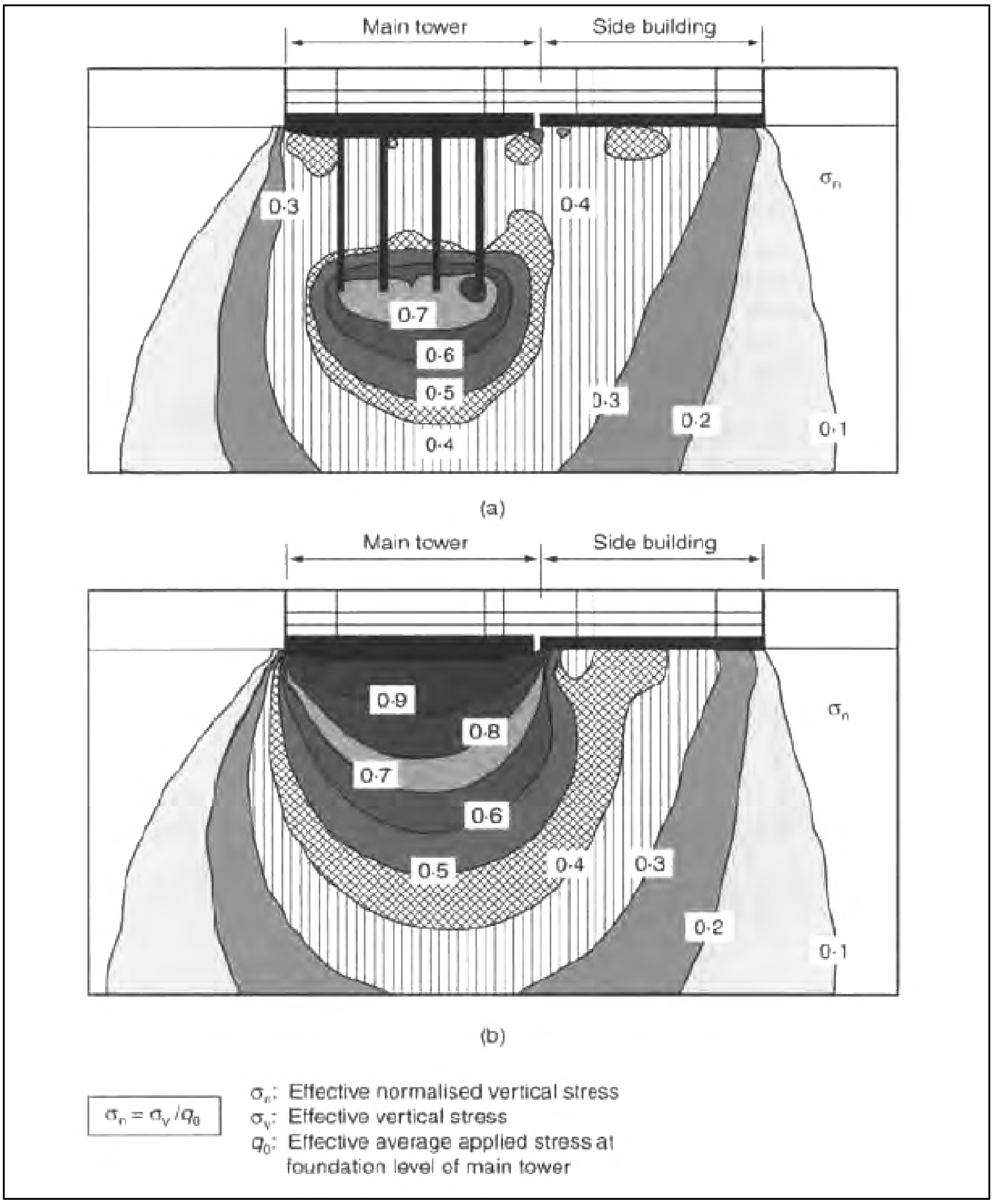

Figure 2.27 Normalized stress contours for a) Piled raft b) Only raft options in Westend Tower Building (Franke et al., 2000)

It is seen in Figure 2.27 (a) that the structural loads are transmitted to deep and stiffer soils by piled raft and this stress regulation reduce of settlement.

2.3.5.3 The Brooklyner Building (Khoury et al., 2011)

The Brooklyner is one of the tallest buildings in New York and it is the first piled raft foundation application in New York City. The Brooklyner Building has a height of 155 m with 51 storeys. Foundation area of the building is approximately 1400 m^2. Total foundation weight of the structure (G+Q) is about 850 MN and average transmitted net pressure to the soil is 625 kN/m^2. Due to existence of shear walls, local high stress points on the foundation plan are present. At that high stress points, foundation contact pressure can exceed 1000 kN/m^2.

Soil profile under Brooklyner Building consists of very dense glacial sands (SP-SM). This thick sand layer stays below an approximately 3 m thick fill layer. Groundwater table is 10 m below the ground surface. Foundation plan, variation of SPT N_{60} blow counts with depth and soil properties site are represented in Figures 2.28, Figure 2.29 and Table 2.8, respectively:

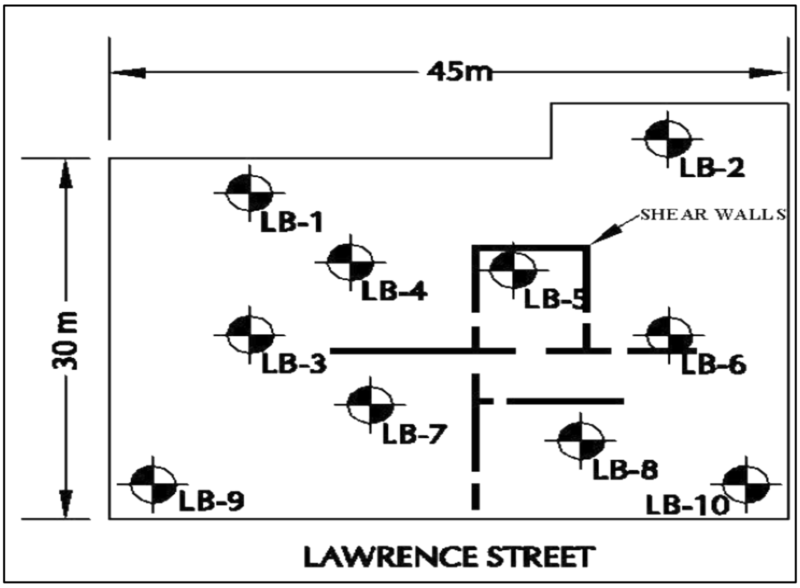

Figure 2.28 Boring location plan of the Brooklyner (Khoury et al., 2011)

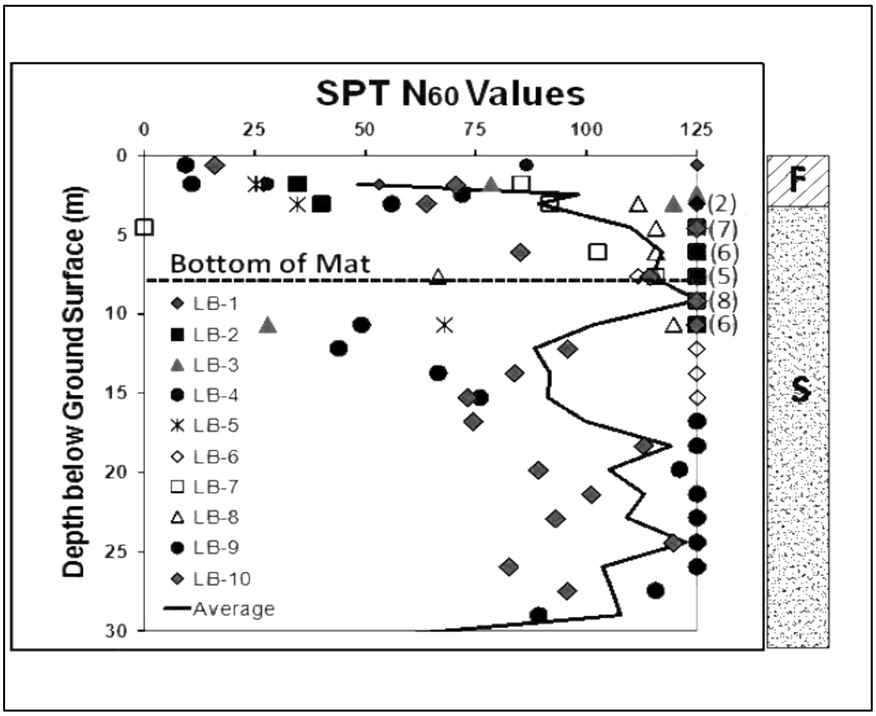

Figure 2.29 Variation of SPT N_{60} values with depth (Khoury et al., 2011)

Table 2.8 Soil properties at construction site (Khoury et al., 2011)

Soil Property	Fiil	Glacial Sand
Unit Weight, γ_n (kN/m^3)	17.5	19.5
Modulus of Elasticity, E (MPa)	24.0	167.5 – 282.5*
Poisson's Ratio, ν (-)	0.32	0.26
Drained Cohesion, c′ (kN/m^2)	1.0	1.0
Internal Friction Angle, φ′ (°)	30	40
Dilatancy Angle, ψ′ (°)	0.0	4.0

(*) Modulus of elasticity increasing with depth linearly

As it is seen in Figure 2.29 and Table 2.8, soil properties below the building is considerably good and only raft foundation case was considered as a first design approach in the foundation design.

In the design of the foundation of the building, first of all, only raft option was evaluated using the commercial finite element analysis software PLAXIS 2D and PLAXIS 3D Foundation. Calculations showed that high maximum and differential settlements would take place. Then, analyses were repeated for different raft thicknesses. Several runs were made and results are shown in Table 2.9. Settlement contours for the case where raft thickness was 1.8 m is given in the Figure 2.30:

Table 2.9 Obtained maximum settlement and angular distortion values for different raft thicknesses (Khoury et al., 2011)

Raft Thickness (m)	Maximum Settlement (cm)	Angular Distortion
1.20	7.50	1/260
1.50	7.00	1/315
1.80	6.50	1/350
2.10	6.00	1/400

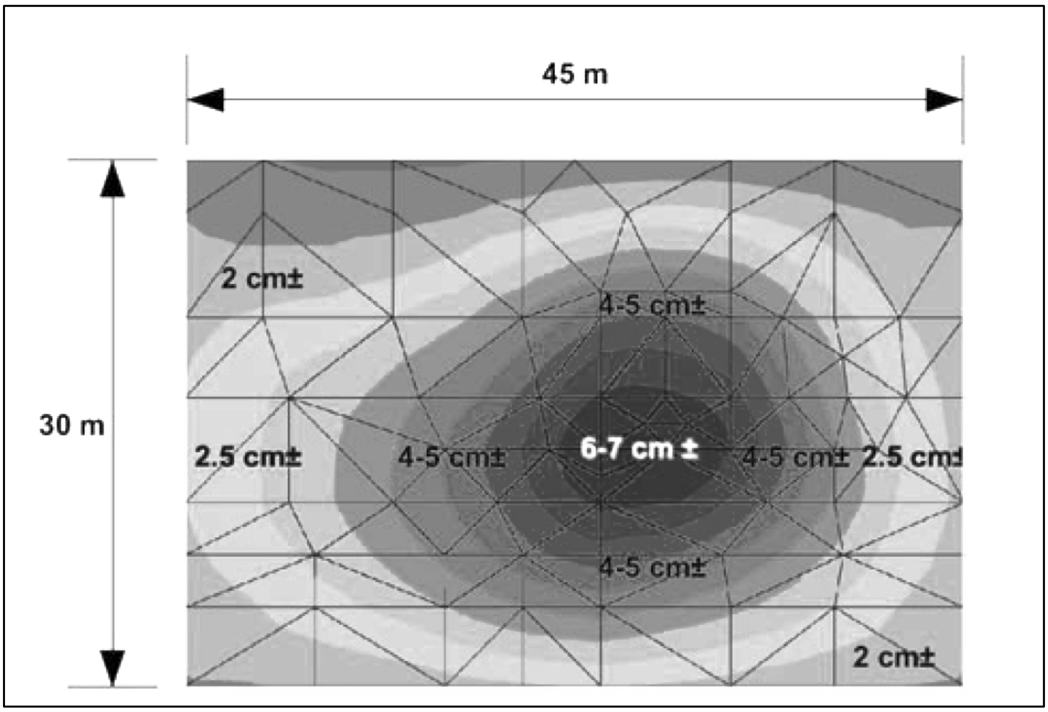

Figure 2.30 Settlement contours when raft thickness is 1.8 m (Khoury et al., 2011)

After the first step of calculations, designers clearly observed that, it was not possible to satisfy maximum settlement and angular distortion limit (in this application example 4 cm and 1/650 in order to avoid adjacent building damage) with only raft option. For that reason, "*piles are settlement reducers*" approach was selected. In order to determine the required number of piles at first stage, designers introduced "*block approach*" which can be defined as improved soil zone by settlement reducer piles and they obtained that "*soil block*" should have a modulus of elasticity value of approximately 1000 MPa. They found out that, with a "*soil block*" with modulus of elasticity value of 1000 MPa, maximum settlement and angular distortion values would have been diminished to 4 cm and 1/850, respectively, satisfying design requirements. This "*soil block*" approach is represented in Figure 2.31:

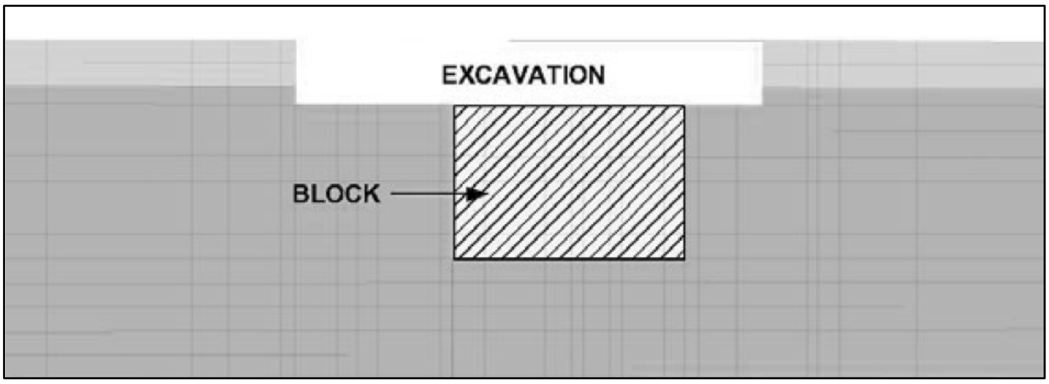

Figure 2.31 "*Soil Block*" Approach (Khoury et al., 2011)

Required number of piles which provide required stiffness increase of "*soil block*" was determined using the following equation:

$$N_p = \frac{E_b A_b - E_s A_s}{E_p A_p} \tag{2.51}$$

where;

N_p =Number of settlement reducer

E_b =Elasticity modulus of the "block"

E_s =Elasticity modulus of the soil

E_p =Elasticity modulus of the pile

A_b =Area of the "block"

A_p =Area of the individual settlement reducer (single pile)

A_s =Area of foundation (soil)

Using this approach, required numbers of piles was determined as 80. Pile type was considered as micro pile with a diameter and length of 0.35 m and 7.50 m, respectively.

Soil properties at the construction site were calibrated after load test results by simulating the pile load test in the PLAXIS 3D Foundation software. Pile load tests were performed at two different pile lengths (SR-1 represents 12 m pile length and SR-2 stands for 7.50 m). In the construction, L=7.50 m piles were selected due to pile installation difficulties. Pile load test results and result of PLAXIS analyses for the test piles are given in Figure 2.32:

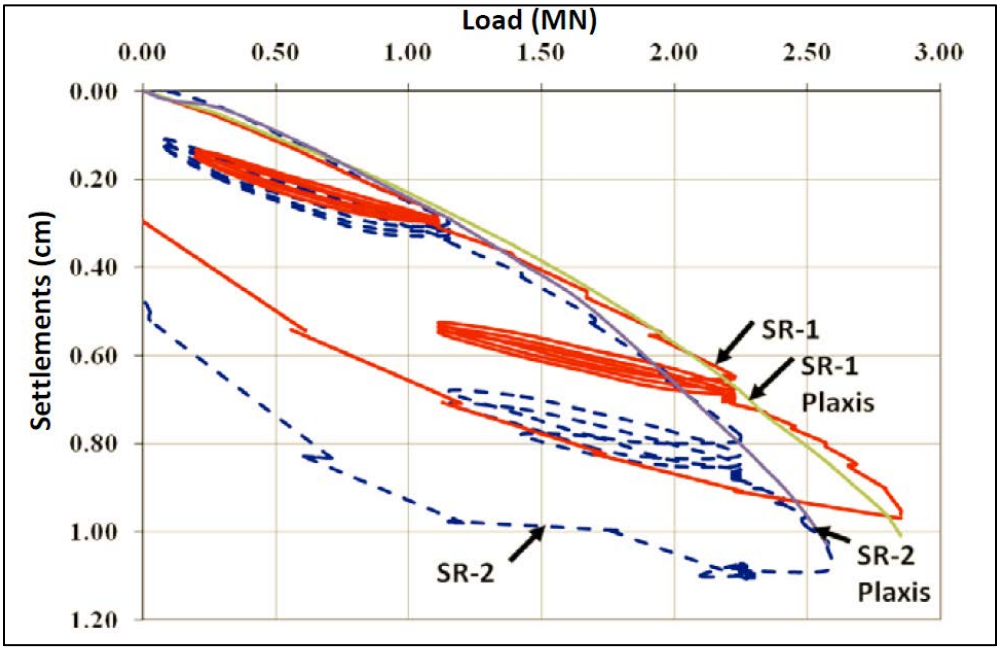

Figure 2.32 Pile load test results and calibration curves (Khoury et al., 2011)

Calibrated soil properties at the construction site after the load test results are given in Table 2.9:

Table 2.9 Calibrated soil properties at the construction site (Khoury et al., 2011)

Soil Property	Fill	Glacial Sand
Unit Weight, γ_n (kN/m^3)	17.5	19.5
Modulus of Elasticity, E (MPa)	24.0	**275 – 375**[*]
Poisson's Ratio, ν (-)	0.32	0.26
Drained Cohesion, c′ (kN/m^2)	1.0	1.0
Internal Friction Angle, φ′ (°)	30	40
Dilatancy Angle, ψ′ (°)	0.0	4.0

(*) Modulus of elasticity increasing with depth linearly

Final piled raft foundation design was performed by creating pile layout and PLAXIS 3D (Finite Element Method) calculations. In the pile layout, 72 micro piles were placed into center of the foundation and 11 micro piles were placed at two edges of the raft. Final pile arrangement and settlement contours in piled raft option are given in Figures 2.33 and Figure 2.34, respectively:

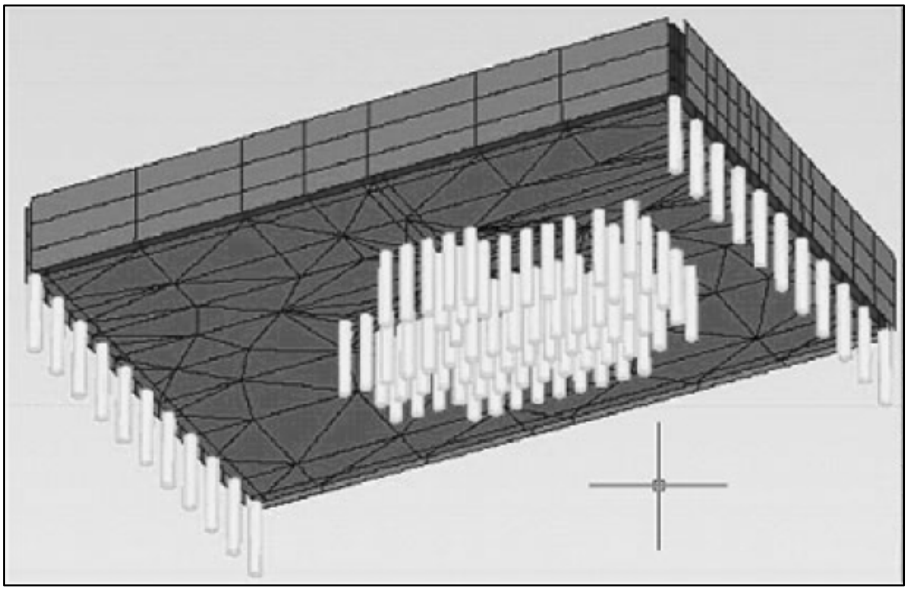

Figure 2.33 Final pile arrangement (Khoury et al., 2011)

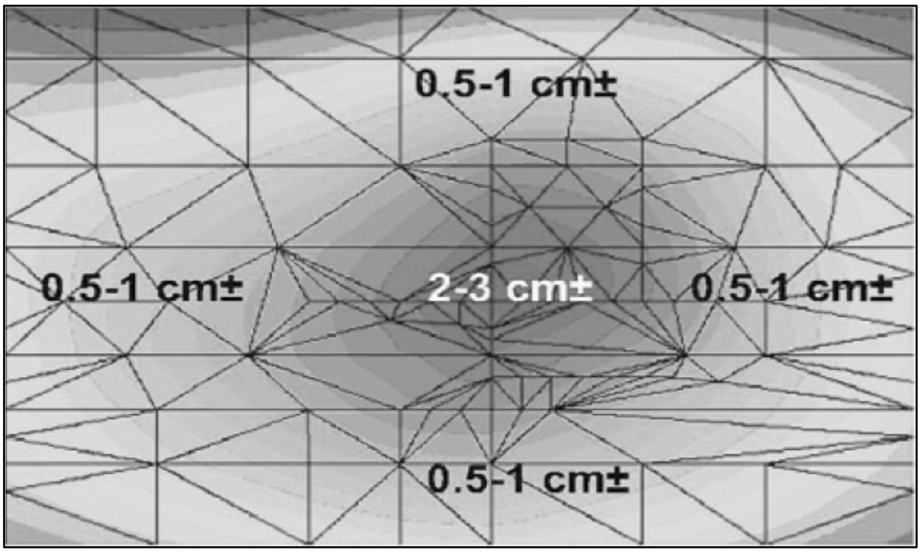

Figure 2.34 Settlement contours for piled raft option (Khoury et al., 2011)

After the construction of the building, settlement of the foundation was observed continuously. Comparison of the calculation results and observed settlement data are shown in Figure 2.35. Note that, observed settlement values were obtained under the only static (G+Q) loads.

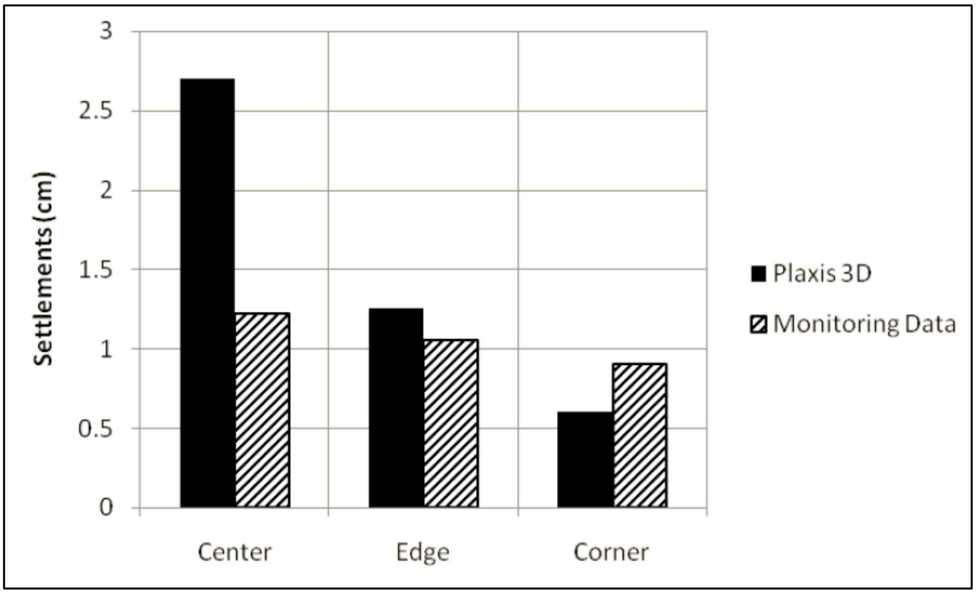

Figure 2.35 Comparison between calculated and observed foundation settlement (Khoury et al., 2011)

If additional settlement due to live load is considered, it can be said that calculated and observed values are in good agreement.

In summary, The Brooklyner Building is a very good example to "*piles are settlement reducers*" approach of piled raft foundation design. Excessive maximum and differential settlements were reduced using piles. In addition, piled raft foundation approach has provided economy in the foundation design. Designers have reported that if the raft's load carrying contribution was ignored, approximately 250 piles would have been necessary. This statement clearly shows the superiority of the piled raft approach over the conventional pile foundation approach.

2.3.6 Estimation of the Raft and the Pile Stiffness

In order to perform the piled raft analysis, estimation of the initial axial stiffnesses of the raft and the pile is required especially while using simplified methods. There are several approaches available in the literature to estimate such stiffnesses.

Poulos & Davis (1974) developed a simple solution for response of the loaded circular rafts in elastic half space. Axial stiffness of raft can be calculated using this tool. In this technique, equivalent radius of the raft can be used for non-circular foundations. General concept of this solution is given is Figure 2.36:

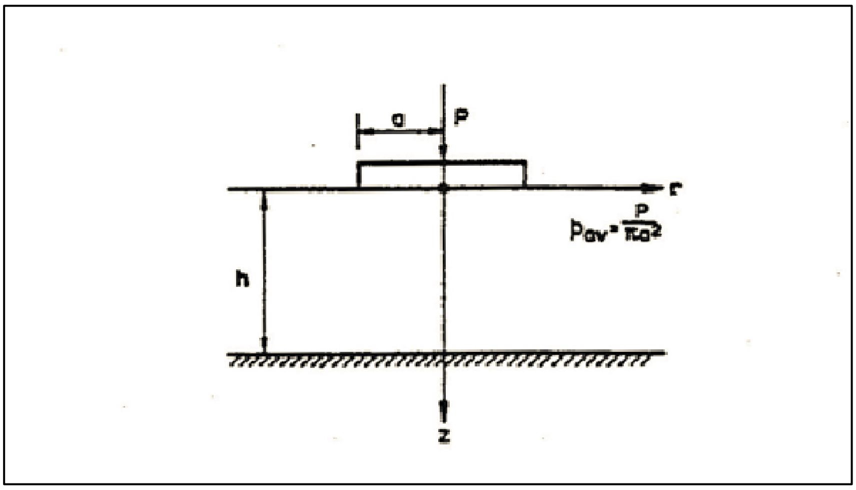

Figure 2.36 General concept of solution (Poulos & Davis, 1974)

Axial stiffness of the raft can be calculated using following equation:

$$K_r = \frac{P}{\rho_z} \tag{2.52}$$

where;
$K_r =$ Axial stiffness of the raft
$P =$ Applied vertical load on the raft
$\rho_z =$ Vertical displacement of the raft

Vertical displacement of the raft (ρ_z) is obtained as shown below:

$$\rho_z = \frac{P_{av} a}{E_s} I_p \tag{2.53}$$

where;

$P_{av} =$ Average stress on the raft

$$P_{av} = \frac{P}{\pi a^2}$$

$a =$ Equivalent radius of the raft

$E_s =$ Elasticity modulus of the soil

$I_p =$ Influence factor

The following chart as a function of Poisson's ratio (ν) and h/a ratio (h represents thickness of compressible soil layer, see Figure 2.36) may be used to obtain the influence factor for vertical displacement calculation:

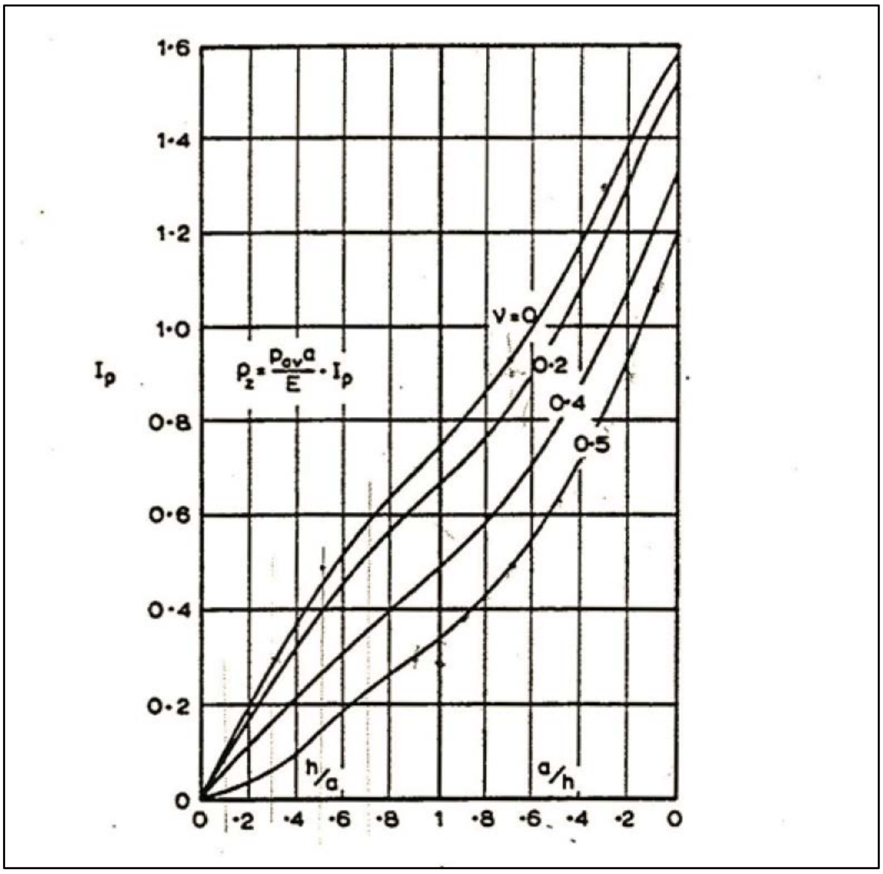

Figure 2.37 Influence factors for vertical displacement of rigid circle (Poulos & Davis, 1974)

Another raft stiffness estimation approach is proposed in FEMA 356 (2000). This calculation method is suitable for embedded rafts which are encountered frequently in real life applications. Formulation of this approach is given as shown:

$$K_{emb} = K_{z,sur} * \beta_z$$

$$K_{z,sur} = \frac{GB}{1-\nu}\left[1.55\left(\frac{L}{B}\right)^{0.75} + 0.80\right] \tag{2.54}$$

$$\beta_z = \left[1 + \frac{1}{21}\frac{D}{B}\left(2 + 2.6\frac{B}{L}\right)\right]\left[1 + 0.32\left(\frac{d(B+L)}{BL}\right)^{2/3}\right]$$

where ;

K_{emb} = Embedded raft's axial stiffness

$K_{z,sur}$ = Axial stiffness of raft which placing on the surface

β_z = Axial stiffness correction factor for embedded rafts

G = Shear modulus of soil below the raft

ν = Poisson's ratio of soil

L, B = Length and width of rafts, respectively

d = Actual embedded depth of raft (if basement floor exists d=D)

D = Depth of raft

There are numerous methods to estimate the pile stiffness just like for the rafts. Sanchez-Salinero (1982) listed different single pile axial stiffness formulations from different researchers in his study. Some of such equations are listed below:

$$k_p = 0.56\frac{E_p A_p}{R}\left(\frac{E_s}{E_p}\right)^{0.50} \quad \text{(Winkler)} \tag{2.55}$$

$$k_p = 0.69\frac{E_p A_p}{R}\left(\frac{E_s}{E_p}\right)^{0.61} \quad \text{(Poulos)} \tag{2.56}$$

$$k_p = 0.79\frac{E_p A_p}{R}\left(\frac{E_s}{E_p}\right)^{0.60} \quad \text{(Blaney)} \tag{2.57}$$

where ;
k_p = Axial stiffness of the single pile
E_p = Modulus of elasticity of pile
E_s = Modulus of elasticity of the soil
A_p = Cross-sectional area of the pile
R = Radius of the pile

A different calculation tool for estimating single pile axial stiffness was developed by Randolph (1994). In this calculation tool, variation of the pile section and shear modulus of soil along the pile, pile-soil stiffness ratio, maximum radius of influence and pile compressibility are considered. This calculation tool is given in Equation 2.58:

$$k_p = \frac{P_t}{w_t} = \frac{\dfrac{4\eta}{(1-\nu)\xi} + \rho\dfrac{2\pi}{\zeta}\dfrac{\tanh(\mu l)}{\mu l}\dfrac{l}{r_0}}{1+\dfrac{1}{\pi\lambda}\dfrac{4\eta}{(1-\nu)\xi}\dfrac{\tanh(\mu l)}{\mu l}\dfrac{l}{r_0}} * (G_l r_0) \tag{2.58}$$

with

$$\begin{aligned}
&\eta = r_b / r_0 \\
&\xi = G_l / G_b \\
&\rho = G_{avg} / G_l \\
&\lambda = E_p / G_l \\
&\zeta = \ln(r_m / r_0) \\
&r_m = \left\{0.25 + \xi\left[2.5\rho(1-\nu) - 0.25\right]\right\} l \\
&\mu l = \sqrt{\frac{2}{\zeta\lambda(l / r_0)}}
\end{aligned} \tag{2.59}$$

where;
k_p =Axial stiffness of the pile
P_t =Applied load on the pile
l =Pile length
G_l =Shear modulus of soil at depth of l
r_o =Pile radius

w_t =Settlement of the pile
r_b =Pile radius at the base of the pile
G_b =Shear modulus of the soil at depth of the pile base
G_{avg} =Average shear modulus of the soil along the pile
E_p =Elasticity modulus of the pile
r_m =Maximum radius of influence

Different single pile axial stiffness estimation techniques are introduced above. However, pile group stiffness is used in the calculations. Pile group stiffness is always lower than the stiffness value that is obtained from adding single pile stiffness values in the group. This concept was introduced and formulated by Randolph (1994). According to pile group efficiency concept, pile group stiffness is calculated as shown below:

$$K_p = k_p * n^{1-e} \tag{2.60}$$

where ;
K_p = Pile group stifness
k_p = Single pile stiffness
n = Number of pile in the pile group
e = Group efficiency exponent

$$e = e_1 * c_1 * c_2 * c_3 * c_4 \tag{2.61}$$

where ;
e_1 = Initial group efficiency exponent depend on slenderness ratio
c_1 = Exponent correction factor depend on stiffness ratio
c_2 = Exponent correction factor depend on pile spacing
c_3 = Exponent correction factor depend on homogenity
c_4 = Exponent correction factor depend on Poisson's ratio

Exponent coefficient factors are given in Figures 2.38 and 2.38, respectively:

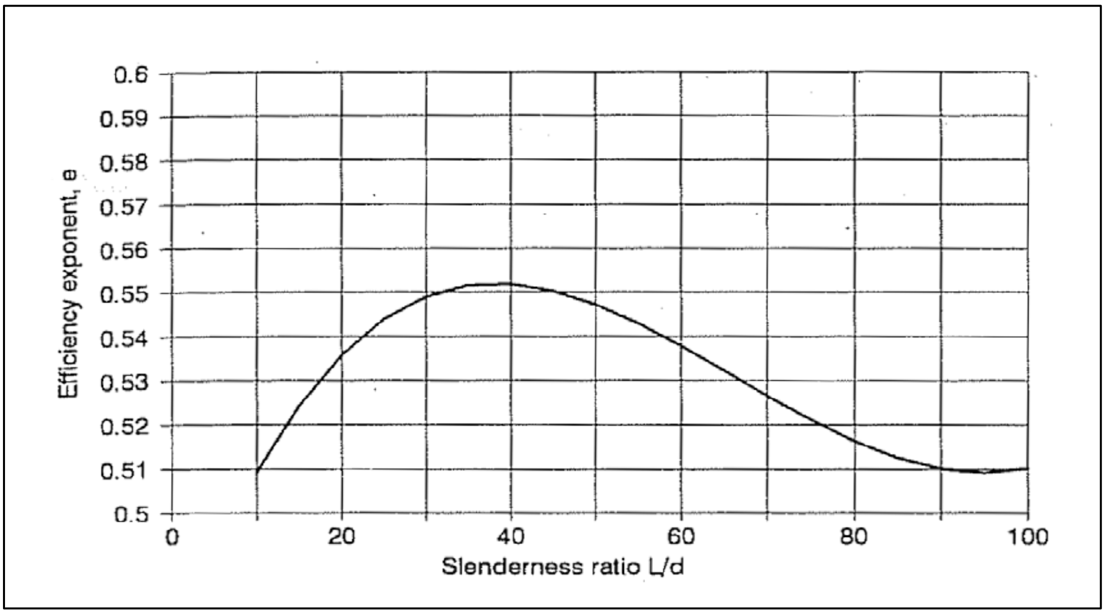

Figure 2.38 Efficiency exponent for pile group stiffness (Randolph, 1994)

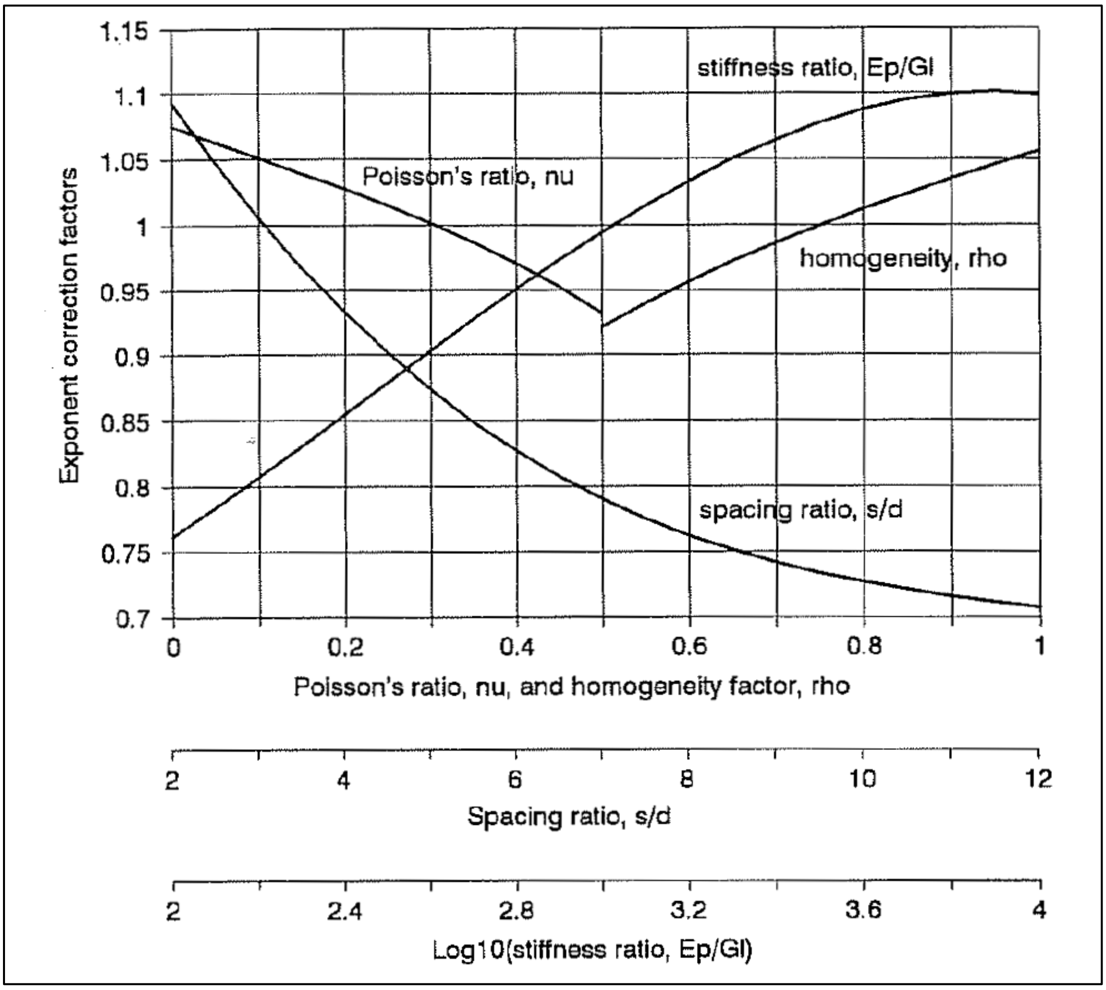

Figure 2.39 Exponent correction factors (Randolph, 1994)

In addition to the above mentioned pile group stiffness calculation method, Poulos (2000) stated a simple approximate approach. This approach is given below:

$$K_p = k_p * \sqrt{n} \tag{2.62}$$

where ;
K_p = Pile group stifness
k_p = Single pile stiffness
n = Number of pile in the pile group

CHAPTER THREE
A PILED RAFT EXAMPLE

3.1 Introduction

This chapter is written with the intention of demonstrating the usage of piled raft analysis techniques which were introduced in the previous chapter. For this purpose; a simple example is created and already explained simplified piled raft analysis techniques are applied on the problem. In addition to such techniques, same problem is handled using commercial computer programs (SAP 2000 and PLAXIS 3D) which are based on the Finite Element Method (FEM) and obtained results have compared. Examination of the results proves that simplified analysis methods yield reasonable solutions as compared with the rigorous solution techniques.

3.2 Definition of Example

The problem mainly consists of 3 x 3 pile group with a single concentric load. Geometry of the problem, soil and pile properties are given in the Figures 3.1 and 3.2 including pile layout and sections

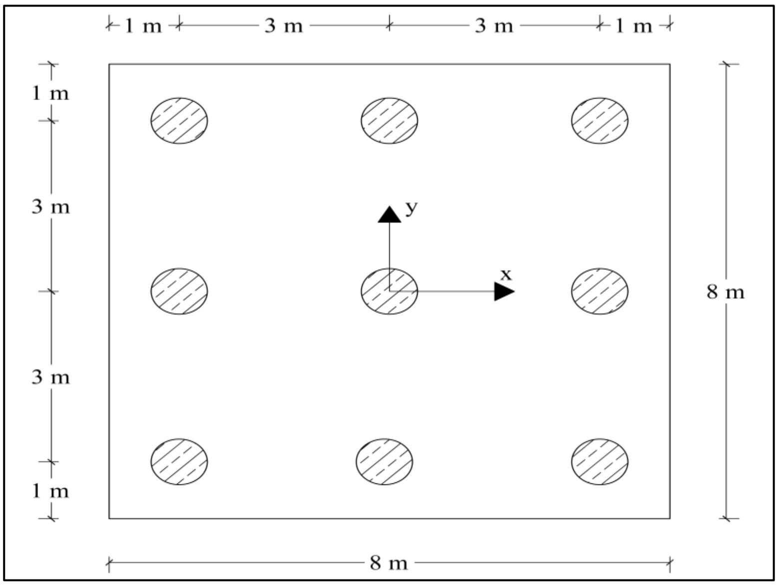

Figure 3.1 Pile layout of problem

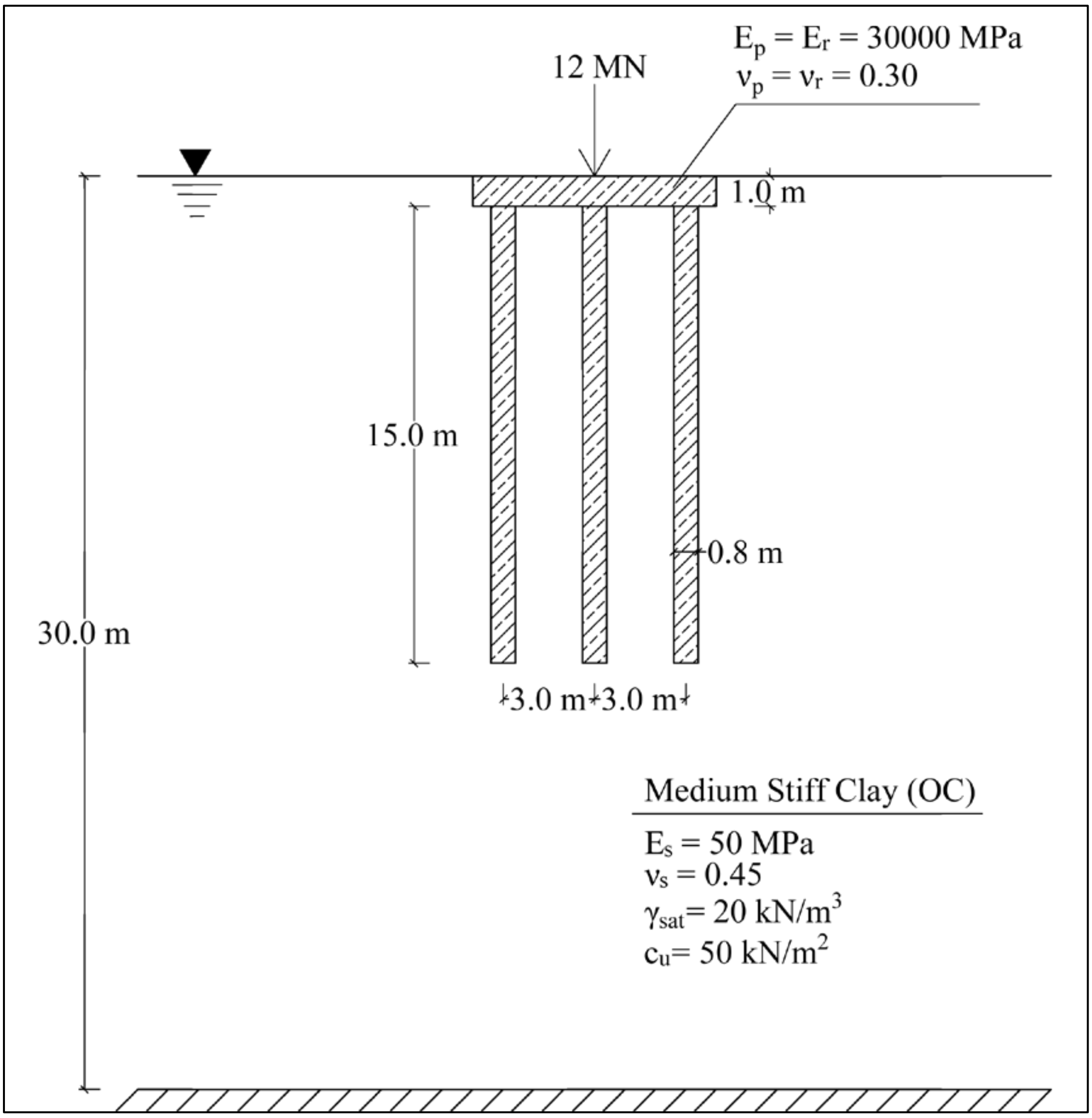

Figure 3.2 Section view and material properties of problem

In order to represent the soil in the analysis, the linear elastic material model is used. However, in some analysis techniques, axial load capacity of pile and raft should be determined separately. For that reason, undrained shear strength (c_u) which is a strength parameter of Mohr-Coulomb (MC) Model is used. Value of c_u is simply estimated from $E_s = 1000c_u$ approach (Bowles, 1997).

Single pile stiffness of the system is calculated utilizing the single pile response to axial load (Randolph, 1994). Single pile stiffness is obtained as 441 MN/m. Pile group stiffness is determined as 1320 MN/m using pile group stiffness approximation in the literature (Poulos, 2000).

Axial raft stiffness is calculated by equivalent circular raft on elastic soil assumption and raft axial stiffness is obtained as 615 MN/m (Poulos & Davis, 1974). Details about the pile and raft stiffness calculations are given in the appendices.

3.3 Performed Calculations and Results

The example was solved using following analysis methods. Calculation details are given in the appendices.

- Randolph Method (Simplified)
- Poulos-Davis-Randolph Method (Simplified)
- Modified version of Poulos-Davis-Randolph Method (Simplified)
- Incremental Load Step Approach (Simplified)
- Plate on Springs Approach with SAP 2000 (Approximate)
- 2D Finite Element Method with SAP 2000 (Advanced)
- 3D Finite Element Method with SAP 2000 (Advanced)
- 3D Finite Element Method with PLAXIS 3D (Advanced)

3.3.1 Randolph Method

Calculation procedure of Randolph Method was explained in Section 2.3.4.1.2. This method yielded load carrying ratio of piles 87% and overall settlement of the foundation was found as 8.85 mm.

3.3.2 Poulos-Davis-Randolph (PDR) Method

In this analysis method, axial load capacity of the pile group is taken into account while obtaining settlement of the system. Pile group bearing capacity is estimated as 19875 kN. Following the calculations load sharing ratio and elastic settlement of the system were obtained as 72% and 7.23 mm, respectively.

3.3.3 Modified version of PDR Method

Non-linear behavior of the foundation system that depends on applied load can be investigated in this analysis method. According to analysis results, 82% of applied load is carried by piles and settlement of the system is 11.60 mm.

3.3.4 Incremental Load Step Approach

In this method, pile group and raft are considered separately and settlement calculations of pile group are performed using equivalent raft approach (Tomlinson & Woodward, 2008). Calculations are repeated with varying load level (defined portion of total load) on the raft and pile group (for details of calculation method, see Section 2.3.4.1.4). According to calculation results load carrying ratio is determined as 70% and elastic settlement of the system is 5.00 mm.

3.3.5 Plate on Spring Approach using SAP 2000

In this approach, a 1x1 grid system is created where soil and piles represented by equivalent springs. Such springs are placed nodes of the grid system. Thus, the raft is supported by equivalent soil and pile springs.

In order to determine equivalent soil springs, axial stiffness of the raft is used. Furthermore, equivalent soil spring stiffnesses are increased gradually from the center to the edges of raft obeying to zoning method. For this purpose, the raft area is divided into suitable sub-areas and stiffness values are assigned in increasing order from center to the edge. The average stiffness value for the soil can be calculated as shown below:

$$k_{s,mean} = \frac{K_r}{A_r} = \frac{615000}{64} \cong 9600 \text{ kN/m/m}^2 \equiv 9600 \text{ kN/m}^3 \tag{3.1}$$

where;
$k_{s,mean}$ = Average stiffness value for soil
K_r = Axial stiffness of raft
A_r = Area of raft

Physical meaning of $k_{s,\ mean}$ is equivalent axial stiffness of soil (spring stiffness) for a 1 m^2 influence area. Thus, $k_{s\ mean}$ value has a different physical meaning compared to subgrade modulus of soil. However, these quantities have same units and $k_{s,\ mean}$ value can be considered as subgrade modulus of soil. This value can be converted into spring constant by multiplying with the influence area. Increasing soil stiffness through the raft area is shown in the Figure 3.3.

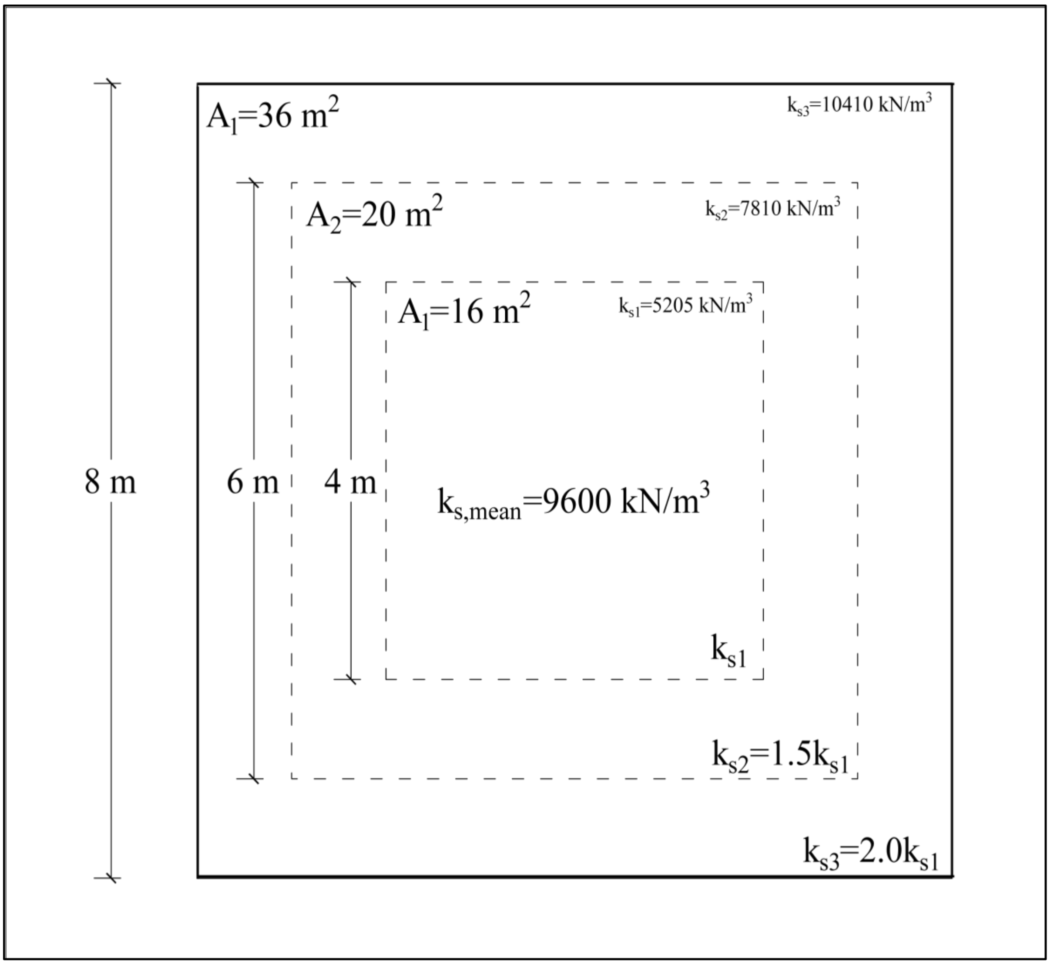

Figure 3. 3 Application of zoning method

Equivalent pile springs are determined considering pile group axial stiffness instead of single pile stiffnesses. For this purpose; equivalent pile stiffness is calculated by dividing pile group stiffness by number of piles in the pile group as shown below. Model geometry, soil and pile springs are shown in Figure 3.4.

$$k_{eq,pile} = \frac{K_{pile\ \mathrm{group}}}{n} = \frac{1320}{9} = 146.7\ \mathrm{MN/m} \tag{3.2}$$

where;

$k_{eq,pile}$ = Equivalent pile stiffnes

$K_{pile\ \mathrm{group}}$ = Pile group stiffness

n = Number of piles in the pile group

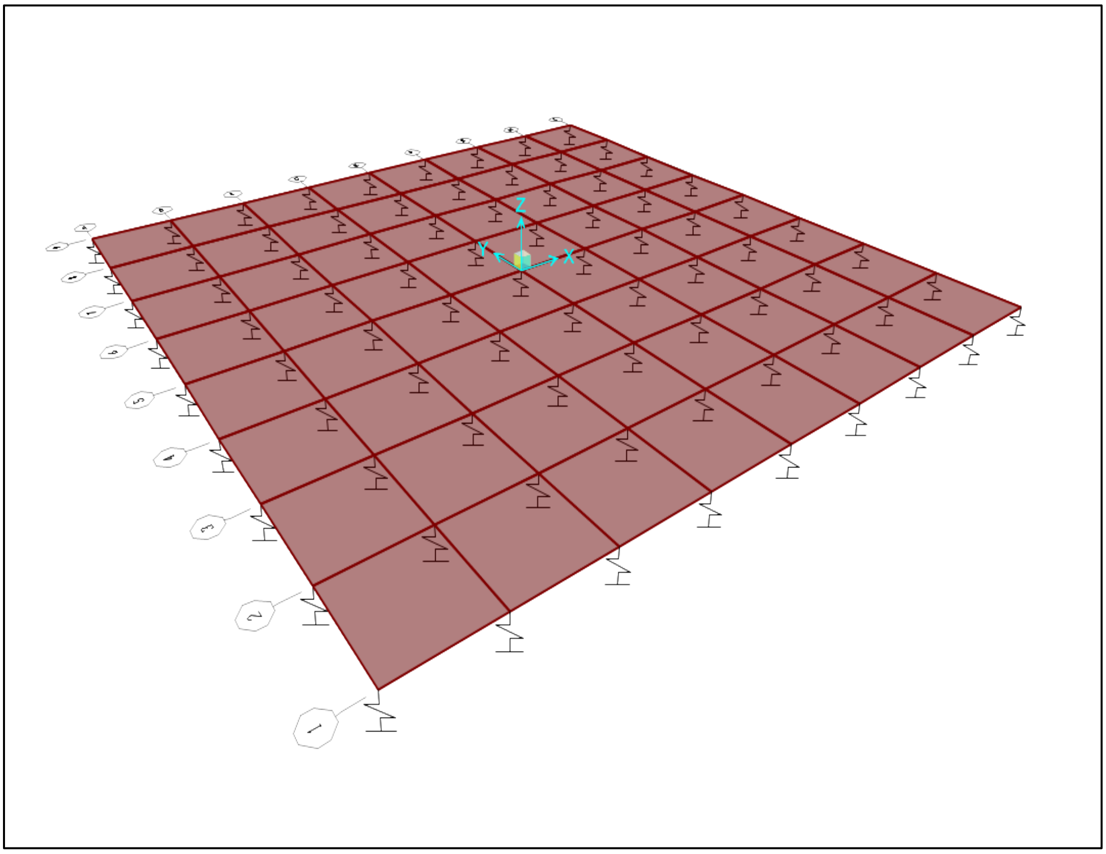

Figure 3.4 Model geometry and presentation of soil and pile springs

It is obtained that load sharing ratio is 75% and maximum settlement is 9.5 mm. Settlement contours of the raft is given in the Figure 3.5.

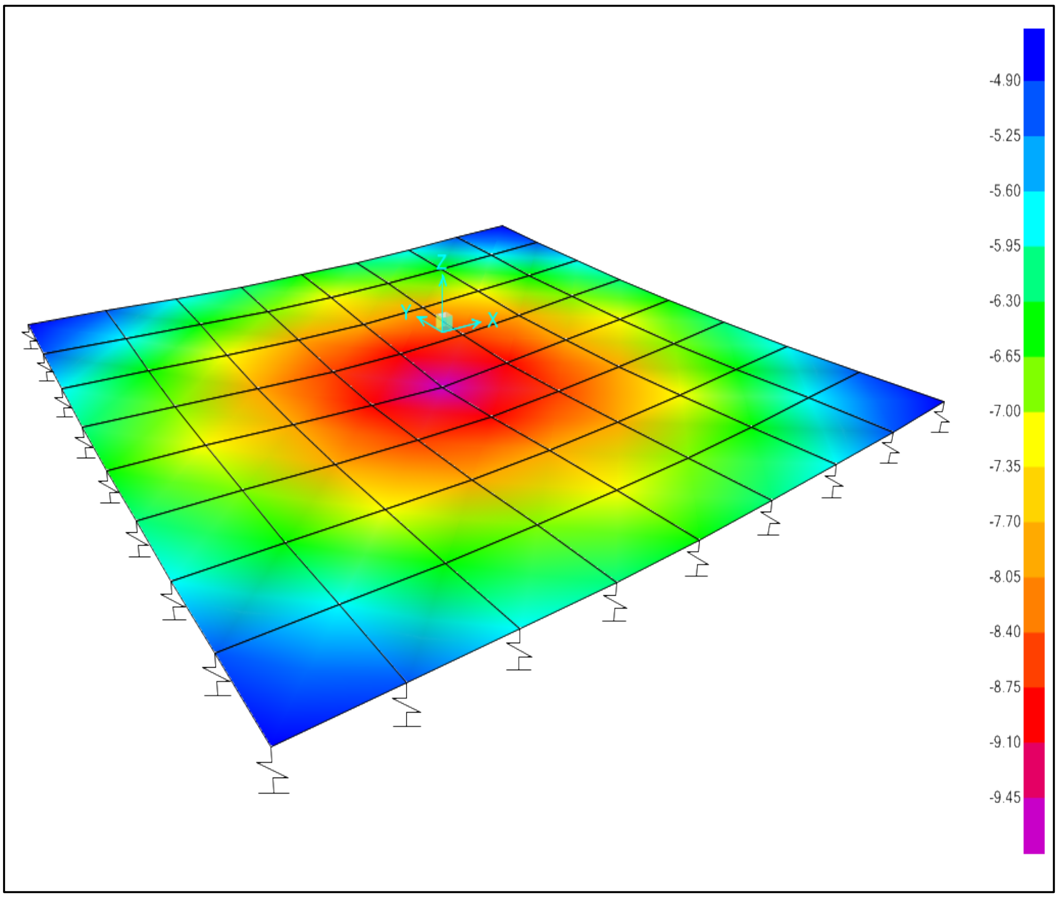

Figure 3.5 Settlement contours of raft (Units are mm)

3.3.6 2D Finite Element Method using SAP 2000

In this analysis method, problem is considered as 2D plain-strain model which can be applied to the soil problems. Soil, raft and piles are modeled as plate elements. Model dimensions are 40 m x 30 m. In order to increase the resolution of the calculations, smaller plate elements are used around the piles and the raft. Load sharing ratio could not be determined in this model because of model restrictions. Maximum settlement is obtained as 9.75 mm. General view of the analysis model and settlement contours of the system are shown in the Figures 3.6 and 3.7, respectively.

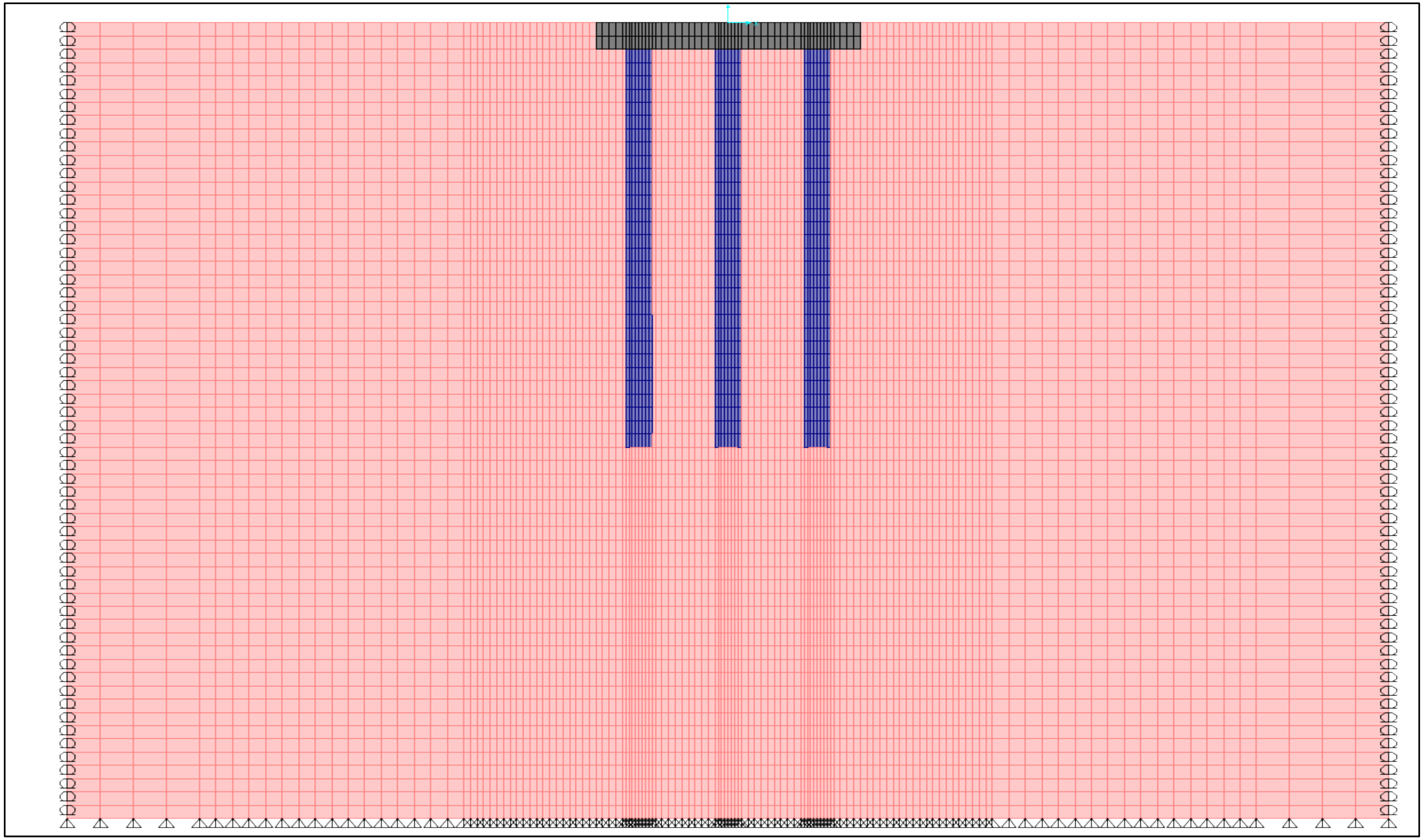

Figure 3.6 General view of analysis model

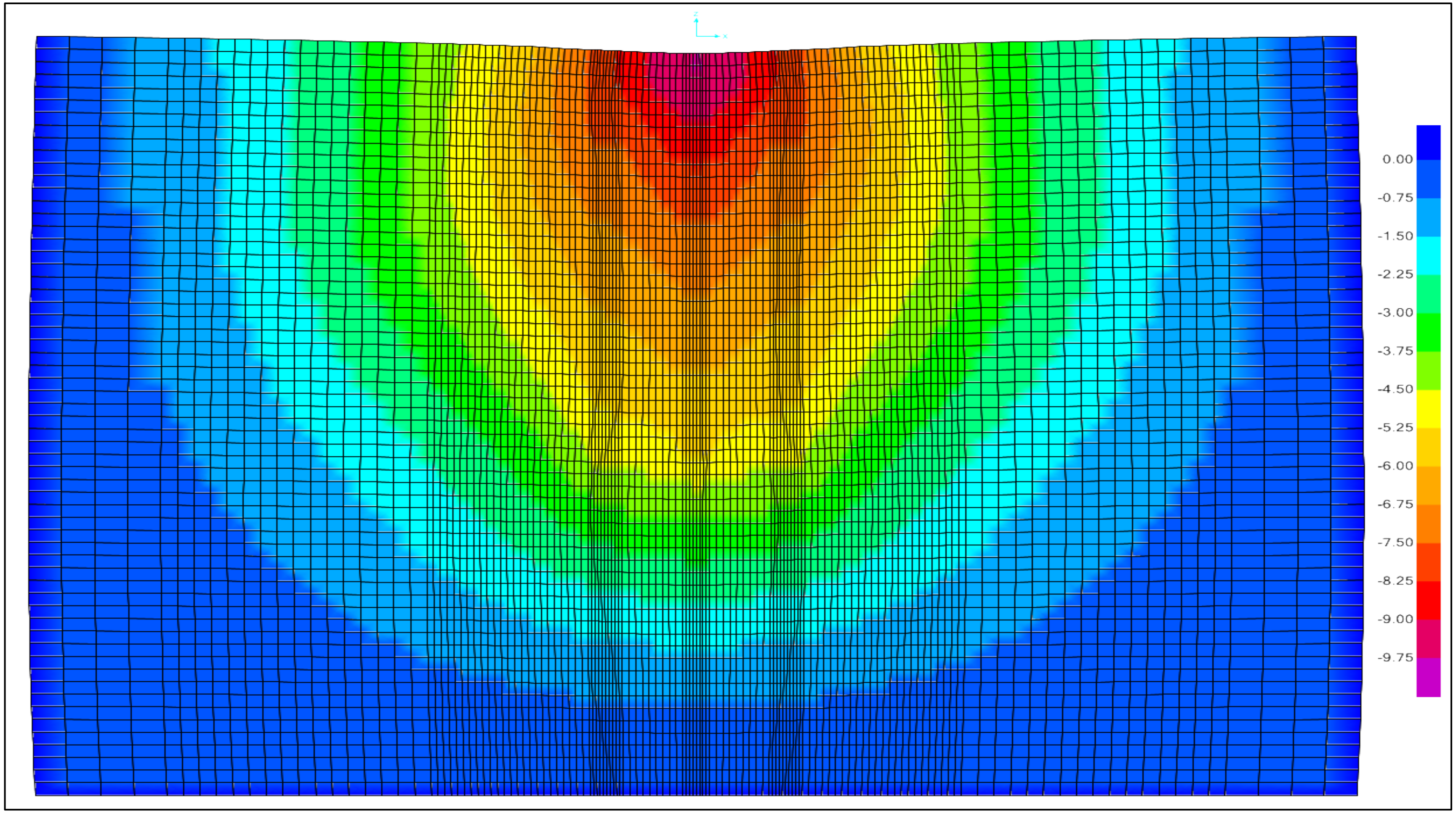

Figure 3.7 Settlement contours of the system (Units are mm)

3.3.7 3D Finite Element Method using SAP 2000

In this model, soil raft and piles are modeled using solid elements in SAP 2000 program. Solid elements are characterized by elastic parameters (E, ν). Model dimensions are 20 m x 20 m x 30 m. General view of the model is given in the Figure 3.8.

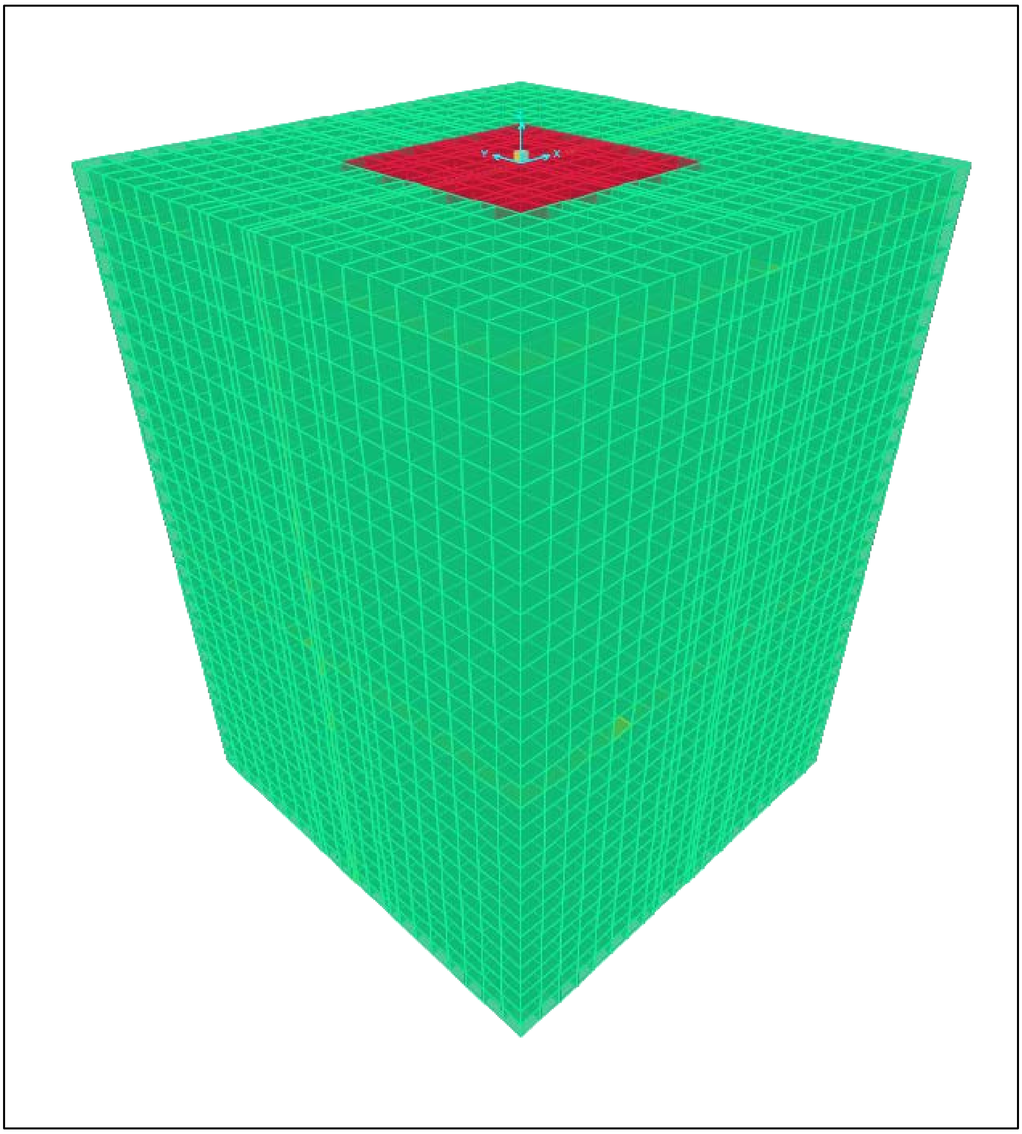

Figure 3.8 General view of analysis model

After the analysis, in order to obtain settlement values of desired sections, very thin (1 mm) which will not affect the results shell elements are defined at the y = 0 and z = -1 planes.

Load sharing ratio between the piles and the raft could not be determined due to model restrictions. Settlement of the system is obtained as 9.00 mm. Settlement contours at y = 0 and z = -1 planes are shown in Figures 3.9 and 3.10, respectively.

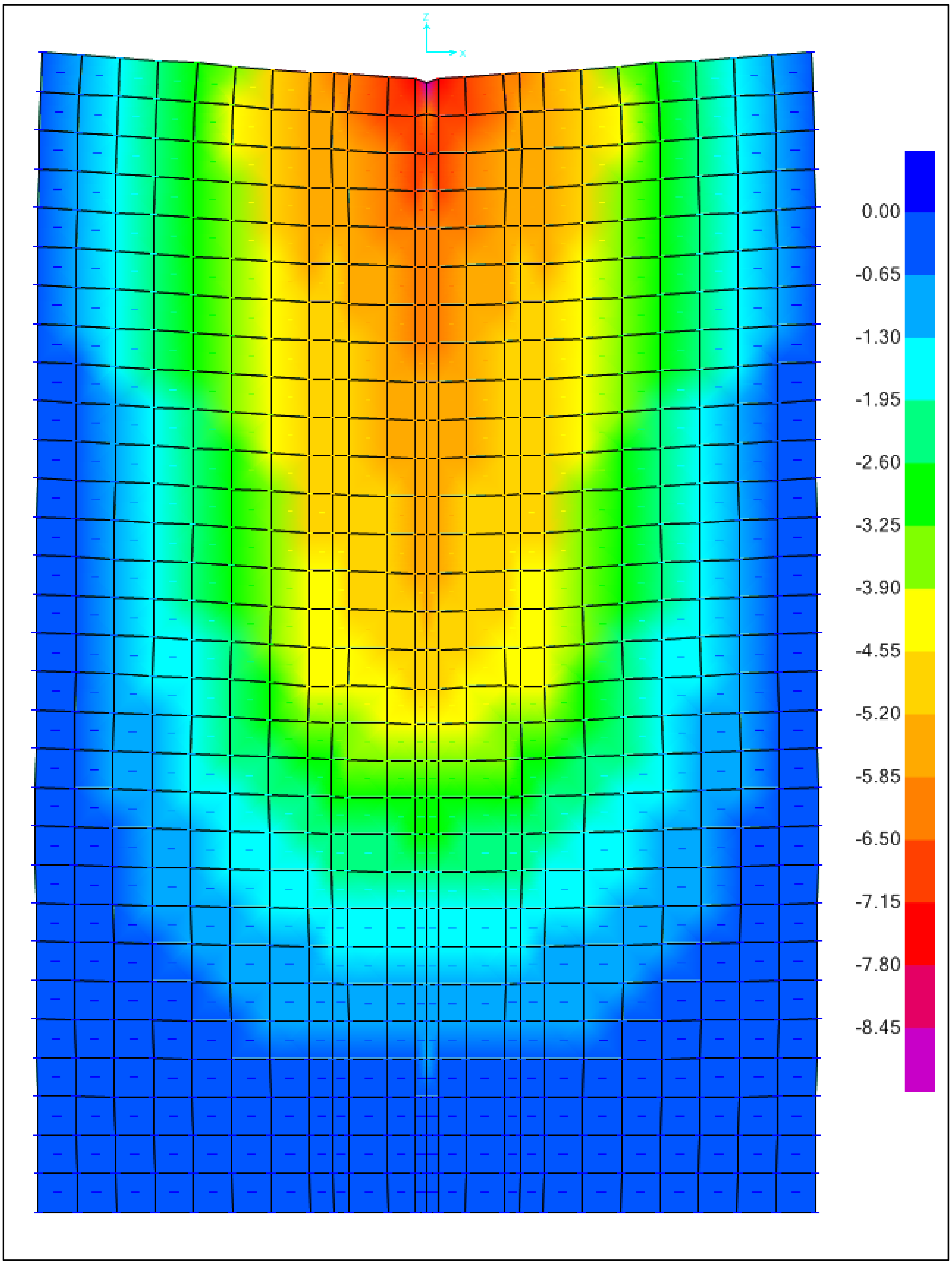

Figure 3.9 Settlement contours at y = 0 plane (Units are mm)

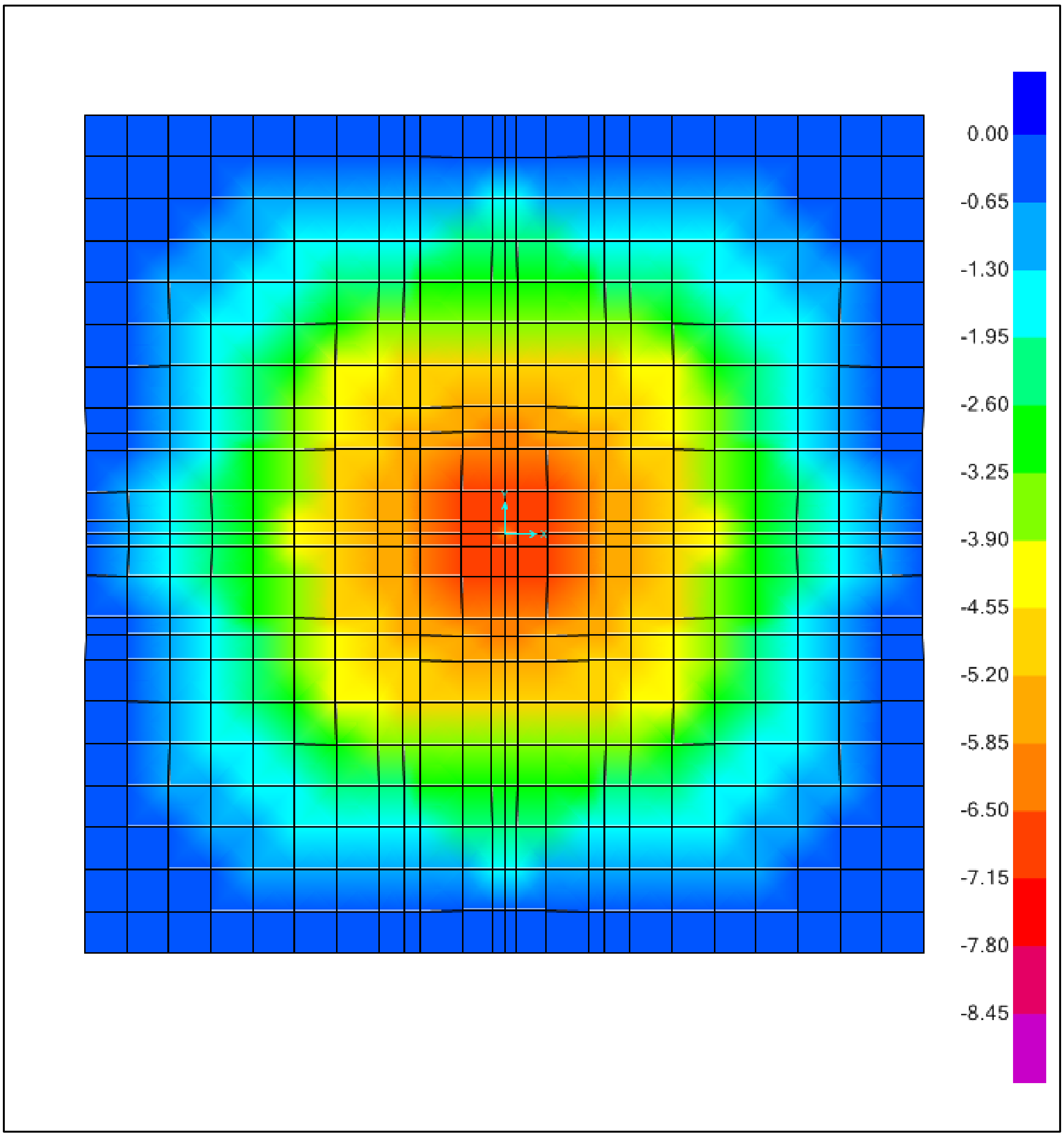

Figure 3.10 Settlement contours at z = -1 plane (Units are mm)

3.3.8 3D Finite Element Method with PLAXIS 3D

In this model the soil can be directly defined with its nonlinear characteristics because of PLAXIS 3D's specialization on geotechnical problems. Raft and piles are defined as "plate" and "embedded piles", respectively (Brinkgreve et al., 2011). Model dimensions are 20 m x 20 m x 30 m. Meshing operations are automatically performed by the software. General view of the model is given in the Figure 3.11.

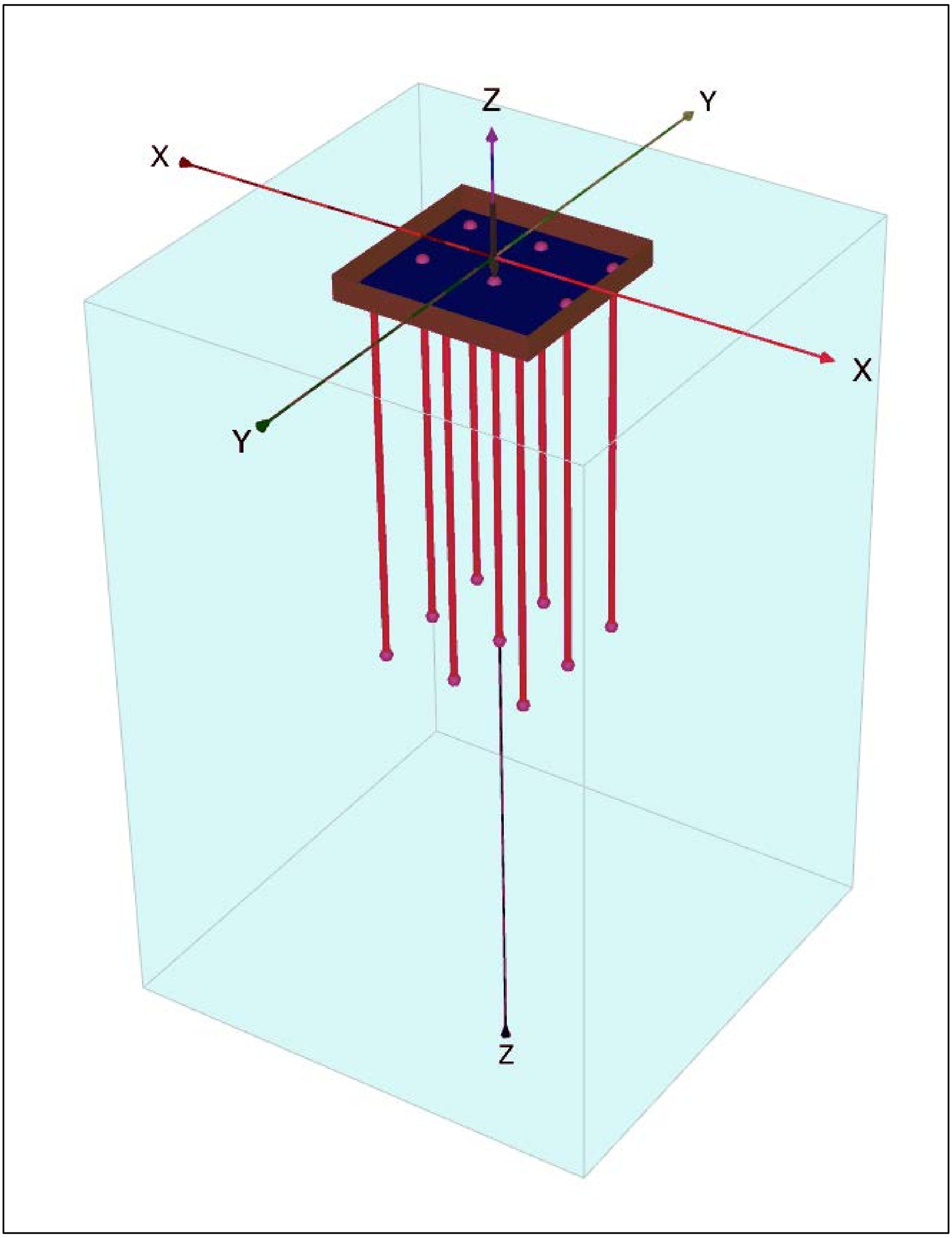

Figure 3.11 General view of PLAXIS 3D model

Load sharing ratio and maximum settlement are obtained 82% and 9.2 mm, respectively. Settlement contours at y = 0 and z = -1 planes are shown in Figures 3.12 and 3.12, respectively.

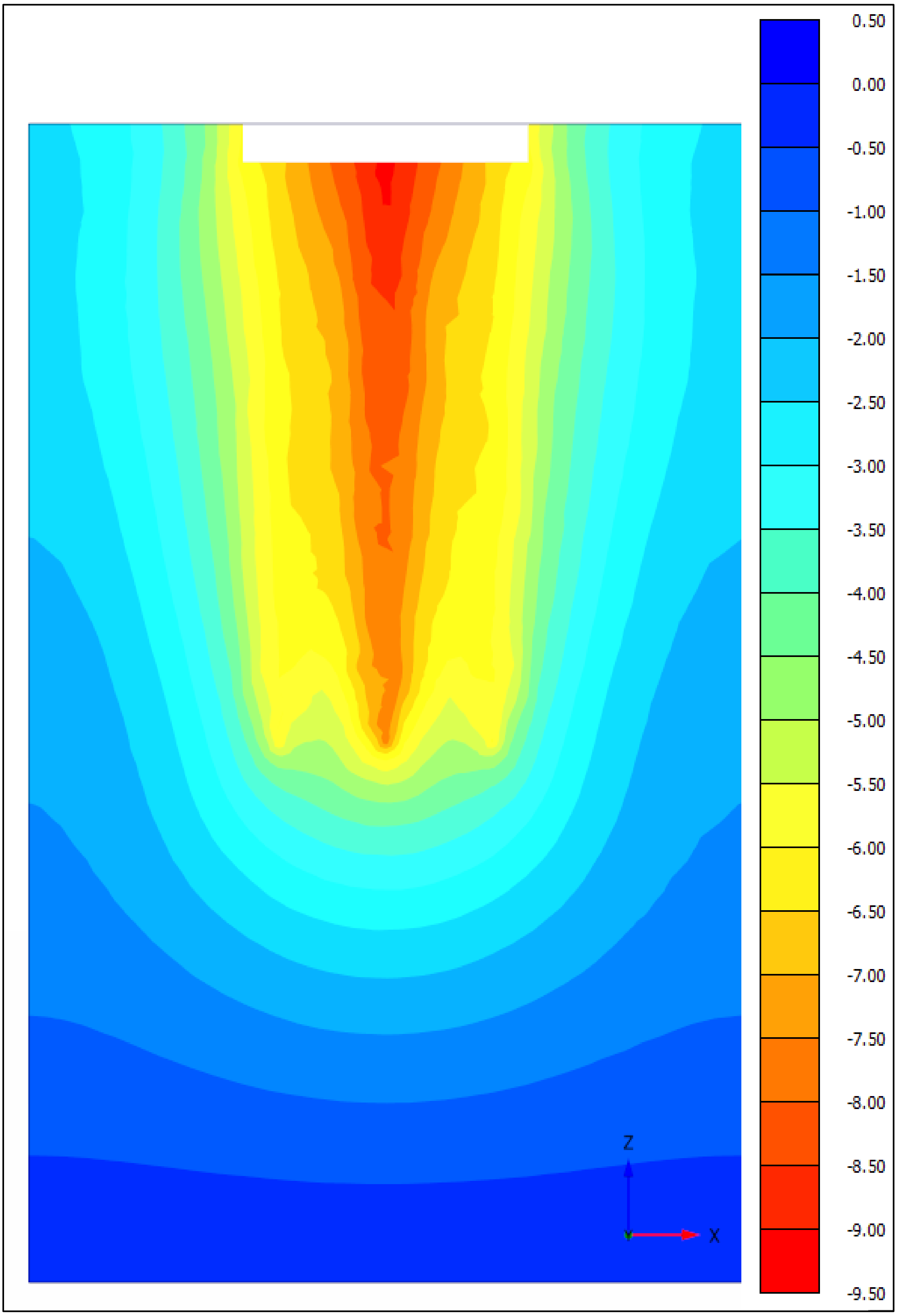

Figure 3.12 Settlement contours at y = 0 plane (Units are mm)

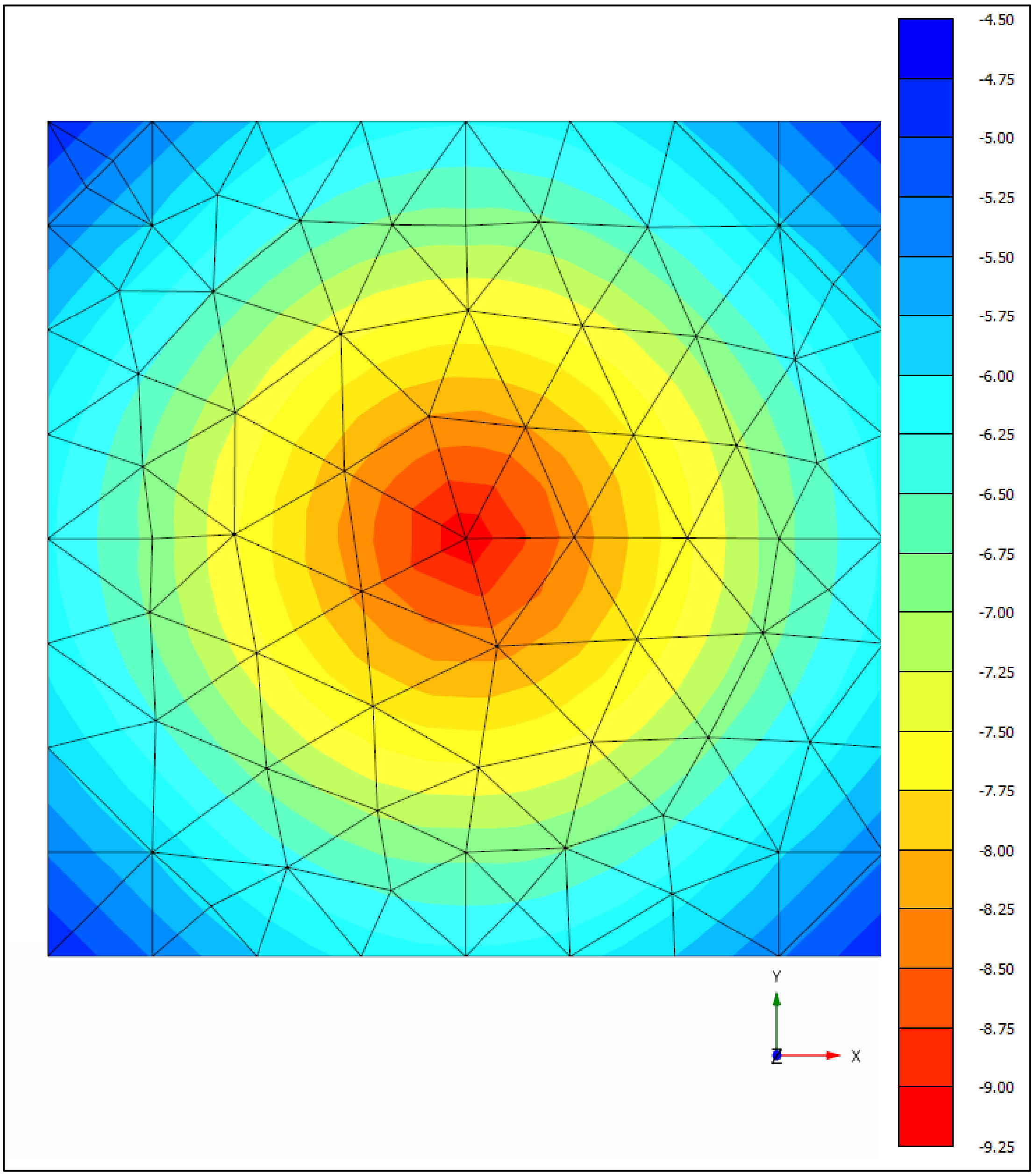

Figure 3.13 Settlement contours at z = -1 plane (Units are mm)

3.4 Overview of Analysis Results

The example problem was solved using eight different calculation methods. In order to compare the obtained results, results are summarized in Table 3.1, Figures 3.14 and 3.15.

Table 3.1 Comparison of obtained results

Method's Type	Method's Name	% of Load Carried by Piles	Settlement (mm)
Simplified	Randolph	87	8.85
	PDR	72	7.23
	Modified of PDR	82	11.60
	Incremental Load Step	70	5.00
Approximate	Plate on Springs (SAP 2000)	75	9.50
Advanced	2D FEM (SAP 2000)	Not Available	9.75
	3D FEM (SAP 2000)	Not Available	9.00
	3D FEM (PLAXIS 3D)	82	9.20

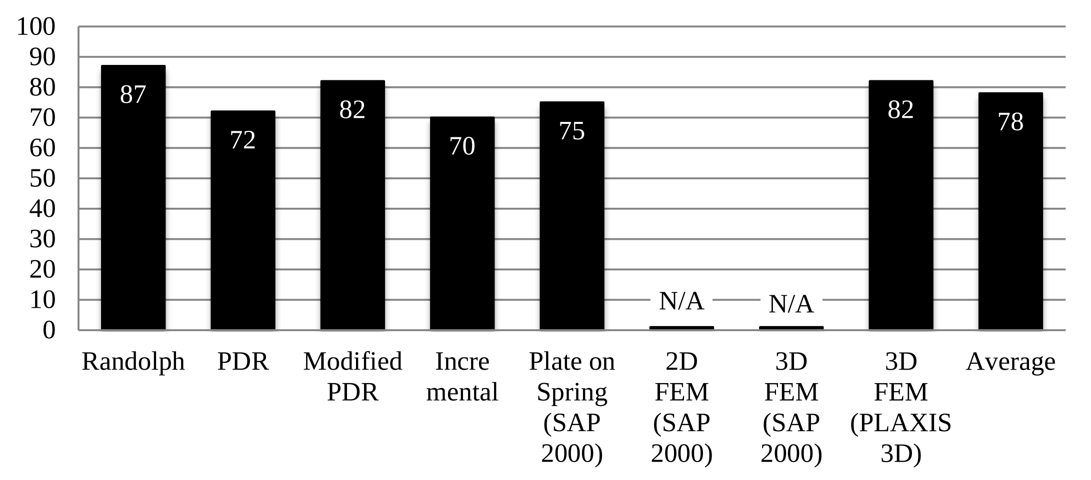

Figure 3.14 Comparison of load carried by piles for different methods (% of Total Load)

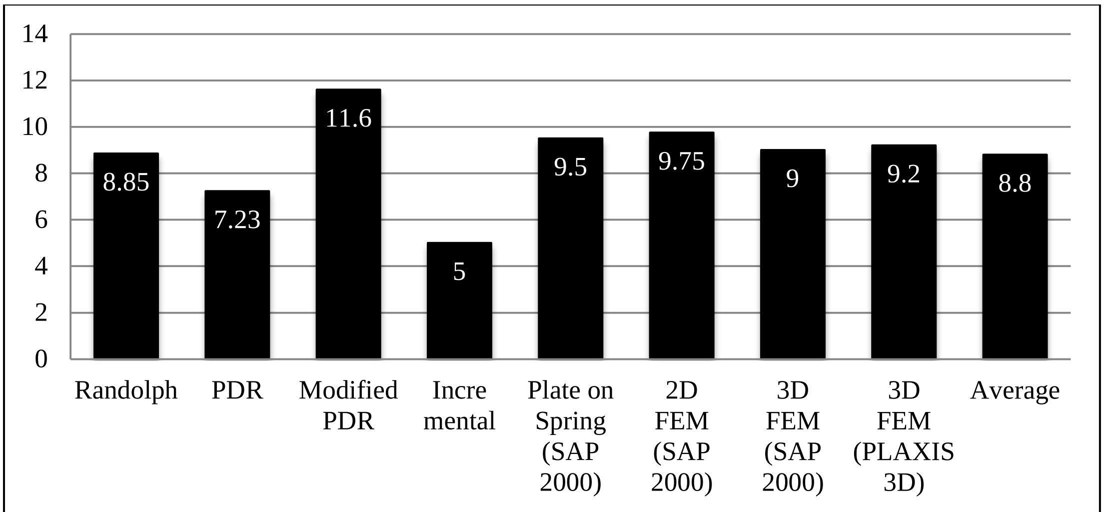

Figure 3.15 Comparison of settlement for different methods (mm)

If the Figure 3.14 and 3.15 are investigated, it can be said that obtained analysis results are in a good agreement. However, incremental load step approach gives lowest values of both % of load carried by piles and settlement. Main reason of this situation is ignoring soil-pile and raft interaction in this analysis method. In addition, obtaining low settlement values in this analysis method may be as a result of it is based on equivalent raft approach. Some application examples in which obtaining lower settlement values using equivalent raft approach are available in the literature (Tomlinson & Woodward, 2008). In addition, Gök (2007) has reported this situation.

In conclusion, evaluation of the results shows that simplified analysis methods provide acceptable results when the results from advanced techniques are considered.

CHAPTER FOUR
CASE STUDY

4.1 Introduction

A piled raft application example is introduced and examined in detail in context of this chapter. For this aim; first of all, structural and soil properties are given. Later on, problem is handled using previously introduced simplified methods and commercial 3D Finite Element Method computer program (PLAXIS 3D), separately. Then obtained results from different methods are compared with each other and measured settlement values in the site. Analysis results show that PLAXIS 3D results are in good agreement with measured values. On the other hand, results from simplified values are higher than in terms of load sharing ratio and overall settlement of the foundation system as compared with PLAXIS 3D results.

4.2 Definition of the Case

4.2.1 Structural Characteristics

Construction site is located in İzmir / Mavişehir region. Different satellite views of the construction site are given in the Figures 4.1, 4.2 and 4.3, respectively.

Construction project mainly consists of two main residence blocks. Each main block includes two sub blocks. Average height of the structure is 70 m. Foundation area of each main block can be calculated as 109.1 m x 27.5 m = 3000.25 m^2. All of the superstructure loads are carried by shear walls. A general view of the construction site and replacement of the residential construction blocks are given in Figure 4.4.

Figure 4.1 Construction site satellite view 1

Figure 4.2 Construction site satellite view 2

Figure 4.3 Construction site satellite view 3

Figure 4.4 General view of construction site and replacement of the structural blocks

4.2.2 Superstructure Loads

Superstructure loads were obtained from structural analysis using the commercial computer program ETABS. Structural analyses were performed for only single block and calculated reaction forces are given in the Table 4.1. Plan view of ETABS model for single block is represented in Figure 4.5. Only static vertical forces (G and Q) are considered in further analysis.

Table 4.1 Superstructure loads for single block

	F_x (kN)	F_y (kN)	F_z (kN)	M_x (kN.m)	M_y (kN.m)
Dead Load (G)			296786.6		
Live Load (Q)			61732.5		
Earthquake X (E_x)	25412.9			1446974.3	
Earthquake Y (E_y)		30560.9			1177367

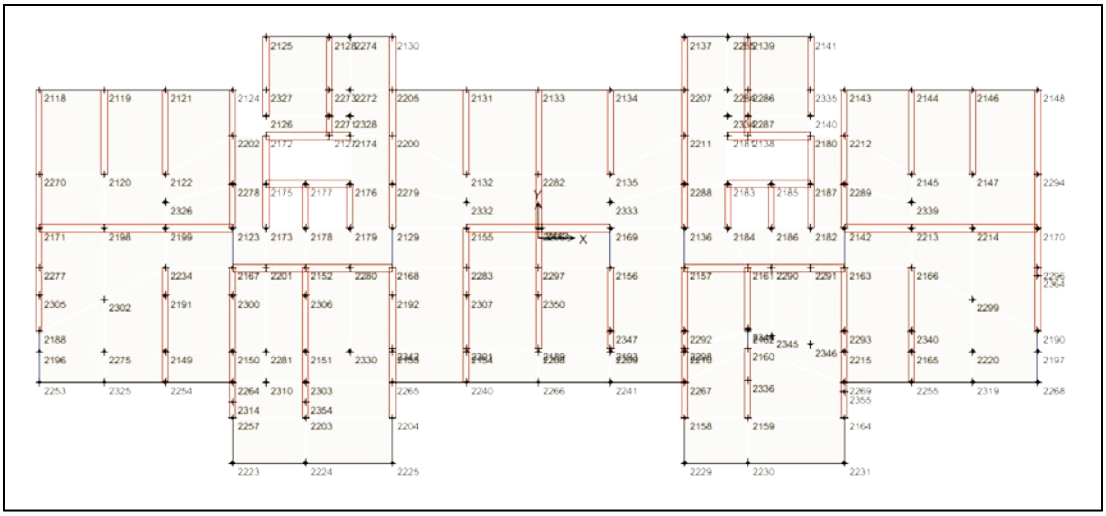

Figure 4.5 Plan view of ETABS model for single structural block

4.2.3 Soil Properties

Soil profile in construction site generally consists of saturated alluvial soils. Groundwater level is 1.0 m. below the ground surface. A boring location map which is related with performed borings is submitted in Figure 4.6. For geotechnical calculation purposes, laboratory experiment results which are performed for recovered soil samples were used. An idealized soil profile was formed using soil investigation report and laboratory test results.

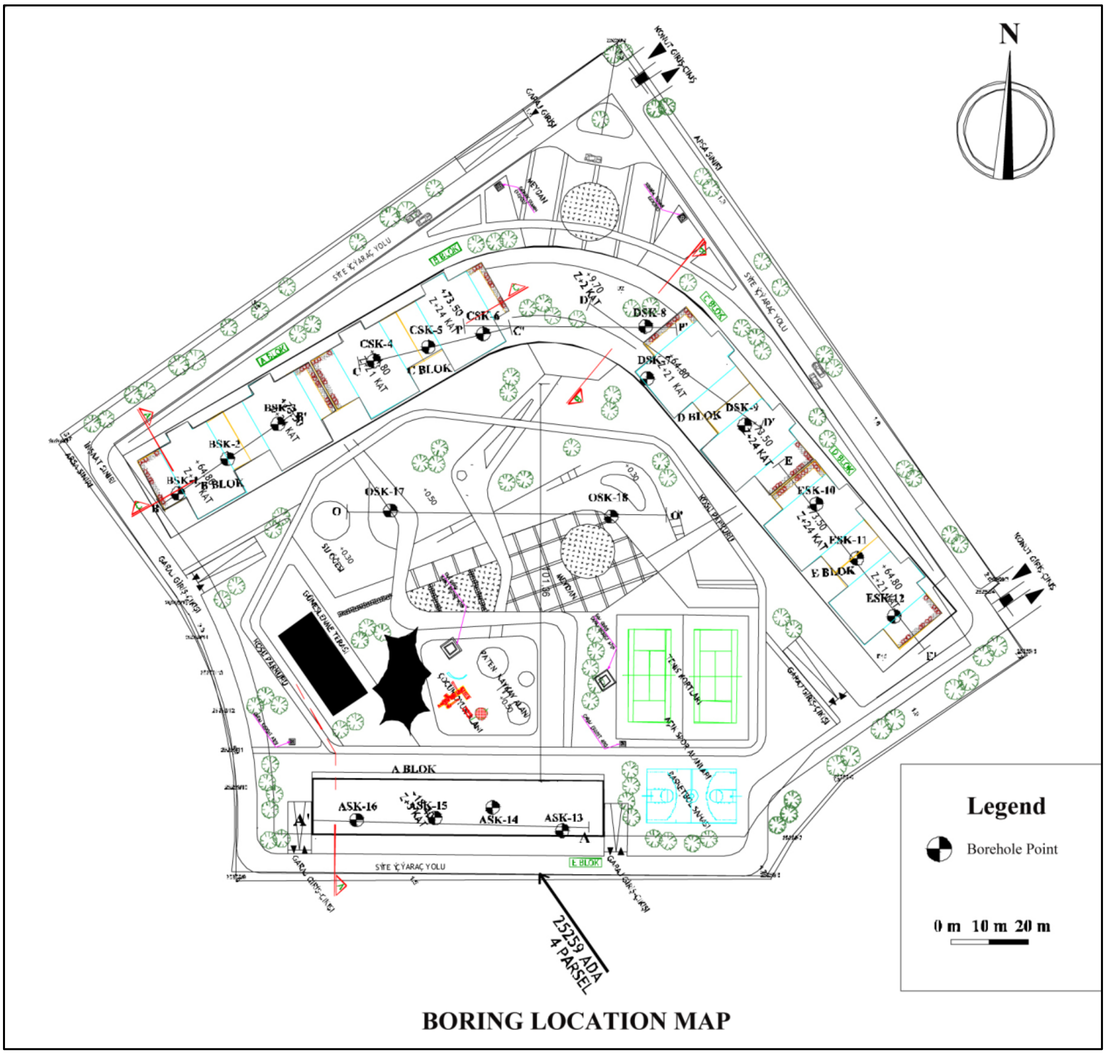

Figure 4.6 Boring location plan

Upon examination of the soil investigation report, it is observed that, there are excessive settlement and liquefaction problems in the soil profile. Thus, shallow foundation option is eliminated. In addition, it is concluded that soil improvement is necessary to prevent liquefaction and to provide extra foundation bearing capacity for piled raft foundation. Soil improvement zone must cover the loose sand and soft clay layers. In the soil profile, below 30 m, fine content of soil is generally higher that 30 % so fine grained soil behavior is expected in clayey gravel and clayey sand layers. In Figure 4.7, idealized soil profile, pile profile and soil improvement zone are illustrated.

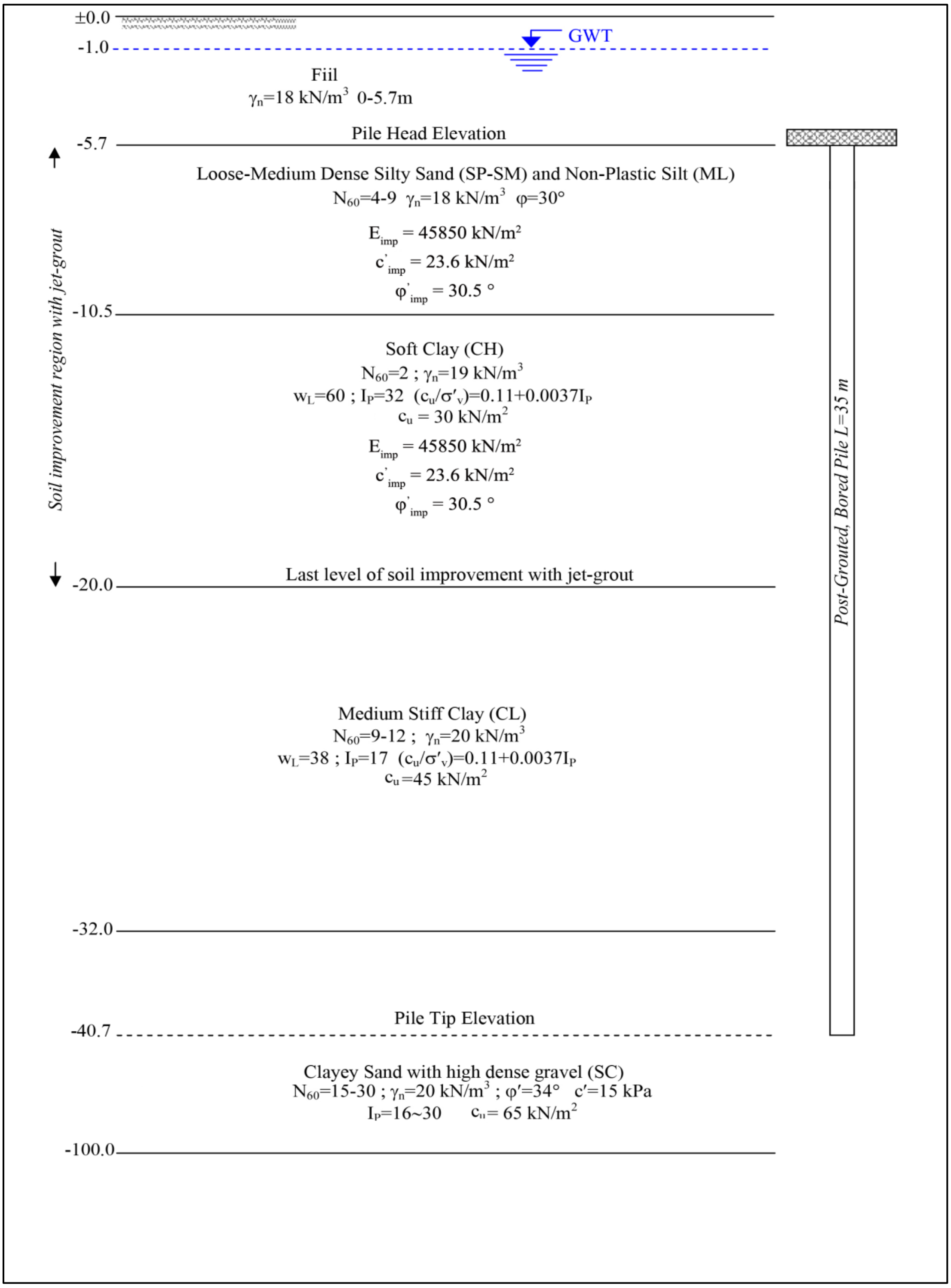

Figure 4.7 Idealized soil profile (with improved soil parameters)

4.2.4 Foundation Properties

General foundation properties are given in the Table 4.2. Calculation details about bearing capacity and axial stiffness calculations for piles and raft are submitted in the appendices.

Table 4.2 General foundation properties

Property	Value
Foundation Type	Piled Raft Foundation
Foundation Dimensions (m)	109.1 x 27.50
Foundation Area (m^2)	3000.25
Raft Thickness (with pile cap) (m)	2.2
Pile Head Elevation (m)	-5.3
Pile Type	Post Grouted Bored Pile
Number of Piles	126
Pile Diameter (m)	1.2
Pile Length (m)	34.50
Pile Spacing in x Direction (m)	6.30
Pile Spacing in y Direction (m)	4.25
Single Pile Axial Load Capacity (kN)	21970
Pile Group Axial Load Capacity (MN)	2768.3
Raft's Axial Load Bearing Capacity (MN)	438.8
Single Pile Axial Stiffness (MN/m)	1037.4
Pile Group Axial Stiffness (MN/m)	14830
Raft Axial Stiffness (MN/m)	4110
Weight of Structure (G+0.5Q) (kN)	655305
Weight of Raft (kN)	154918
Weight of Landscape Fiil (kN)	27000
Weight of Excavation (kN)	-286223
Net Weight Transmitted to Foundation (kN)	551000

4.3 Performed Analyses and Results

Problem was analyzed using following simplified and advanced analysis methods. Calculation details about simplified methods are given in the appendices.

- Randolph Method (Simplified)
- Poulos-Davis-Randolph (PDR) Method (Simplified)
- Modified version of PDR Method (Simplified)
- 3D Finite Element Method with PLAXIS 3D (Advanced)

4.3.1 Randolph Method

According to calculation results, 93 % of total load is carried by piles and overall settlement of the system is 36.7 mm.

4.3.2 PDR Method

As a result of this simplified method, load sharing ratio between piles and raft is determined as 79%. In other words, 79% of total load is carried by the piles. Overall settlement of the system is obtained as 29.8 mm.

4.3.3 Modified Version of PDR Method

Load sharing ratio is determined as 93% and overall settlement of the foundation system is obtained as 40.5 mm from this analysis method.

4.3.4 3D Finite Element Method using PLAXIS 3D

3D Finite Element Method is applied on problem with two different calculation models. Both of these models have same geometry with different loading conditions. Model dimensions of both models are 150 x 50 x 100 m. Meshing operations were performed automatically by PLAXIS 3D and accordingly generated model consists of 36438 elements with 56769 nodes. Average finite element size in the model is 4.537 m. General view of PLAXIS 3D model and pile group layout are shown in Figures 4.8 and 4.9, respectively.

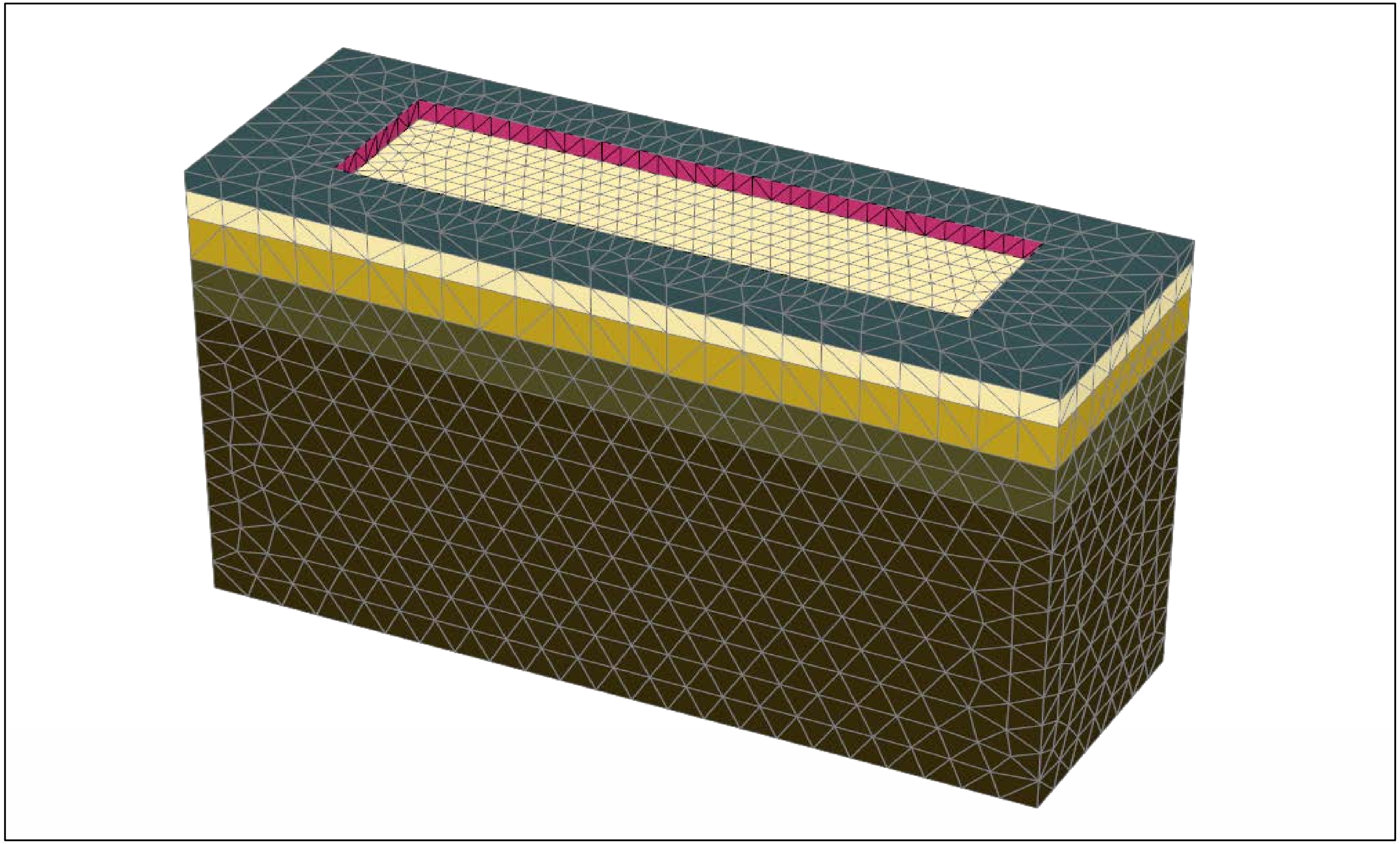

Figure 4.8 General view of PLAXIS 3D model

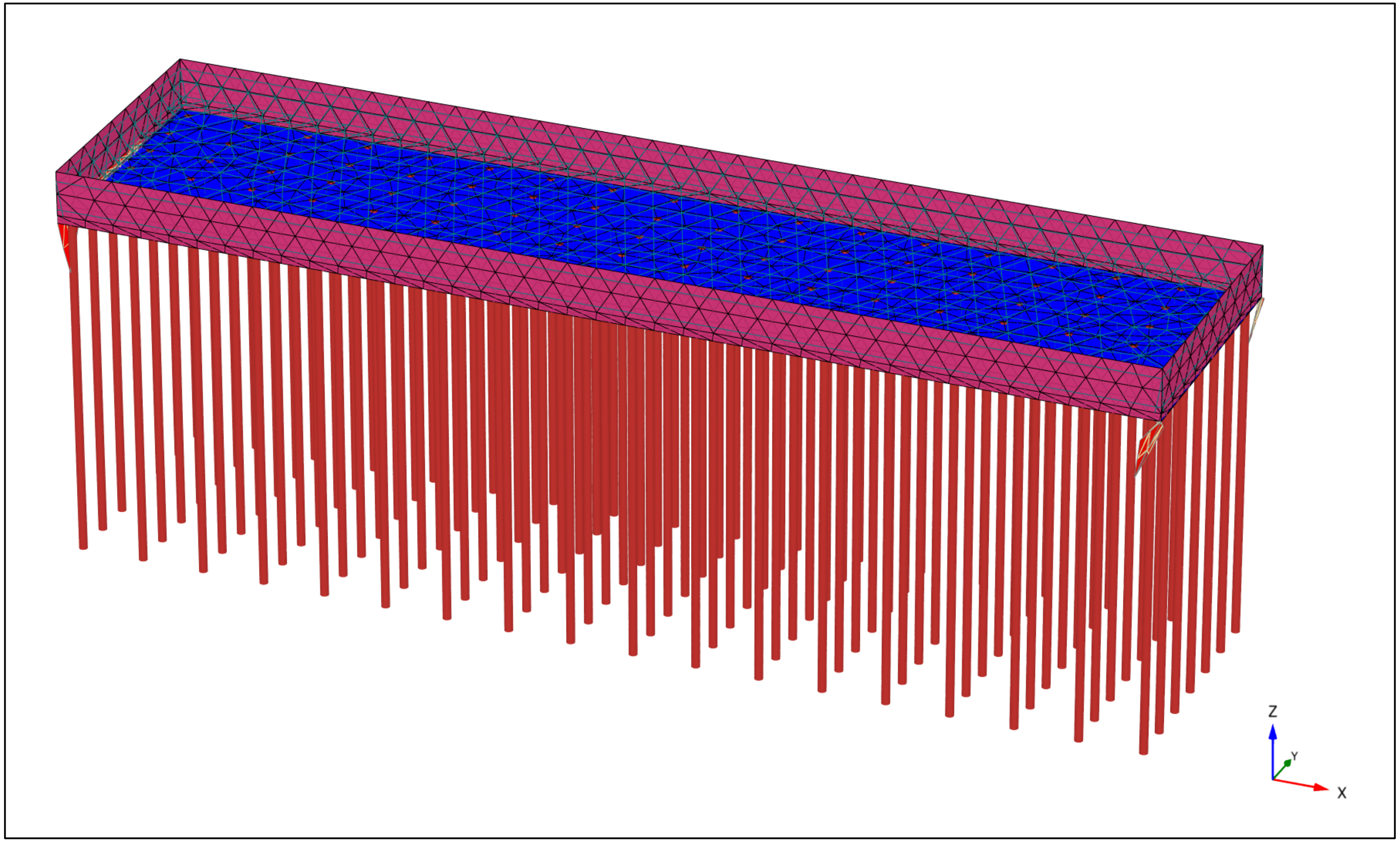

Figure 4.9 Pile group layout

Pile group was created using “embedded pile” elements. There are 126 piles with horizontal spacing as 6.30 m and vertical spacing as 4.25 m. Raft was defined as “plate” element. Plate elements were also defined at the perimeter of the excavation area. Pile layout plan of the model is shown in the Figure 4.10.

In the first model, structural loads were applied to the raft as distributed uniform load. The value of the distributed uniform load is 272 kN/m^2 and it includes the weight of the raft. Thus, unit weight of the raft was defined as a negligible small value. In the second model, structural loads were applied to raft as line loads. The location of the line loads were based on replacement of the shear walls on the basement floor plan. In order to determine the values of the line loads, structural analysis were performed under (G+0.5Q) load combination using ETABS and axial forces at the location of the shear walls are obtained. Such axial forces were converted into equivalent line loads by considering the length of the shear walls. On the other hand, weight of raft is not included in line loads, so real unit weight value of the raft was assigned in the model. Locations of the line loads on the raft are shown in the Figure 4.11.

In order to represent soil properties of the problem, Mohr-Coulomb (MC) soil model was used. Different soil layers were defined using “borehole” in PLAXIS 3D. Idealized soil profile with improved soil properties was based on while creating the “borehole” and defining soil properties in each soil layer. The interface coefficient for soil-structure (piles and raft) interaction was assumed as 0.80 because of post grout operation on the piles. Piles and raft are modeled as linear elastic materials. Skin resistance of the piles was calculated automatically using “layer dependent skin resistance” option in PLAXIS 3D. Details of material properties (soil, raft and pile) are given in appendices.

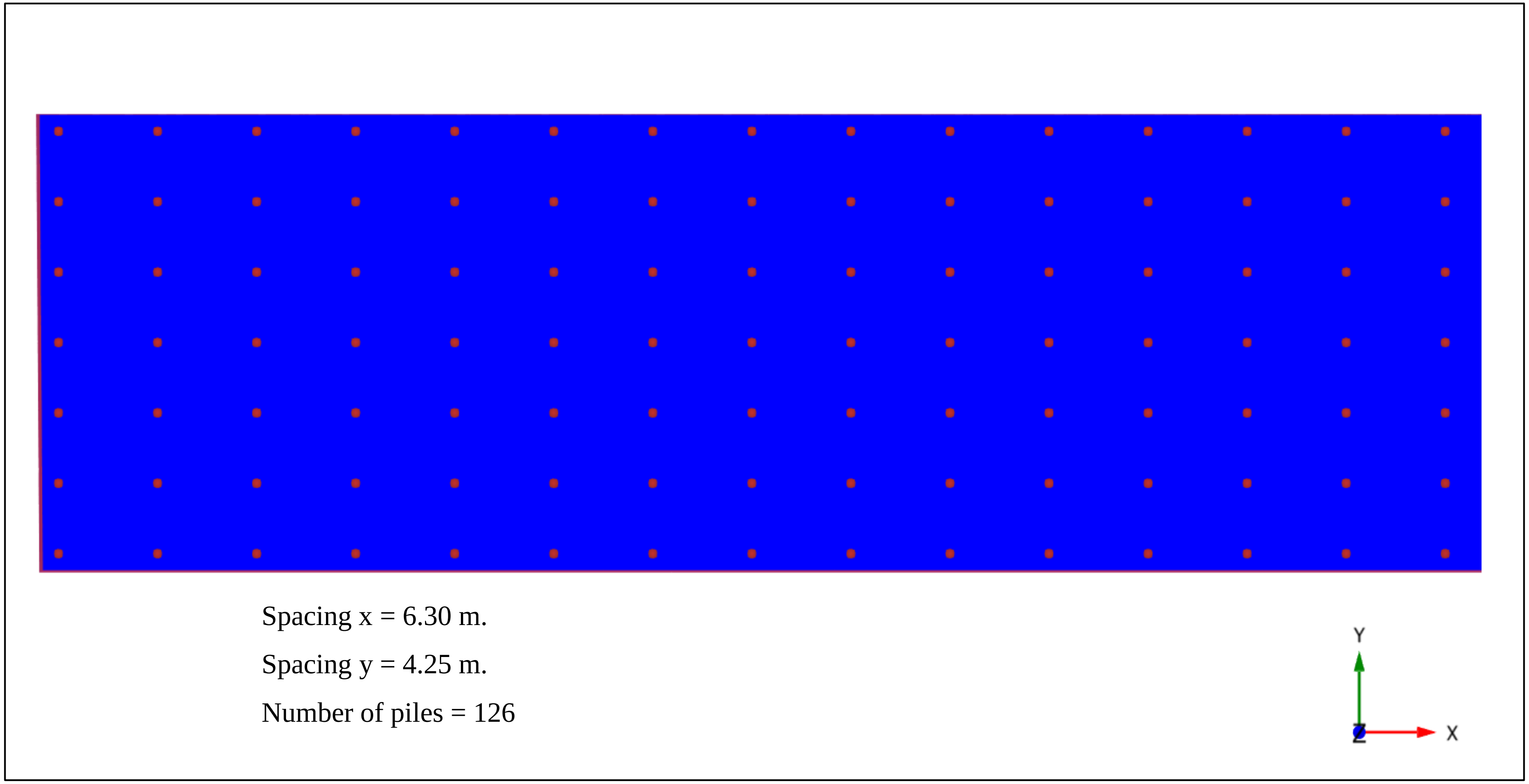

Figure 4.10 Pile layout plan of the model.

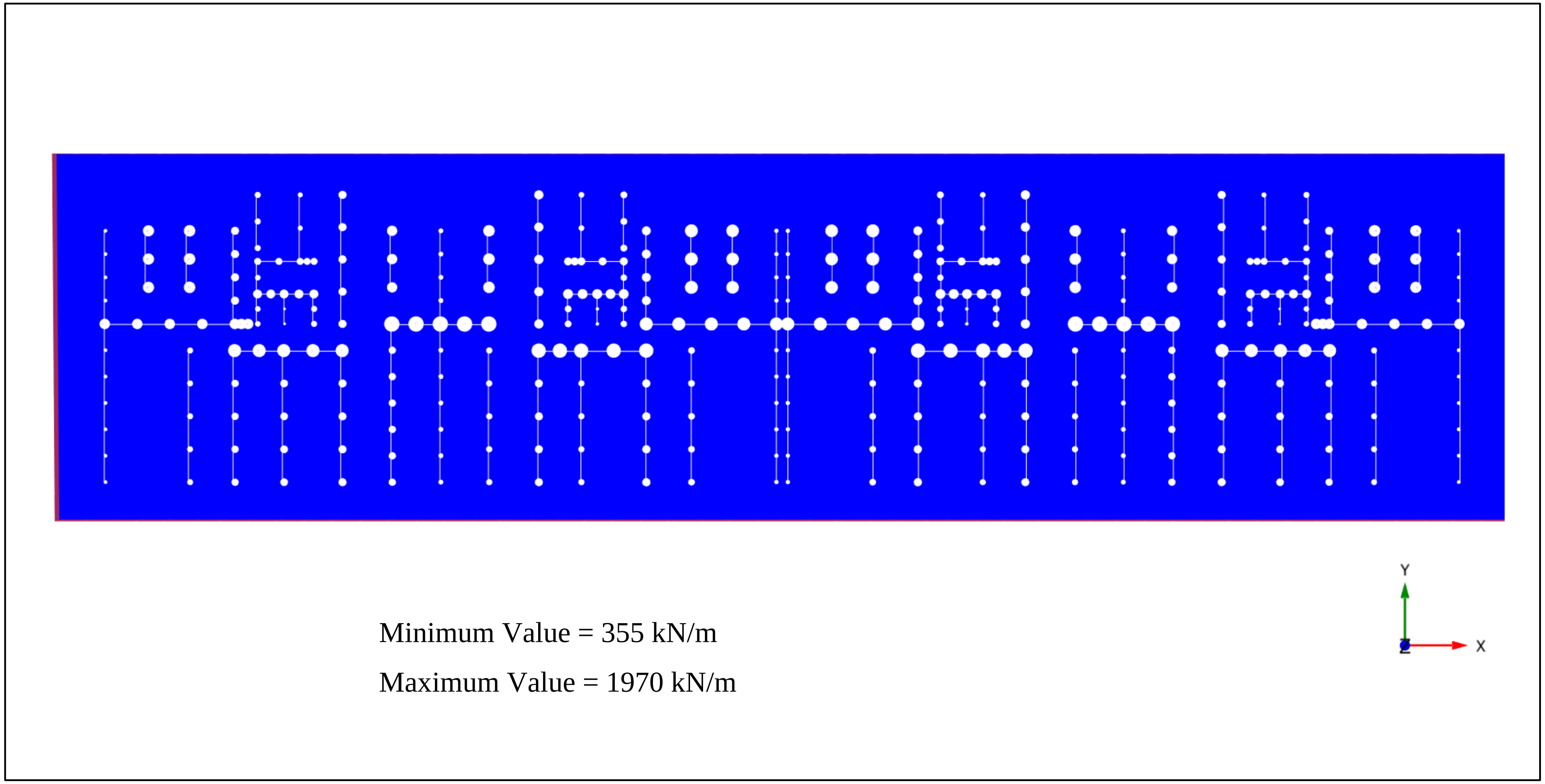

Figure 4.11 Representation of the line loads on the raft with maximum and minimum values (Dots show the relative magnitude of the line load)

When obtained results are examined, load sharing ratio is determined as 71% and 75% of the total load for first (distributed load) and second (line load) model, respectively. In addition, settlement values are obtained as 28 mm and 34 mm in a similar way. Settlement contours for both models are given in the Figures 4.12 thru 4.15 for z = -5.3 m and y = 0 m planes. Higher settlement values in the second model are expected due to the load arrangement differences between two models. In the first model, majority of the piles take approximately same loads and the system tends to work uniformly. On the other hand, in the second model, piles located at the center are exposed to higher stress than corner and edge piles do. This situation causes an increase in computed settlements. Pile load contours for each model are represented in Figures 4.16 and 4.17. From these figures, it is clearly seen that there is a stress accumulation at the center piles. Plastic points of the systems are shown in Figures 4.18 and 4.19. A closer look to Figures 4.18 and 4.19 reveal that number of plastic points at the center of the model is higher than in the second model. Such plastic points at the center may cause higher displacement with larger stress levels.

Effects of load application style on the foundation get a more dramatic situation when the raft moments are investigated. Obtained raft moments for the second model are approximately twice of the results from the first model. However, computed moments are considerably high as compared with real life applications since contribution of superstructure stiffness to that of the foundation is ignored in the calculation model. Raft moments for the models are shown in Figures 4.20 thru 4.23.

It can be inferred from examination of the results that distributed load approach should only be used at the initial design steps. Detailed design must be performed using real loading conditions and considering effect of superstructure stiffness on the raft.

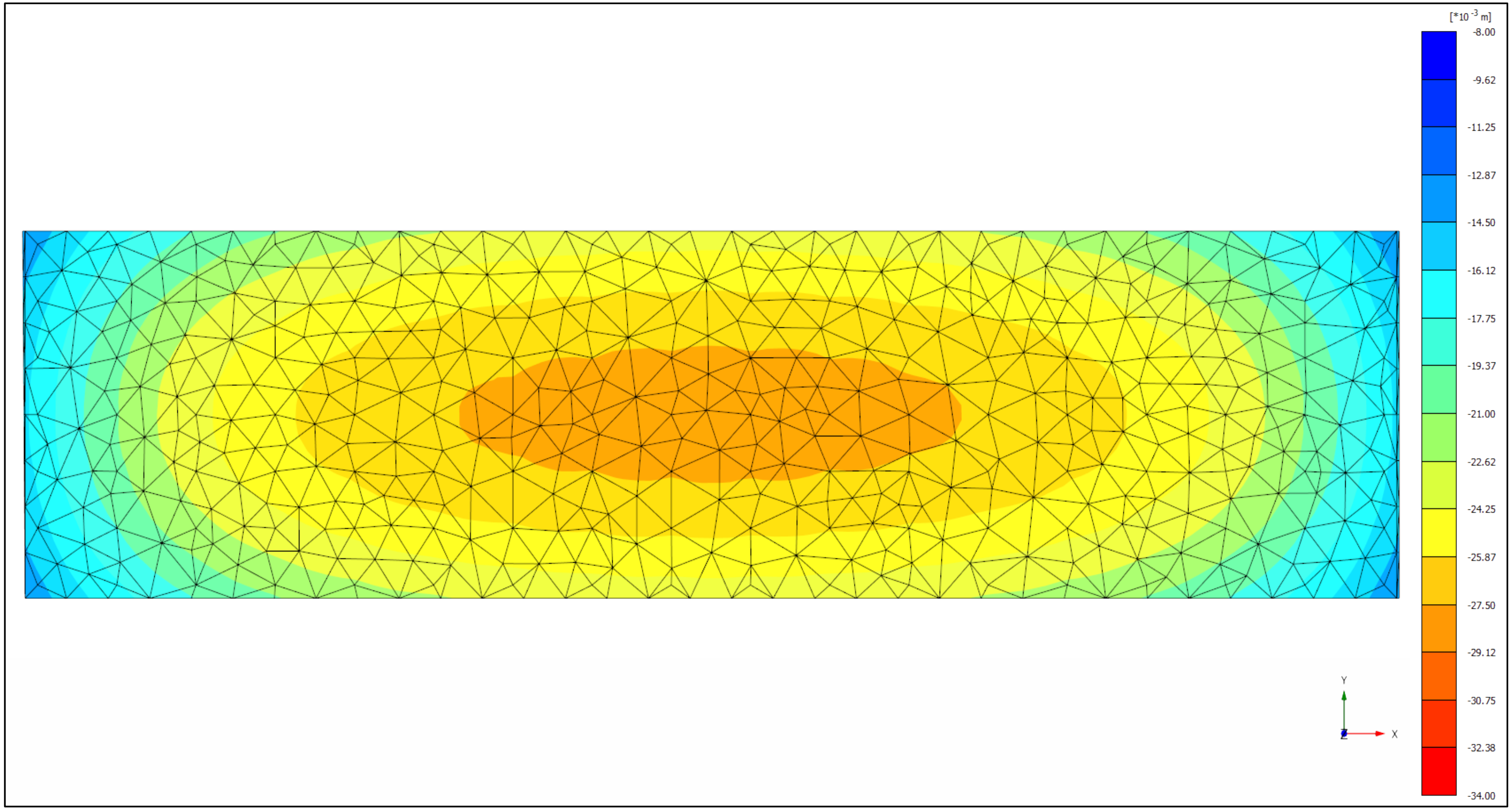

Figure 4.12 Settlement contours for first (distributed load) model at z = -5.3 plane (Units are mm)

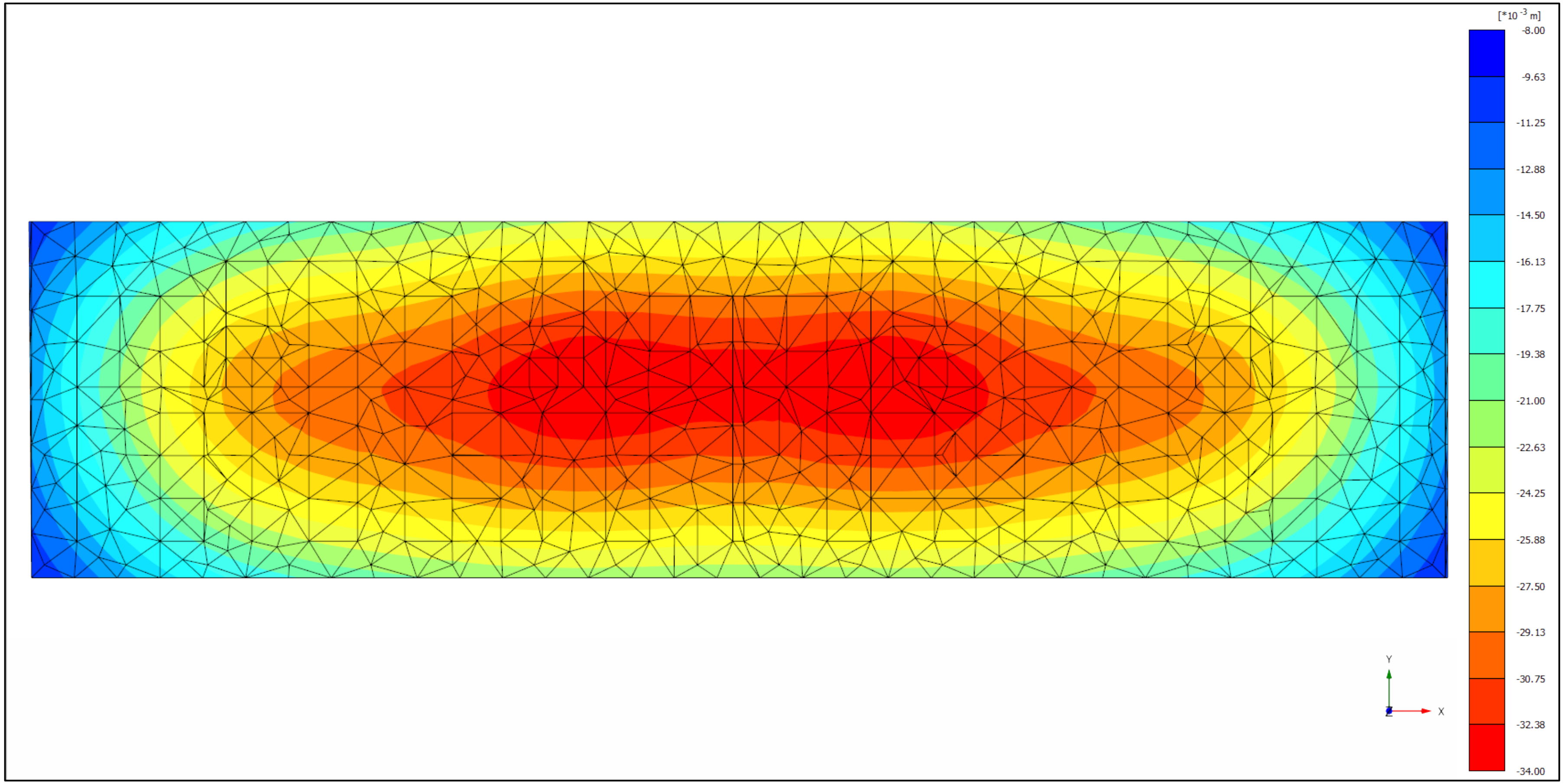

Figure 4.13 Settlement contours for second (line load) model at z = -5.3 plane (Units are mm)

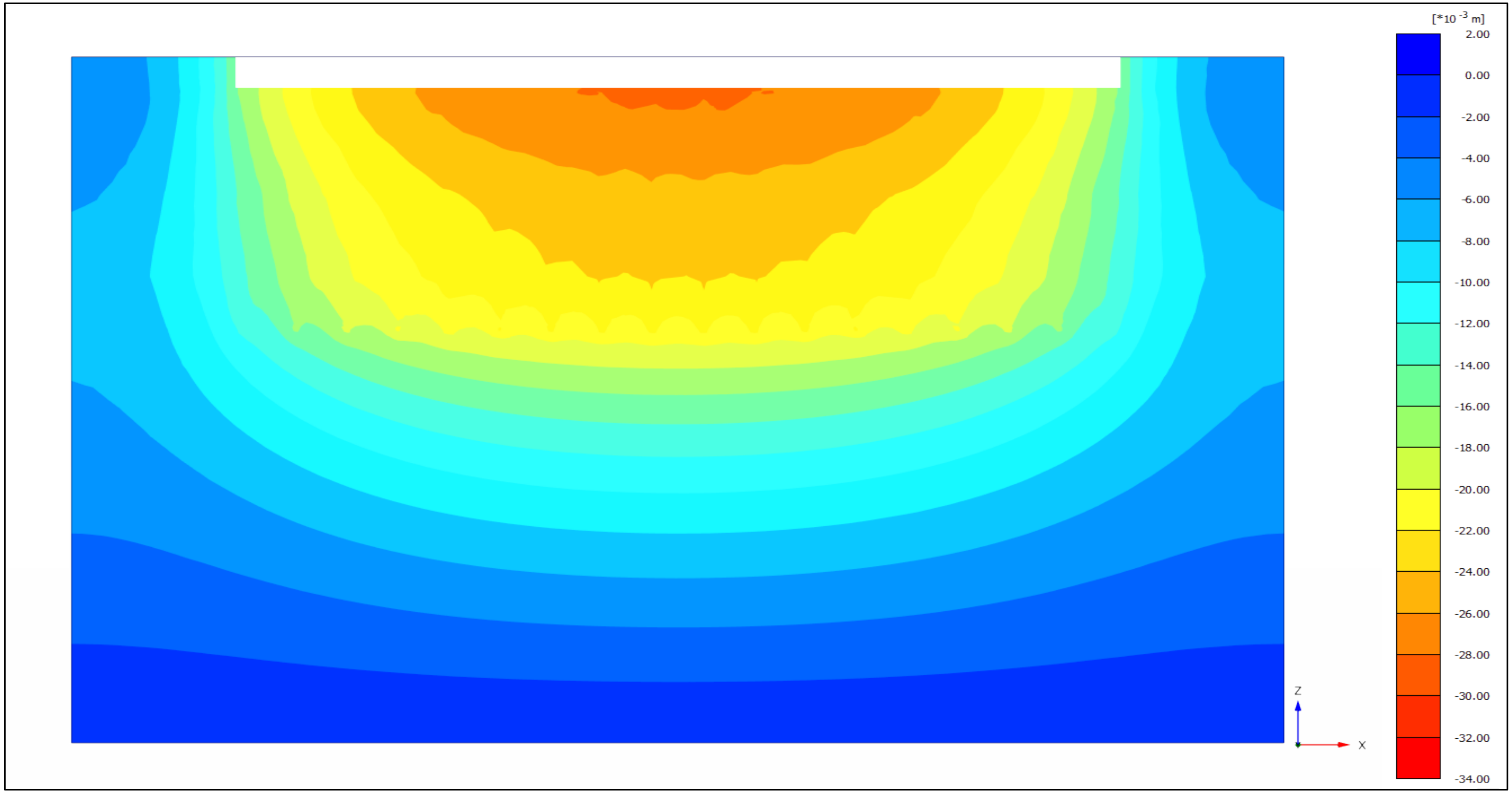

Figure 4.14 Settlement contours for first (distributed load) model at y = 0 m. plane (Units are mm)

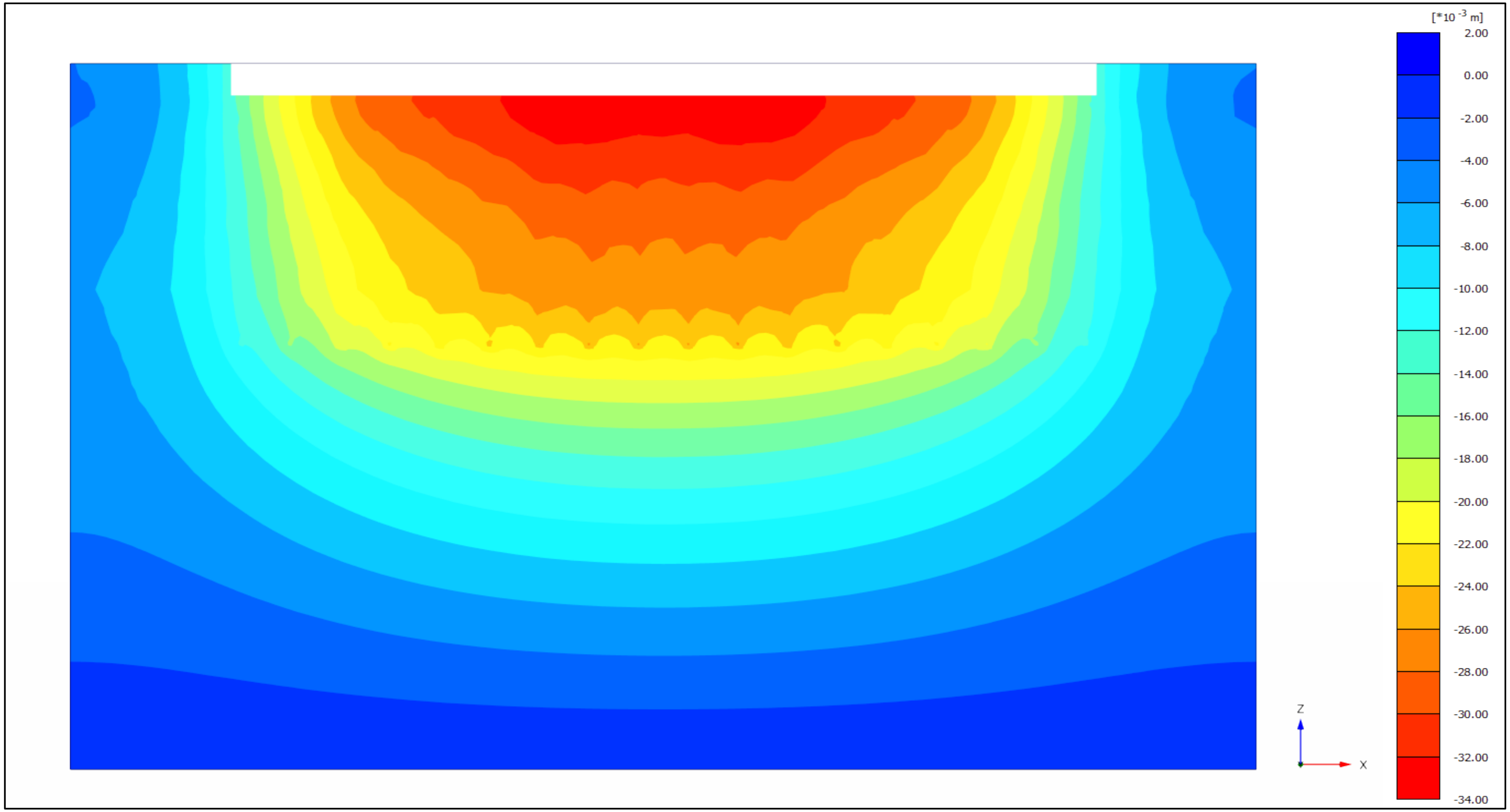

Figure 4.15 Settlement contours for second (line load) model at y = 0 m. plane (Units are mm)

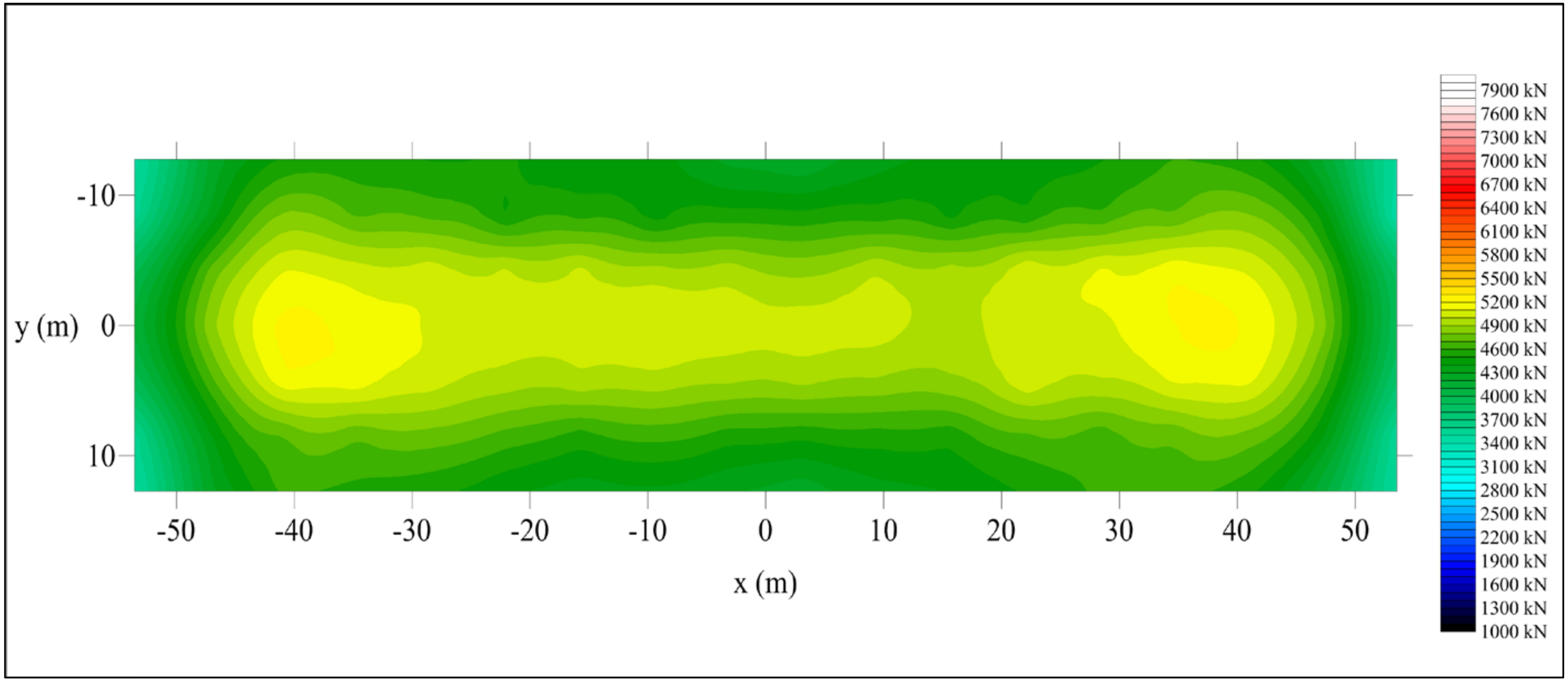

Figure 4.16 Pile load distributions for first model (Units are kN)

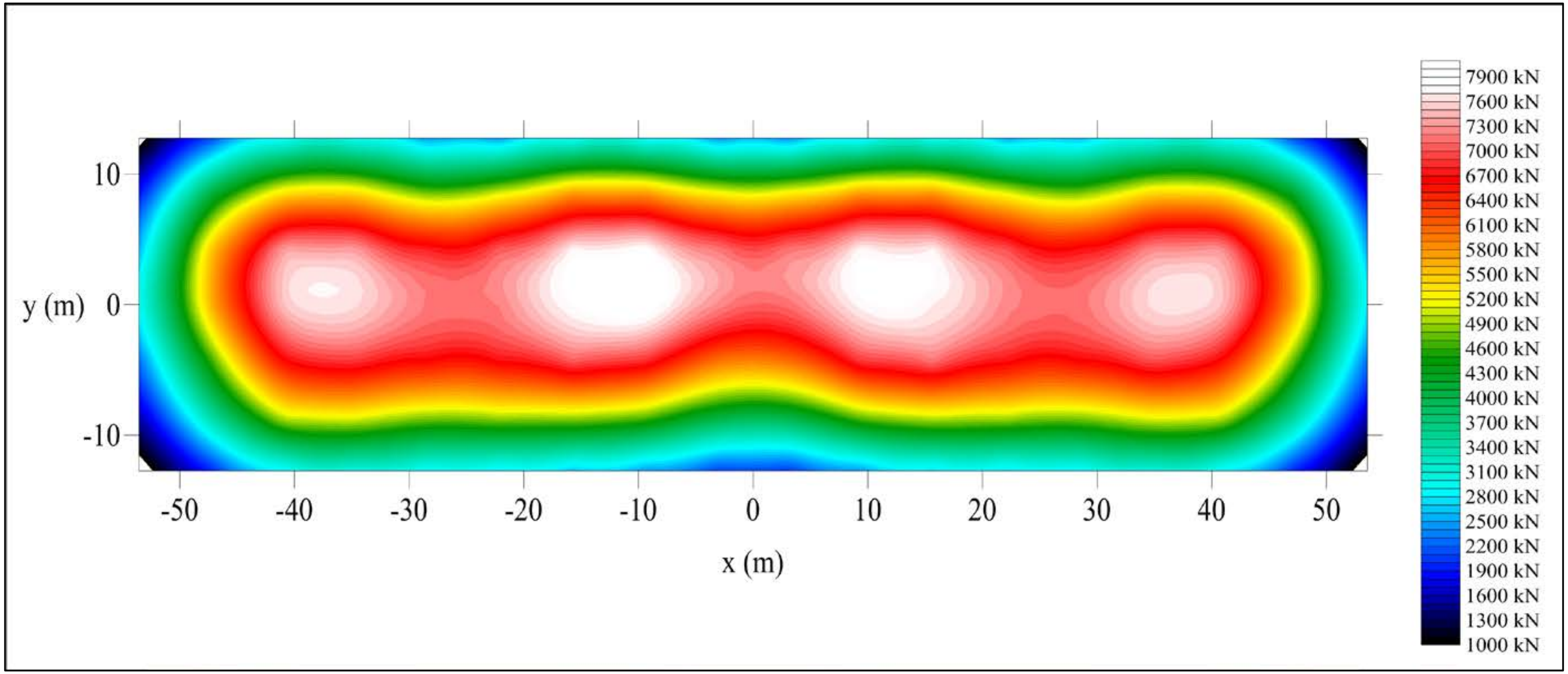

Figure 4.17 Pile load distributions for second model (Units are kN)

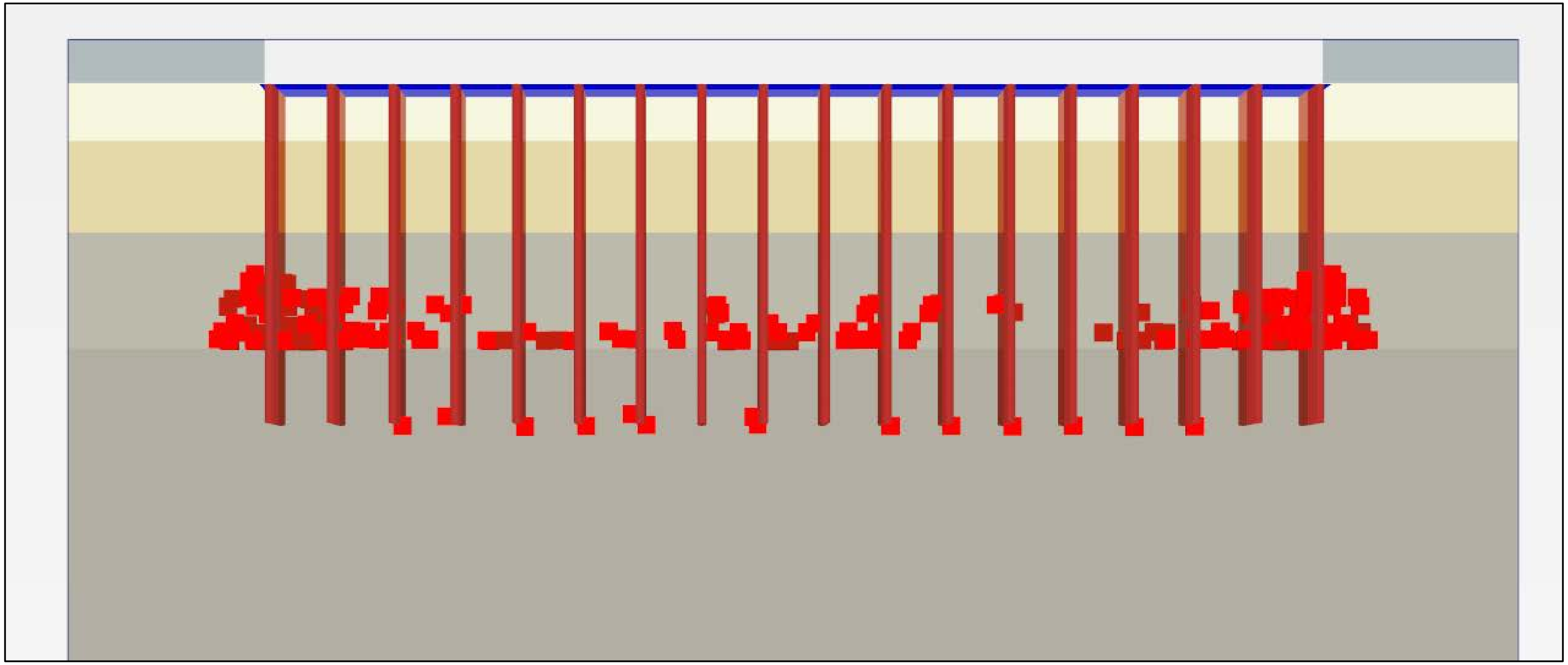

Figure 4.18 Plastic points for first model (Red dots indicate the plastic points)

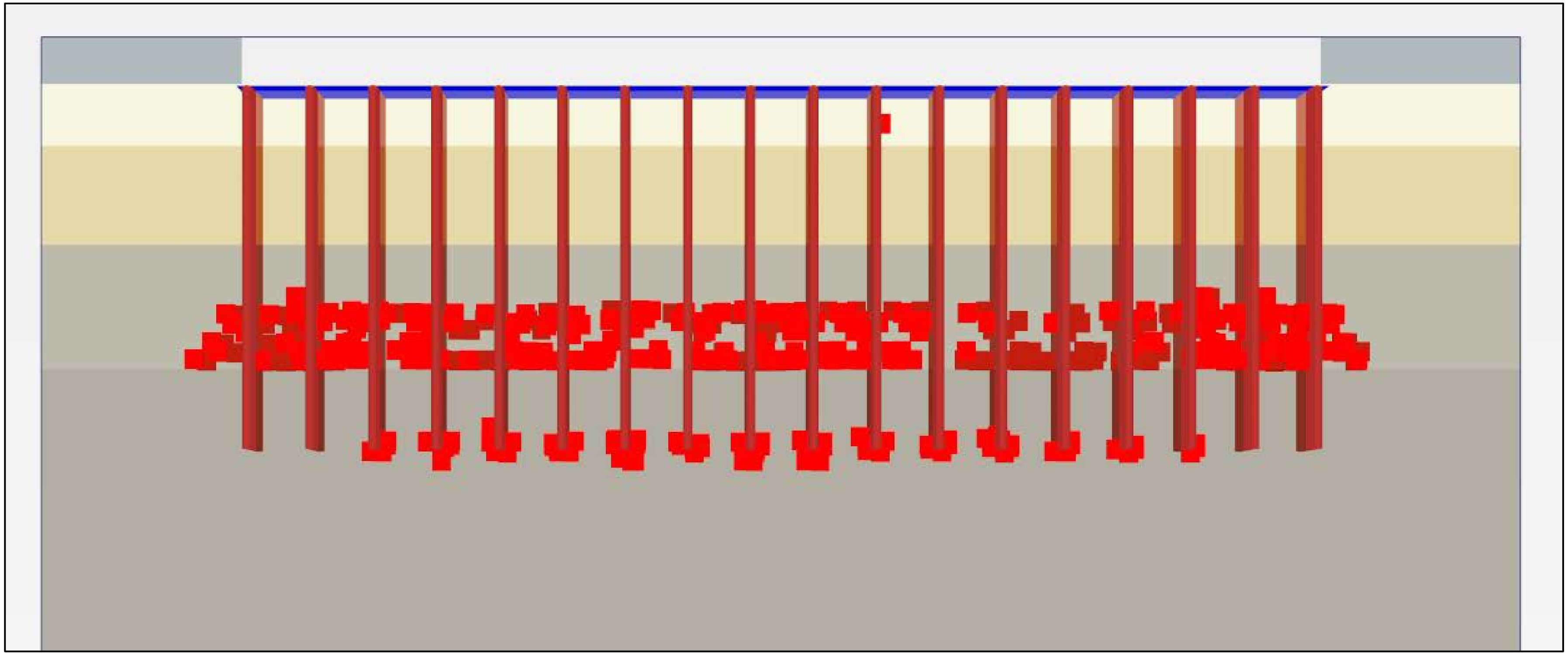

Figure 4.19 Plastic points for second model (Red dots indicate the plastic points)

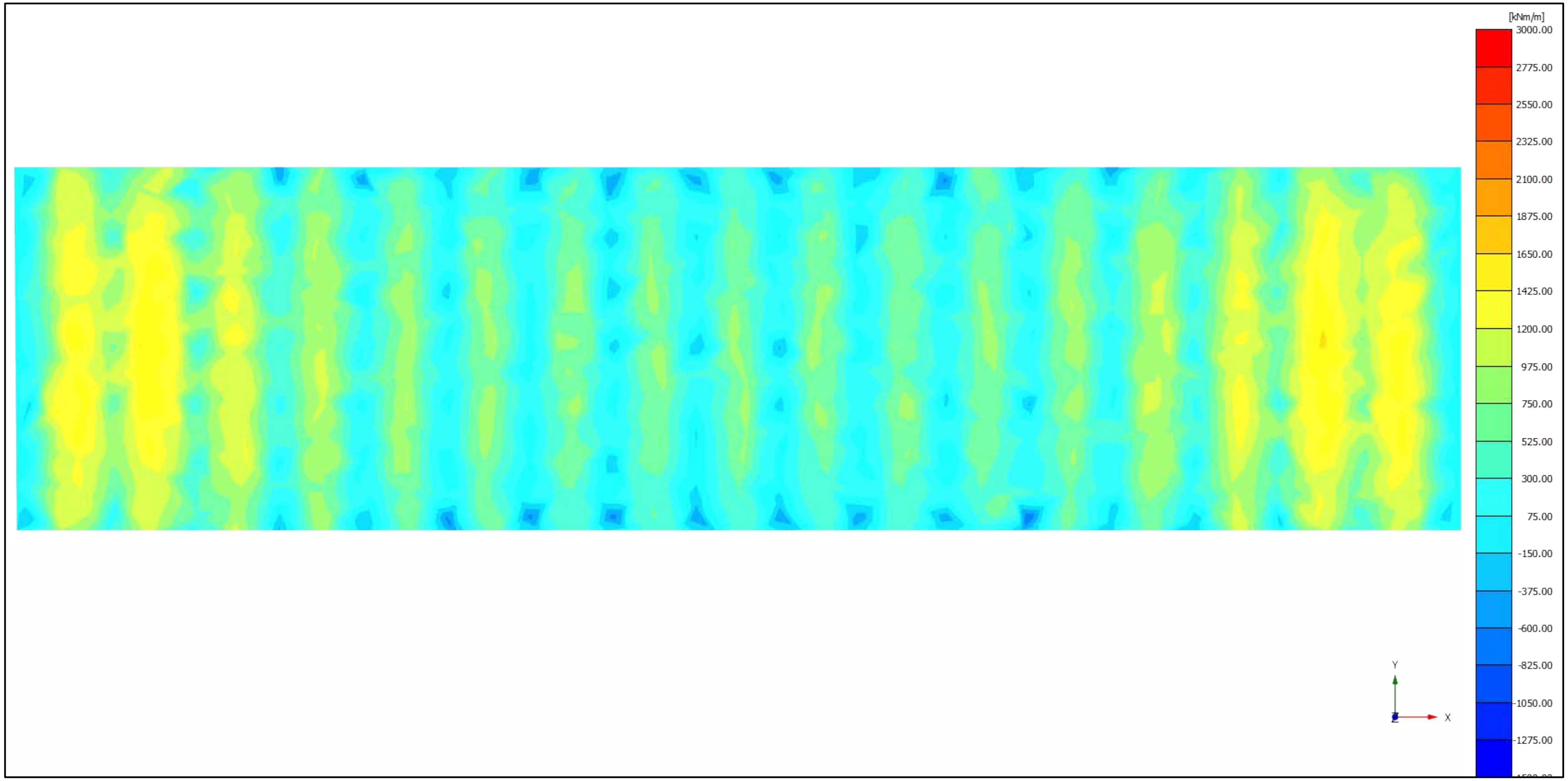

Figure 4.20 Raft moments for first model about to y-y axis (Units are kNm)

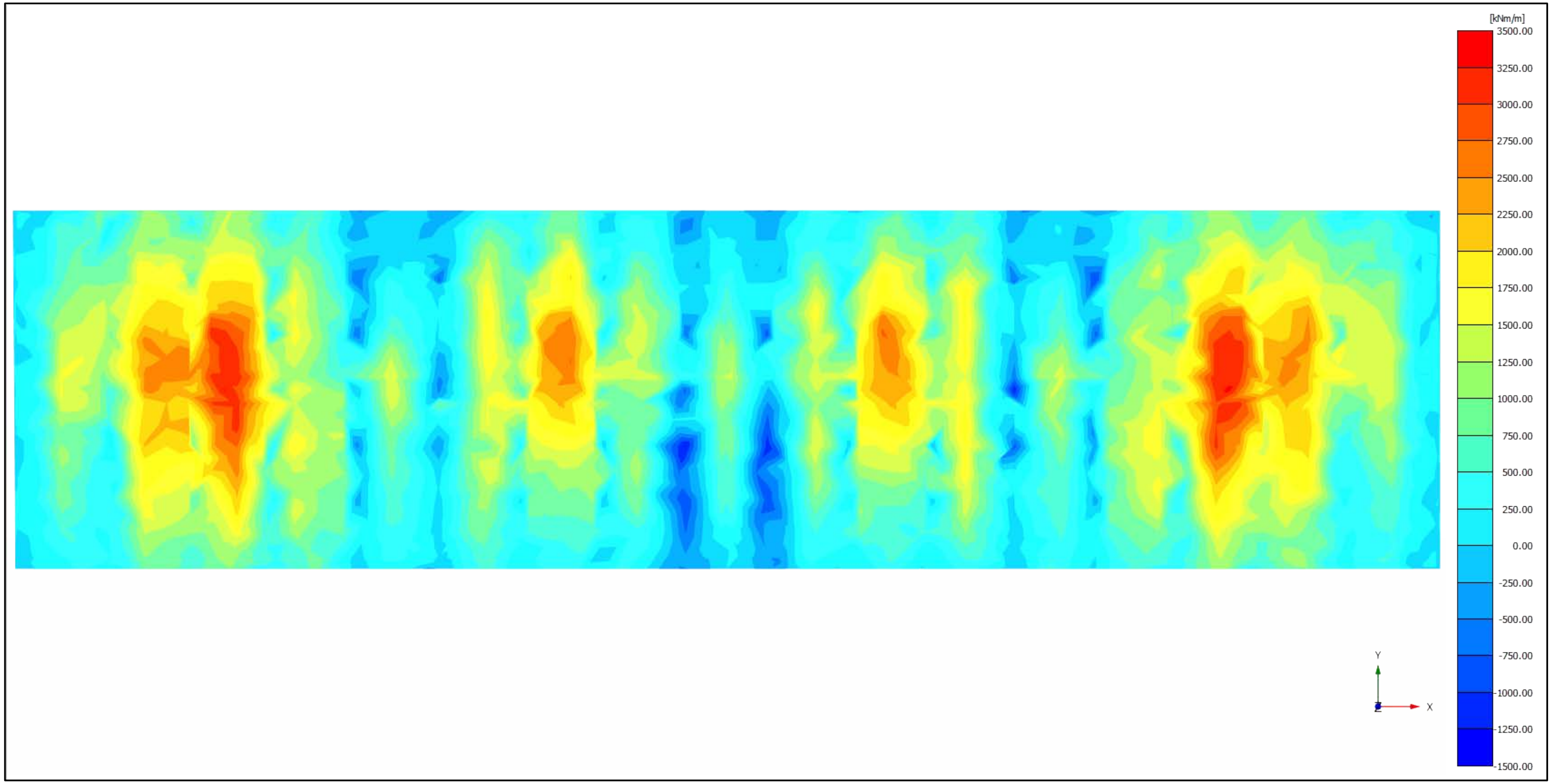

Figure 4.21 Raft moments for second model about to y-y axis (Units are kNm)

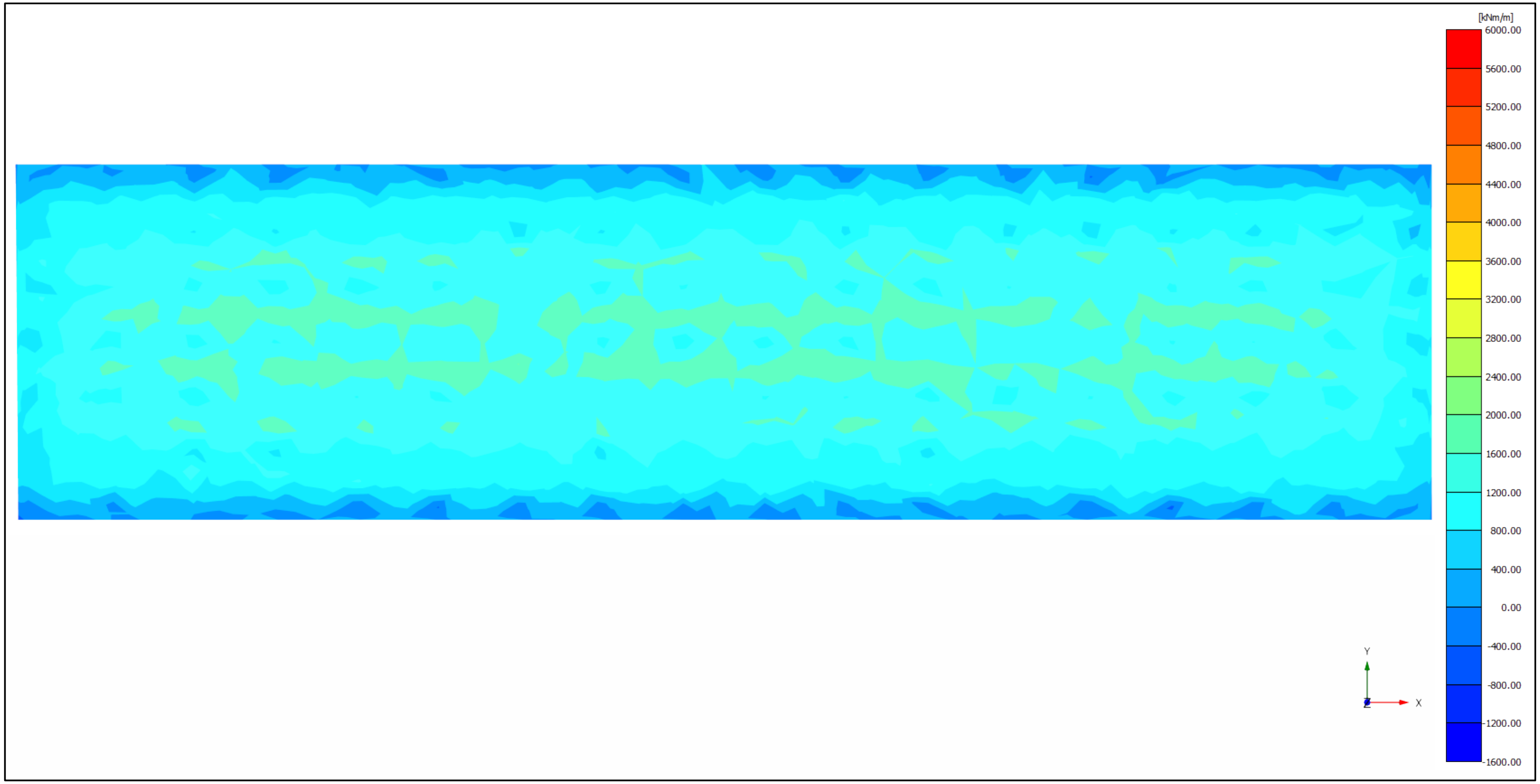

Figure 4.22 Raft moments for first model about to x-x axis (Units are kNm)

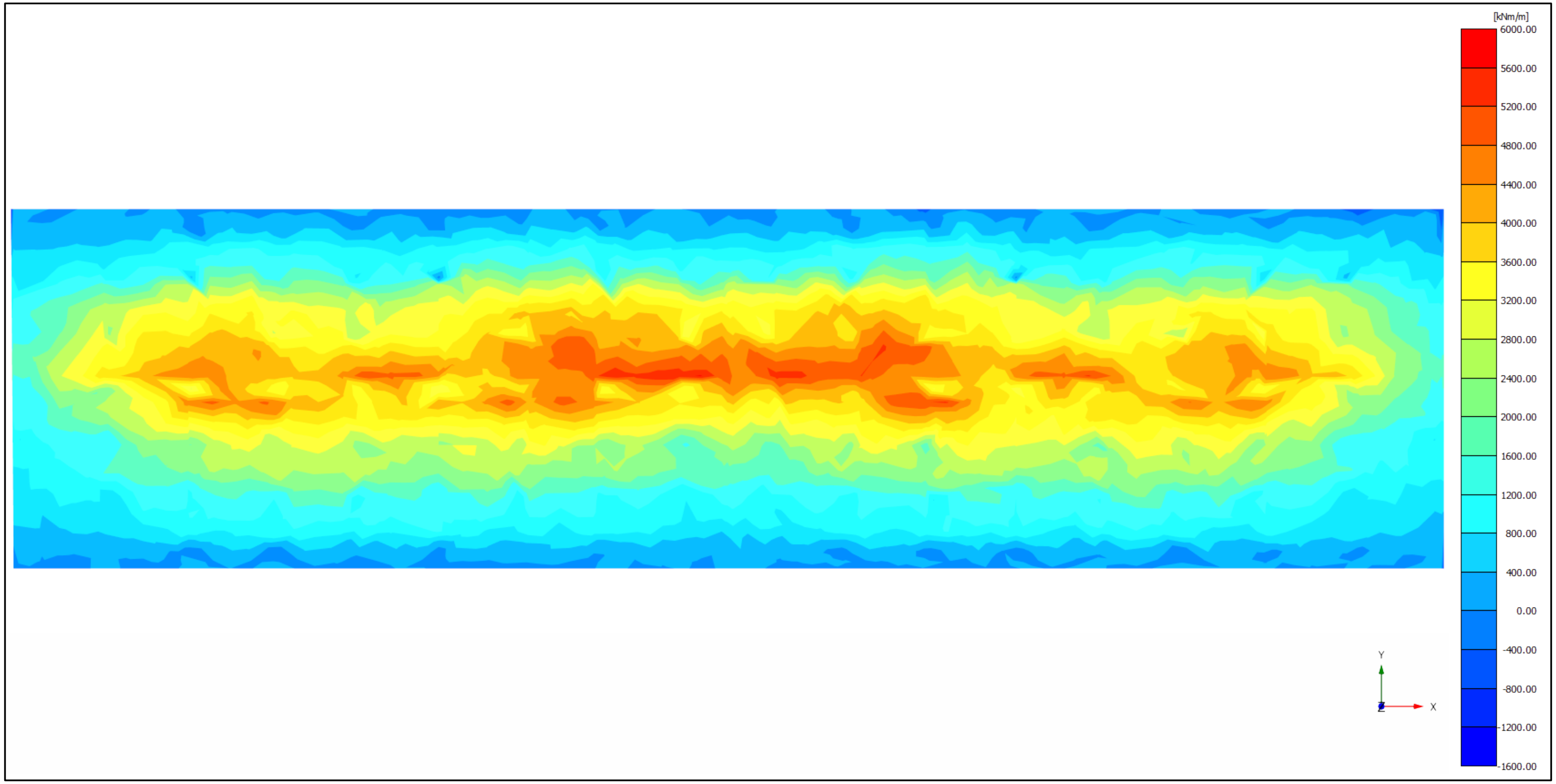

Figure 4.23 Raft moments for second model about to x-x axis (Units are kNm)

4.4 Overview of Analysis Results

The case history problem was analyzed using four different analysis methods. In order to compare obtained results with each other and field settlement values, results are summarized in Table 4.3, Figures 4.24 and 4.25, respectively.

Table 4.3 Comparison of obtained results

Method's Type	Method's Name	% of Load Carried by Piles	Settlement (mm)
Simplified	Randolph	93	36.7
	PDR	79	29.8
	Modified of PDR	93	40.5
Advanced	3D FEM (PLAXIS 3D) (Distributed Load)	71	28
	3D FEM (PLAXIS 3D) (Line Load)	75	34
-	Measured	Not Available	27.5

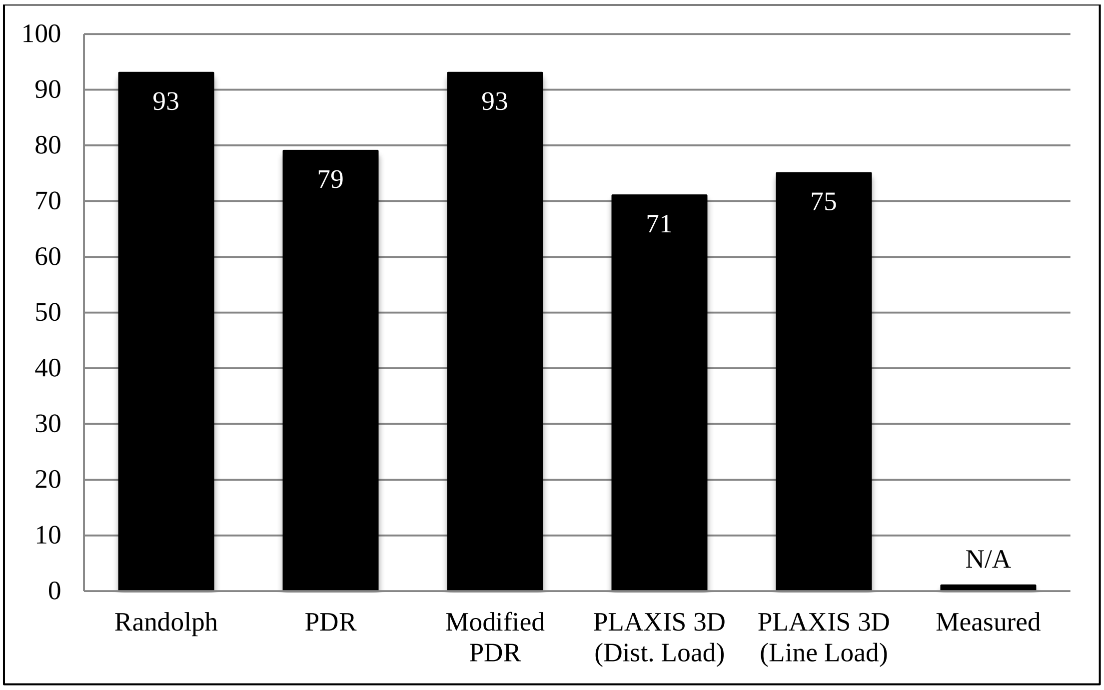

Figure 4.24 Comparison of load carried by piles according to various analysis methods (% of Total Load)

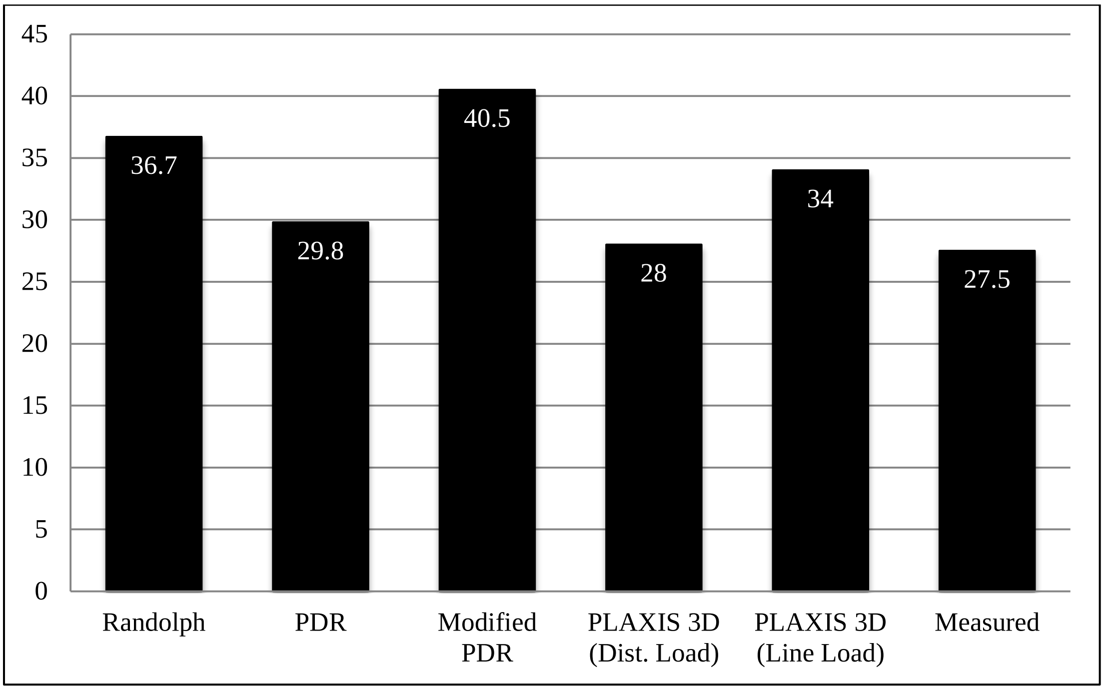

Figure 4.25 Comparison of settlement according to various analysis methods (mm)

As it is seen in Figure 4.24, load sharing ratio obtained from simplified methods is relatively higher than 3D Finite Element calculation results. Results from Randolph and Modified PDR Methods give the same and highest load sharing ratio. Both of these methods use the same load sharing calculation procedure and in this procedure, the interaction factor between raft and piles (α_{rp}) is assumed as 0.80 (for details, see Section 2.3.4.1.2). This assumption gives reasonably good results when foundation aspect ratio (foundation length / foundation width) is equal to 1 (square foundation) as shown in the hypothetical piled raft example in Chapter 3. In this example, foundation aspect ratio is relatively high (109.1 / 27.5 = 4) and α_{rp} = 0.80 assumption is not capable to represent real situation. In contrast to Randolph and Modified PDR Methods, in PDR method, the α_{rp} value is calculated by considering radius of the pile and pile influence radius (see Equation 2.31). This calculation improves the load sharing calculation ability of the method. Thus, load sharing ratio is determined as approximately 10% different -which is acceptable- from the result of 3D Finite Element Method.

Obtained maximum settlement values from different methods are compared with each other and measured settlement values in Figure 4.25. Field settlement value and computed settlement from PLAXIS 3D (distributed load model) are almost the same. Settlement from other PLAXIS 3D model (line load) is considerably higher than the measured value. It was already mentioned in section regarding PLAXIS 3D analysis results that the second (line load) model gives more realistic results than the distributed load model. It can be concluded from this situation that foundation system response in the field is better than expected. This means that soil parameters (E, c, φ) were defined relatively lower than actual soil properties. In addition, this settlement difference may be caused by ignoring superstructure stiffness in the finite element model. It is found that simplified methods give acceptable settlement values. Especially, in PDR method, obtained settlement value is very close to the measured one. Highest settlement value is obtained from Modified PDR Method because of using hyperbolic model that reduces stiffness coefficients which may improve the representation ability of the foundation response under higher load levels.

To sum up, examination of the analysis results proves that it is possible to represent almost real conditions in situ using advanced analysis techniques (3D Finite Element Method). In addition, simplified methods are valuable calculation tools for preliminary design of the piled raft foundations.

CHAPTER FIVE
CONCLUSIONS AND RECOMMENDATIONS

In scope of this thesis, the concept of piled raft foundations is introduced comprehensively with design philosophies and application examples. Calculation abilities of the piled raft analysis methods which are available in the literature are compared and such analysis methods are applied on a hypothetical piled raft example and a real life piled raft application. A back analysis is performed using analysis results from different piled raft analysis methods and real settlement measurement. Thus, efficiency of those methods is determined.

As a result of performed analyses in context of this thesis, raft's contribution on the bearing capacity of the foundation system is clearly observed. The amount of load carried by the raft primarily depends on soil strength parameters below the raft and portion of the attained load by the raft increases with increasing stiffness of the soil. Thus, stiffness of soil which supports the raft affects the design philosophy of the piled raft foundation. In circumstances where soil stiffness is relatively low (still adequate for piled raft application), load carried by the raft decreases and this minor contribution helps for reducing the required number of the piles in the foundation design (conventional approach). On the other hand, if the soil below the raft is satisfactory, significant portion of the load is carried by the raft and piles are used for controlling the overall and differential settlements (piles as settlement reducers approach). In addition, raft's bearing behavior can be enhanced by performing soil improvement. Moreover, soil profiles that are inadequate for pile raft application can gain enough strength and stiffness by means of soil improvements.

A close look to the analysis results of the hypothetical example and the case study (Chapter 3 & Chapter 4) proves that simplified methods provide valuable information at the initial stage of the foundation design. Results obtained using simplified methods are even very close to those obtained from approximate and advanced techniques when the foundation aspect ratio (L/B) is near the unity. However, achieved results deviate from each other as the aspect ratio increases. This situation is due to the simplifying assumptions regarding the determination of the interaction coefficient between the piles and the raft. Nevertheless, in some other simplified methods, this interaction factor is calculated by considering both single pile and pile group properties. These sort of simplified methods -for instance PDR Method- yield very satisfactory results as compared with advanced techniques. In a conclusion, simplified methods for piled raft analysis are essential tools for designers in estimating overall settlement of the foundation and pile-raft load sharing ratio. However, capabilities and calculation procedures of simplified methods should be investigated very carefully and they should be used depending on the problem’s properties in order to avoid misleading results.

Advanced analysis techniques, as it is expected, give the most accurate results. Especially, in the case study, 3D Finite Element Method provided very satisfactory settlement values when measured settlements are considered. However, the manner of the load assignment on the model has a considerable effect on analysis results. In the performed analysis using two different -uniformly distributed loads on the raft versus line load at the location of shear walls- load assignments, significantly different results (up to two folds) regarding the pile axial loads and raft’s internal forces are obtained. However, in the analyses, effect of superstructure stiffness on the raft was ignored and such internal forces were obtained higher than their actual values. Nevertheless, these differences become important at the structural design stage of the foundation members (piles, raft). Therefore, in situ loading conditions should be applied in the advanced piled raft analysis model. If one considers the required time and computational effort –which is significantly high- to represent field conditions, it is more convenient to perform such complex analysis methods at the final design stage.

In the piled raft concept, the load carrying capacity of the raft, which is ignored and considered as reserved bearing capacity in the conventional pile foundation approach is utilized effectively. In addition, in the piled raft approach, preliminary calculations are performed with lower safety factors. Therefore, the importance of the proper determination of the soil parameters in the piled raft foundation design is higher than the conventional pile foundation approach. Poulos et al. (2001) stated this situation as "*the key to successful prediction is more the ability to choose appropriate geotechnical parameters rather than the details of the analysis employed*". For that reason, validation of the accuracy of estimated soil parameters must be performed by conducting pile load test and required revisions should be done.

This study is focused on response of piled rafts under the static vertical loads. However, in many circumstances, dynamic loads control the design of the foundations. There is not enough study about the dynamic behavior of the piled rafts in the literature. For that reason, this study may be extended and dynamic response of the piled rafts may be investigated using suitable dynamic mathematical and physical models in the future.

REFERENCES

Bowles, J. E. (1997). *Foundation analysis and design* (5th ed.). Singapore: The McGraw-Hill Companies, Inc.

Broms, B. B. (1976). Pile foundations-pile groups, 6th ECSMFE, Vienne, Austria

Brinkgreve, R. B. J., Engin, E, & Swolfs, W. M. (2011). *Plaxis 3D 2011 reference manual*. Delft: Plaxis bv

Brown, P. T., & Wiesner, T. J. (1975). The behaviour of uniformly loaded piled strip footings. *Soils and Foundation*, 15, *13*-21.

Burland, J. B., Broms, B. B, & De Mello, V. F. B. (1977). Behaviour of foundations and structures, 9th ICSMFE, Tokyo, Japan

Burland, J. B. (1995). Piles as settlement reducers, 18th Italian Congress of Soil Mechanics, Pavia, Italy

Butterfield, R., & Banerjee, P. K. (1971). The problem of pile group-pile cap interaction. *Géotechnique, 21* (2), 135-142.

Clancy, P., & Randolph, M. F. (1993). An approximate analysis procedure for piled raft foundation. *International Journal for Numerical and Analytical Methods in Geomechanics, 17* (12), 849-869.

De Sanctis, L., Mandolini, A, Russo, G, & Viggiani, C. (2002). Some remarks on the optimum design of piled rafts. *Deep Foundations 2002: An international perspective on theory, design, construction and performance* (405-425). New York: ASCE Publication

De Sanctis, L., & Russo, G. (2008). Analysis and performance of piled rafts designed using innovative criteria. *ASCE Journal of Geotechnical and Geoenviromental Engineering*, *134* (8), 1118-1128.

Desai, C.S., Johnson, L. D., & Hargett, C. M. (1974). Analysis of pile supported gravity lock. *ASCE Journal of Geotechnical Engineering*, *100* (9), 1009-1029.

El-Mossallamy, Y. (2002). Innovative application of piled raft foundation in stiff and soft subsoil. *Deep Foundations 2002: An international perspective on theory, design, construction and performance* (426-440). New York: ASCE Publication

FEMA 356 (2000). *Prestandard and commentary for the seismic rehabilitation of buildings.* Washington D. C. : Federal Emergency Management Agency & ASCE Publications

Fleming, K., Weltman, A, Randolph, M, & Elson, K. (2009). *Piling engineering* (3rd ed.). New York: Taylor & Francis

Franke, E., Lutz, B, & El-Mossallamy, Y. (1994). Measurement and numerical modeling of high-rise building foundations on Frankfurt Clay. *Geotechnical special publication No. 40* (1325-1336). New York: ASCE Publication

Franke, E., El-Mossallamy, Y, & Wittmann, P. (2000). Calculation methods for raft foundations in Germany. *Design applications of raft foundations* (283-322). London: Thomas Telford Ltd.

Gök, S. (2007). *Kazıklı radye temellerin tasarımı.* PhD thesis. İstanbul, September 2007.

Griffiths, D. V., Clancy, P, Randolph, M. K. (1991). Piled raft foundations analysis by finite elements, 7th International Conference of Computer Methods and Advances in Geomechanics, Cairns, Australia

Hain, S. J., & Lee, I. K. (1978). The analysis of flexible raft-pile systems. *Géotechnique*, *28* (1), 65-83.

Hewitt, P. B., & Gue, S. S. (1994). Piled raft foundation in a weathered sedimentary formation, Proceedings of Geotropika, Kuala Lumpur, Malaysia

Hooper, J. A. (1973). Observations on the behavior of a piled raft foundation on London clay. *Proceedings of the Institution of Civil Engineers, 55* (2), 77-90.

Horikoshi, K., & Randolph, M. F. (1998). A contribution to optimum design of piled rafts. *Géotechnique, 48* (3), 301-317.

Katzenbach, R., Arslan, U, & Moormann, C. (2000). Piled raft foundation projects in Germany. *Design applications of raft foundations* (283-322). London: Thomas Telford Ltd.

Katzenbach, R., & Moormann, C. (2001). Recommendations for the design and construction of piled rafts, 15th ICSMFE, İstanbul, Turkey

Khoury, M. C., Alzamora, A. J, & Ciancia, A. J. (2011). A piled-raft foundation for the tallest building in Brooklyn. *Geo-Frontiers 2011: Advances in geotechnical engineering* (3818-3827). New York: ASCE Publication

Kuwabara, F. (1989). An elastic analysis for piled raft foundations in a homogeneous soils. *Soils and Foundations, 29* (1), 82-92.

Lee, I. K. (1993). Analysis and performance of raft and raft-pile system, 3rd International Conference on Case History in Geotechnical Engineering, St. Louis, Australia

Liang, F.Y., Chen, L. Z., & Shi, X. G. (2003). Numerical analysis of composite piled raft with cushion subjected to vertical load. *Computers and Geotechnics, 30* (6), 443-453.

Love, J. P. (2003). Use of settlement reducing piles to support a raft structure. *Geotechnical Engineering, 156* (4), 177-181.

Mindlin, R. D. (1936). Force at a point interior of a semi-infinite solid. *Physics, 7*, 195-202.

Ottoviani, M. (1975). Three dimensional finite element analysis of vertically loaded pile groups. *Géotechnique, 25* (2), 159-174.

Poulos, H. G. (1991). Piled raft foundations analysis by finite elements, 7th International Conference of Computer Methods and Advances in Geomechanics, Cairns, Australia

Poulos, H. G. (1993). Piled rafts in swelling or consolidating soils. *ASCE Journal of Geotechnical Engineering, 119* (2), 374-380.

Poulos, H. G. (1994). An approximate numerical analysis of pile-raft interaction. *International Journal for Numerical and Analytical Methods in Geomechanics, 18* (2), 73-92.

Poulos, H. G. (2000). Practical design procedures for piled raft foundations. *Design applications of raft foundations* (425-468). London: Thomas Telford Ltd.

Poulos, H. G. (2001a). Methods of analysis of piled raft foundations, ISSMGE TC18 Subcommittee Report

Poulos, H. G. (2001b). Piled raft foundations: Design and applications. *Géotechnique*, *51* (2), 95-113.

Poulos, H. G., & Davis, E. H. (1974). *Elastics solutions for soil and rock mechanics*. New York: John Wiley & Sons

Poulos, H. G., & Davis, E. H. (1980). *Pile foundation analysis and design*. New York: John Wiley & Sons

Poulos, H. G., Carter, J. P, & Small, T. C. (2001). Foundations and retaining structures- Research and practice, 15th ICSMFE, İstanbul, Turkey

Prakoso, W. A., & Kulhawy, F. H. (2001). Contribution to piled raft optimum design. *ASCE Journal of Getechnical and Geoenviromental Engineering, 127* (1), 17-24.

Pressley, J. S., & Poulos, H. G. (1986). Finite element analysis of mechanism of pile group behavior. *International Journal for Numerical and Analytical Methods in Geomechanics, 10* (2), 213-221.

Randolph, M. F. (1994). Design methods for pile groups and piled rafts, 13th ICSMFE, New Delhi, India

Reul, O., & Randolph, M. F. (2003). Piled rafts in overconsolidated clay: Comparison of in situ measurements and numerical analyses. *Géotechnique, 53* (3), 301-315.

Sanchez-Salinero, I. (1982). *Static and dynamic analysis of single pile.* MSc thesis. Texas, USA.

Sinha, J. (1997). *Piled raft foundations subjected to swelling and shrinking soils.* PhD thesis. Sydney, Australia.

Ta, L. D., & Small, J. C. (1996). Analysis of piled raft system in layered soils. *International Journal for Numerical and Analytical Methods in Geomechanics, 20* (1), 57-72.

Tomlinson, M., & Woodward, J. (2008). *Pile design and construction practice* (5th ed.). New York: Taylor & Francis

Yamashita, K., & Yamada, T. (2009). Settlement and load sharing of a piled raft with ground improvement on soft ground, 17th ICSMGE, Alexandria, Egypt

APPENDICES

APPENDIX A

Solution of Piled Raft Example in Chapter 3

Solution of the Hypothetical Example

Determination of the Stiffness Parameters of the System

Raft Stiffness (Poulos & Davis, 1974)

Applied load on the foundation : P=12 MN=12000 kN

Area of the raft : A=8*8=64 m^2

Radius of equivalent circular raft : a=$\sqrt{\frac{64}{\pi}} = 4.51$ m

Depth of soil layer to incompressible level : h=30 m

$P_{av} = \frac{P}{\pi a^2} = \frac{12000}{\pi * 4.51^2} = 187.5$ kN/m^2 and $a/h = 4.51/30 = 0.15$

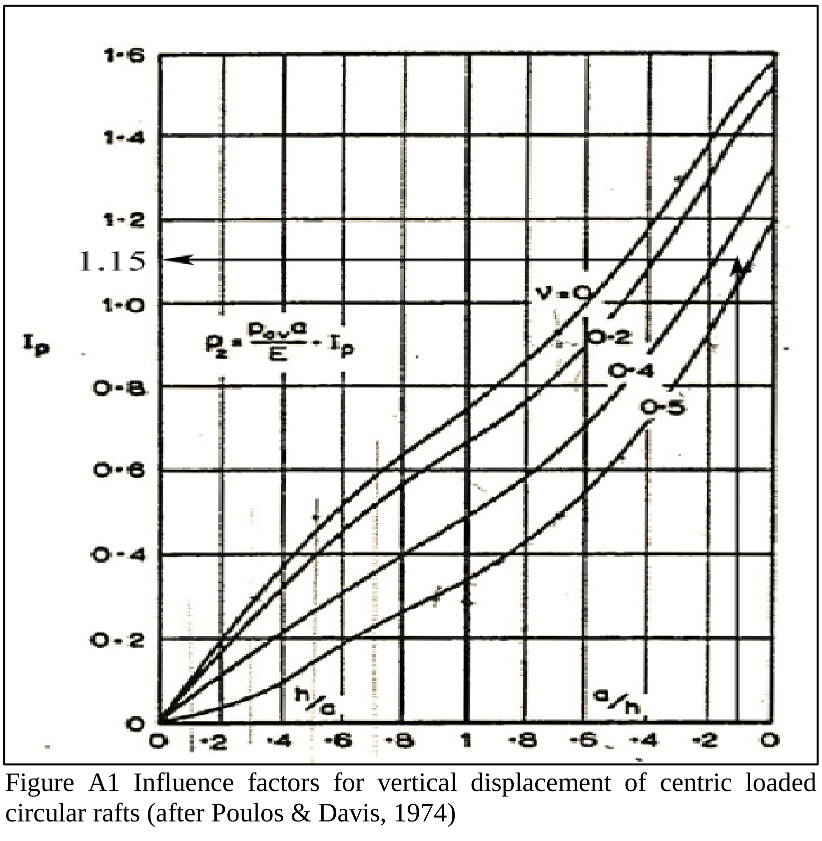

Figure A1 Influence factors for vertical displacement of centric loaded circular rafts (after Poulos & Davis, 1974)

Using Figure A1 I_p is obtained as 1.15.

Vertical displacement : $\rho_z = \dfrac{P_{av}a}{E_s} I_p = \dfrac{187.5*4.51}{50000}*1.15 = 0.0194m$

Axial stiffness of the raft : $K_r = \dfrac{P}{\rho_z} = \dfrac{12000}{0.0194} = 615$ MN/m

Single Pile and Pile Group Stiffnesses (Randolph, 1994)

Applied load on pile : P_t = 1000 kN (Arbitrary Value)

Pile length : l=15 m

Shear modulus of soil at depth of l : $G_l = \dfrac{E_l}{2(1+\nu)} = \dfrac{50000}{2(1+0.45)} = 17250$ kN/m^2

Pile radius : r_o =0.40 m

Pile radius at the base of the pile : r_b =0.40 m

Shear modulus of soil at depth of pile base : G_b =17250 kN/m^2

Average shear modulus of soil along the pile : G_{avg} =17250 kN/m^2

Elasticity modulus of pile : E_p =30000 MPa

$\eta = r_b / r_0 = 1$

$\xi = G_l / G_b = 1$

$\rho = G_{avg} / G_l = 1$

$\lambda = E_p / G_l = 1739.130$

$r_m = \left\{0.25 + \xi\left[2.5\rho(1-\nu) - 0.25\right]\right\} l = 20.625$

$\zeta = \ln(r_m / r_0) = 3.942$

$\mu l = \sqrt{\dfrac{2}{\zeta\lambda(l/r_0)}} = 0.002789$

$$\frac{P_t}{G_l r_0 w_t} = \frac{\dfrac{4\eta}{(1-\nu)\xi} + \rho\dfrac{2\pi}{\zeta}\dfrac{\tanh(\mu l)}{\mu l}\dfrac{l}{r_0}}{1 + \dfrac{1}{\pi\lambda}\dfrac{4\eta}{(1-\nu)\xi}\dfrac{\tanh(\mu l)}{\mu l}\dfrac{l}{r_0}} \text{ and } w_t = 0.0023 \text{ m}$$

Single pile stiffness : $k_p = \dfrac{P_t}{w_t} = \dfrac{1000}{0.0023} = 441$ MN/m

Pile group stiffness : $K_p = k_p\sqrt{n} = 441*\sqrt{9} = 1320$ MN/m

Randolph Method (Randolph, 1994)

Load Sharing Ratio between Piles and Raft

$$\frac{P_r}{P_p} = \frac{0.2}{1-0.8\left(\frac{K_r}{K_p}\right)}\frac{K_r}{K_p} = \frac{0.20}{1-0.80\left(\frac{615}{1320}\right)} * \frac{615}{1320} = 0.15 = \alpha$$

$$\frac{P_p}{P_t} = \frac{1}{1+\alpha} = \frac{1}{1+0.15} = 0.87 \text{ (87\% of total load carried by piles)}$$

Settlement of the Foundation (Elastic)

Stiffness of piled raft : $K_{pr} = \dfrac{1-0.6\left(\frac{K_r}{K_p}\right)}{1-0.64\left(\frac{K_r}{K_p}\right)} K_p$

$$K_{pr} = \frac{1-0.60\left(\frac{615}{1320}\right)}{1-0.64\left(\frac{615}{1320}\right)} * 1320 = 1355 \text{ MN/m}$$

Elastic settlement of the system : s $= \dfrac{P}{K_{pr}} = \dfrac{12MN}{1355MN/m} = 8.85$ mm

Poulos-Davis-Randolph Method (Poulos, 2001)

Ultimate Vertical Load Capacity of Pile Group

Pile diameter : D=0.80 m

Pile length : l=15 m

Undrained cohesion of the soil : $c_u = 50$ kN/m^3

Adhesion factor for pile : α=0.65

Single pile load capacity : Q_{c1} = Friction resistance + Tip resistance

Pile group capacity : Q_c = Number of pile * Q_{s1}

$$Q_c = n(\pi D L c_u \alpha + 9c_u) = 9(\pi * 0.80 * 15 * 50 * 0.65 + 9 * 50) = 15075 \text{ kN}$$

Raft contributes the bearing capacity of the pile group via its direct contact area with soil.

Bearing capacity of the raft (stress) : $q_b = N_c c_u \cong 6c_u = 300 \text{ kN/m}^2$

Raft contact area outside of the pile group $\cong$ (2*0.60*5.20)+(2*8*0.60)=16 m^2

Raft's contribution $= q_b A_{conctact} = 300 * 16 = 4800$ kN

Bearing capacity of the pile group: $P_{up} = 15075 + 4800 = 19875$ kN

Load Sharing Ratio between Piles and Raft

Pile-raft interaction factor : $\alpha_{rp} = 1 - \dfrac{\ln(r_c / r_0)}{\zeta}$

$$r_c = \frac{\text{Area of raft}}{\text{Number of piles}} = \frac{64}{9} = 7.11 \text{ m}$$

$\zeta = 3.942$ (from pile stiffness calculations)

$$\alpha_{rp} = 1 - \frac{\ln(7.11/0.4)}{3.942} = 0.27$$

$$\frac{P_r}{P_r + P_p} = X = \frac{K_r\left(1-\alpha_{rp}\right)}{K_p + \left(1-2\alpha_{rp}\right)K_r} = \frac{615*(1-0.27)}{1320+(1-2*0.27)*615} = 0.28$$

$1 - X = 0.72$ (72% of total load carried by piles)

Settlement of the Foundation (Elastic)

$$K_{pr} = \frac{K_p + \left(1-2\alpha_{rp}\right)K_r}{1-\alpha_{rp}{}^2\left(\dfrac{K_r}{K_p}\right)} = \frac{1320+\left(1-2*0.27\right)*615}{1-0.27^2*\left(\dfrac{615}{1320}\right)} = 1660 \text{ MN/m}$$

$$P_1 = \frac{P_{up}}{1-X} = \frac{19875}{1-0.27} = 27604 \text{ kN}$$

$P = 12000$ kN < P_1 =27604 kN

Elastic settlement of the system : $s = \dfrac{P}{K_{pr}} = \dfrac{12 \text{ MN}}{1660 \text{ MN/m}} = 7.23 \text{ mm}$

Modified Version of Poulos-Davis-Randolph Method (Poulos, 2000)

Load Sharing Ratio between Piles and Raft

Vertical load at "Point A" : $\mathrm{V}_A = \dfrac{V_{pu}}{\beta_p}$

V_{pu} :Ultimate vertical load capacity (equal to P_{up} from previous section)

$V_{pu} = P_{up} = 19875 \text{ kN}$

β_p is assumed as 0.85 for first approximation.

$V_A = \dfrac{V_{pu}}{\beta_p} = \dfrac{19875}{0.85} = 23380 \text{ kN}$

V_p and V_r : Load carried by piles and raft, respectively

$V_p = 0.85 * 12000 = 10200 \text{ kN}$

$\mathrm{V}_r = (1 - 0.85) * 12000 = 1800 \text{ kN}$

V_{pu} and V_{ru} : Ultimate load capacity of piles and raft, respectively

$V_{pu} = 19875 \text{ kN}$

$V_{ru} = A_{raft} * 6c_u = (8*8)*6*50 = 19200 \text{ kN}$

K_{pi} and K_{ri} = Initial stiffnesses of pile group and raft

$K_{pi} = 1320 \text{ MN/m}$

$K_{ri} = 615 \text{ MN/m}$

R_{fp} and R_{fr} =Hyperbolic factor for pile group and raft

$R_{fp} = 0.50$ and $\mathrm{R}_{fr} = 0.75$ (Poulos, 2000)

$K_p = K_{pi}\left(1 - R_{fp}\dfrac{V_p}{V_{pu}}\right) = 1320 * \left(1 - 0.50 * \dfrac{10200}{19875}\right) = 981 \text{ MN/m}$

$$K_r = K_{ri}\left(1 - R_{fr}\frac{V_r}{V_{ru}}\right) = 615 * \left(1 - 0.75 * \frac{1800}{19200}\right) = 571 \text{ MN/m}$$

$$a = \frac{0.2}{1 - 0.8(K_r / K_p)}\left(\frac{K_r}{K_p}\right) = \frac{0.20}{1 - 0.80(571/981)} * \left(\frac{571}{981}\right) = 0.22$$

$$\beta_{p,calculated} = \frac{1}{1+\alpha} = \frac{1}{1+0.22} = 0.82$$

$$\beta_{p,calculated} \neq \beta_{p,assumed}$$

New assumed $\beta_p = 0.82$

$$V_p = 0.82 * 12000 = 9840 \text{ kN}$$

$$\mathrm{V}_r = (1 - 0.82) * 12000 = 2160 \text{ kN}$$

$$K_p = K_{pi}\left(1 - R_{fp}\frac{V_p}{V_{pu}}\right) = 1320 * \left(1 - 0.50 * \frac{9840}{19875}\right) = 993 \text{ MN/m}$$

$$K_r = K_{ri}\left(1 - R_{fr}\frac{V_r}{V_{ru}}\right) = 615 * \left(1 - 0.75 * \frac{2160}{19200}\right) = 563 \text{ MN/m}$$

$$a = \frac{0.2}{1 - 0.8(K_r / K_p)}\left(\frac{K_r}{K_p}\right) = \frac{0.20}{1 - 0.80(571/981)} * \left(\frac{563}{993}\right) = 0.21$$

$$\beta_{p,calculated} = \frac{1}{1+\alpha} = \frac{1}{1+0.21} \cong 0.82$$

$\beta_{p,calculated} = \beta_{p,assumed} = 0.82$ (82% of total load carried by piles)

Settlement of the Foundation (Elastic)

$$X = \frac{1 - 0.60\left(\frac{K_r}{K_p}\right)}{1 - 0.64\left(\frac{K_r}{K_p}\right)} = \frac{1 - 0.60 * \left(\frac{563}{993}\right)}{1 - 0.64 * \left(\frac{563}{993}\right)} = 1.04$$

$$V = 12000 \text{ kN} < V_A = 23380 \text{ kN}$$

$$S = \frac{V}{XK_{pi}\left(1-\frac{R_{fp}\beta_p V}{V_{pu}}\right)} = \frac{12}{1.04*1320*\left(1-\frac{0.5*0.82*12}{19.875}\right)} = 11.60 \text{ mm}$$

Elastic settlement of the system : S = 11.60 mm

Incremental Load Step Method (Gök, 2007)

In this method, pile group and raft are considered separately and their individual settlement values were calculated from elastic settlement formulation as shown below.

$$\rho = \frac{\mu_0 * \mu_1 * q * B}{E}$$

where;

ρ = Elastic settlement of the raft

q = Applied vertical stress

B = Width of raft

E = Elasticity modulus of soil

μ_0, μ_1 = Correction factors depend on L/B, H/B and D/B (see Figure A1.2)

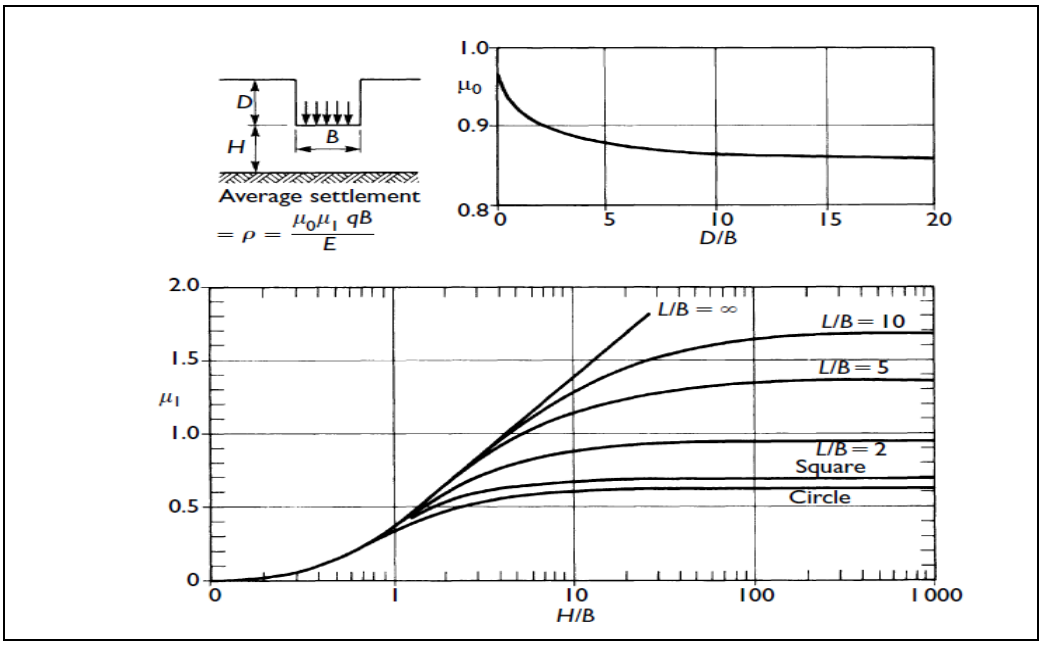

Figure A2 Elastic raft settlement correction factors, μ_1, μ_2 (Tomlinson & Woodward, 2008)

In order to obtain the settlement of the pile group, equivalent raft approach was used.

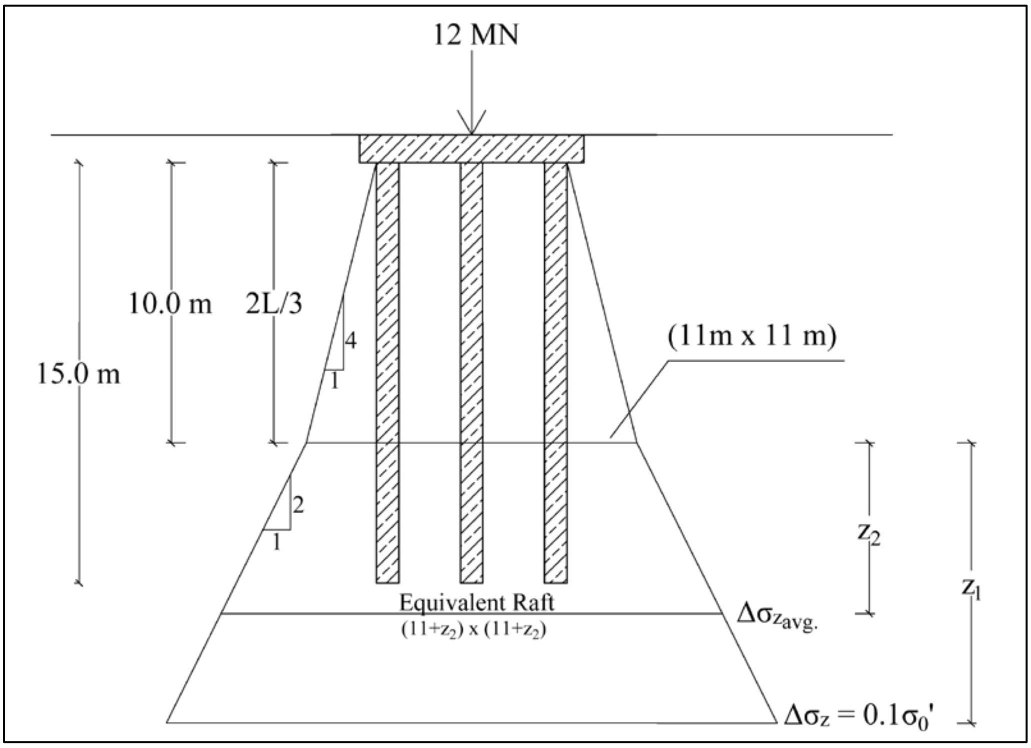

Figure A3 Representation of equivalent raft

Load-settlement response of raft and pile group is shown in the Table A1.1

Table A1 Incremental load step approach load-settlement table

% of Load Ratio (P_{Pile}/P_{total})	P_{raft} (kN)	$P_{pile\ Group}$ (kN)	Depth of $\Delta\sigma_Z=0.1\sigma_0'$ from 2L/3 z_1 (m)	Average Stress Increase of Equivalent Raft (kN/m^2)	Depth of Equivalent Raft from 2L/3 z_2 (m)	Width of Equivalent Raft (m)	Settlement of Raft Alone (mm)	Settlement of Pile Group (mm)
0	12000	0	-	-	-	8	15.91	0
10	10800	1200	0	9.91	0	11	14.32	0.96
20	9600	2400	2.73	15.89	1.29	12.29	12.73	1.72
30	8400	3600	4.67	20.9	2.12	13.12	11.14	2.41
40	7200	4800	6.21	25.4	2.75	13.75	9.55	3.07
50	6000	6000	7.51	29.56	3.25	14.25	7.96	3.71
60	4800	7200	8.65	33.46	3.67	14.67	6.36	4.32
70	3600	8400	9.67	37.18	4.03	15.03	4.77	4.92
80	2400	9600	10.52	40.88	4.32	15.32	3.18	5.51
90	1200	10800	11.44	44.21	4.63	15.63	1.59	6.08
100	0	12000	12.23	47.55	4.89	15.89	0.00	6.65

Load sharing ratio and the overall settlement of the system was obtained by plotting the % of total load versus settlement of the raft and pile group separately. Intersection point gives the system's load sharing ratio and overall settlement.

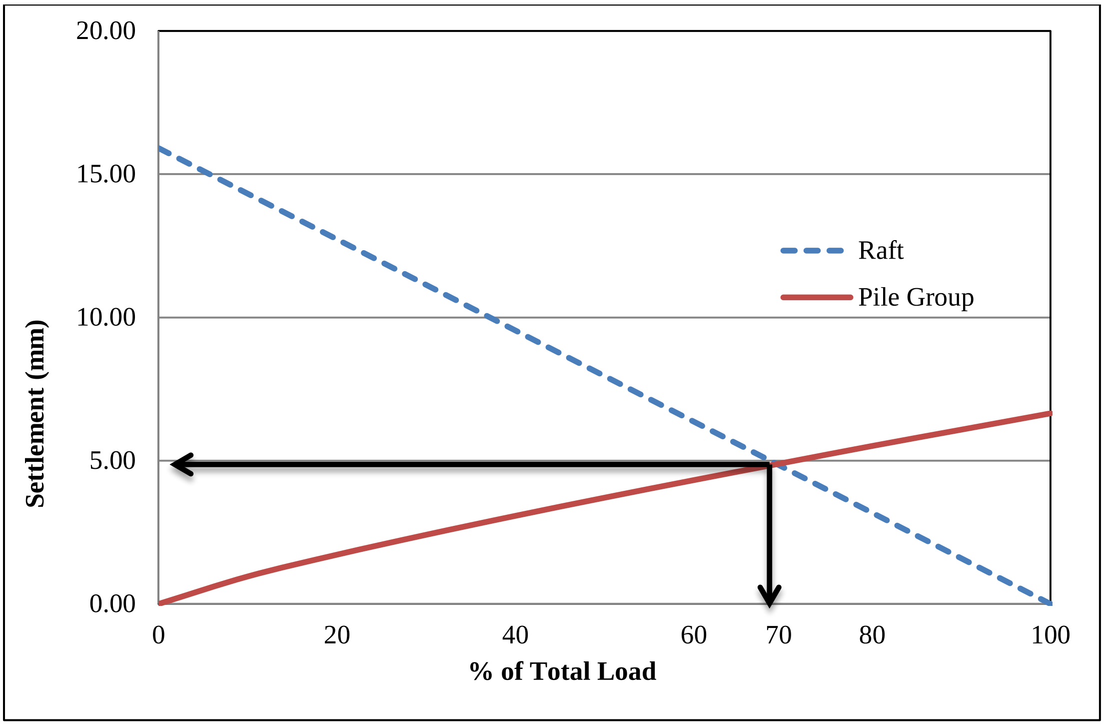

Figure A4 Load-settlement relationship of raft and pile group

APPENDIX B

Solution of the Case Study in Chapter 4

Solution of the Case Study

Determination of the Stiffness Parameters of the System

Raft Stiffness (FEMA 356, 2000)

$$K_{emb} = K_{z,sur} * \beta_z$$

$$K_{z,sur} = \frac{GB}{1-\nu}\left[1.55\left(\frac{L}{B}\right)^{0.75} + 0.80\right]$$

$$\beta_z = \left[1+\frac{1}{21}\frac{D}{B}\left(2+2.6\frac{B}{L}\right)\right]\left[1+0.32\left(\frac{d(B+L)}{BL}\right)^{2/3}\right]$$

where ;

K_{emb} = Embedded raft's axial stiffness

$K_{z,sur}$ = Axial stiffness of raft which placing on the surface

β_z = Axial stiffness correction factor for embedded rafts

G = Shear modulus of soil below the raft

ν = Poisson's ratio of soil

L, B = Length and width of rafts, respectively

d = Actual embedded depth of raft (if basement floor exists d=D)

D = Depth of raft

$$G = \frac{E}{2(1+\nu)} = \frac{45850}{2(1+0.30)} = 17635 \text{ kN/m}^2 \quad \text{and } \nu = 0.30$$

$L = 109.1$ m. B=27.5 m. d=5.3 m. D=5.3 m.

$$K_{z,sur} = \frac{17635*27.50}{1-0.30}\left[1.55\left(\frac{109.1}{27.50}\right)^{0.75} + 0.80\right] = 3575 \text{ MN/m}$$

$$\beta_z = \left[1+\frac{1}{21}*\frac{5.3}{27.50}*\left(2+2.6*\frac{27.50}{109.1}\right)\right]\left[1+0.32*\left(\frac{5.3*(27.50+109.1)}{(27.50*109.1)}\right)^{2/3}\right]$$

$$\beta_z = 1.15$$

$$K_{z,emb} = 3575*1.15 = 4110 \text{ MN/m}$$

Axial stiffness of the raft = 4110 MN/m

Single Pile and Pile Group Stiffnesses (Randolph, 1994)

Single Pile Stiffness (Randolph, 1994)

Applied load on pile : P_t = 1000 kN (Arbitrary Value)
Pile length : l = 34.50 m
Shear modulus of soil at depth of l : $G_l = \dfrac{E_l}{2(1+\nu)} = \dfrac{100000}{2(1+0.30)} = 38460$ kN/m^2
Pile radius : r_o = 0.60 m
Pile radius at the base of the pile : r_b = 0.60 m
Shear modulus of soil at depth of pile base : G_b = 38460 kN/m^2
Average shear modulus of soil along the pile : G_{avg}

$$G_{avg} = \frac{E_{avg}}{2(1+\nu)} = \frac{\dfrac{(5.2*45850)+(9.5*38400)+(12*25000)+(7.8*100000)}{34.50}}{2(1+0.30)}$$

G_{avg} = 18765 kN/m^2
Elasticity modulus of pile : E_p = 30000 MPa

$\eta = r_b / r_0 = 1$
$\xi = G_l / G_b = 1$
$\rho = G_{avg} / G_l = 0.488$
$\lambda = E_p / G_l = 780.03$
$r_m = \left\{0.25 + \xi\left[2.5\rho(1-\nu) - 0.25\right]\right\} l = 29.46$
$\zeta = \ln(r_m / r_0) = 3.892$
$\mu l = \sqrt{\dfrac{2}{\zeta\lambda(l/r_0)}} = 0.003384$

$$\frac{P_t}{G_l r_0 w_t} = \frac{\dfrac{4\eta}{(1-\nu)\xi} + \rho\dfrac{2\pi}{\zeta}\dfrac{\tanh(\mu l)}{\mu l}\dfrac{l}{r_0}}{1 + \dfrac{1}{\pi\lambda}\dfrac{4\eta}{(1-\nu)\xi}\dfrac{\tanh(\mu l)}{\mu l}\dfrac{l}{r_0}} \quad \text{and } w_t = 0.0009639 \text{ m}$$

Single pile stiffness : $k_p = \dfrac{P_t}{w_t} = \dfrac{1000}{0.0009639} = 1037.4$ MN/m

Pile Group Stiffness (Randolph, 1994)

$$K_p = k_p * n^{1-e}$$

where ;
K_p = Pile group stifness
k_p = Single pile stiffness
n = Number of pile in the pile group
e = Group efficiency exponent

$$e = e_1 * c_1 * c_2 * c_3 * c_4$$

where ;
e_1 = Initial group efficiency exponent depend on slenderness ratio
c_1 = Exponent correction factor depend on stiffness ratio
c_2 = Exponent correction factor depend on pile spacing
c_3 = Exponent correction factor depend on homogenity
c_4 = Exponent correction factor depend on Poisson's ratio

Slenderness ratio: L/d
$L / d = 34.50 / 1.20 = 28.75$
Stiffness ratio: E_p / G_l
$E_p / G_l = 3*10^7 / 38460 = 780$
$\log(E_p / G_l) = 2.90$
Pile spacing: s/d
$s_{avg} = (6.30 + 4.25) / 2 = 5.275$ m
$s_{avg} / d = 5.275 / 1.2 = 4.4$
Homogenity: ρ
$\rho = G_{avg} / G_l = 18765 / 38460 = 0.50$
Poisson's ratio: ν
$\nu = 0.30$

Obtained coefficients are shown in the Figures B1 and B2 below:

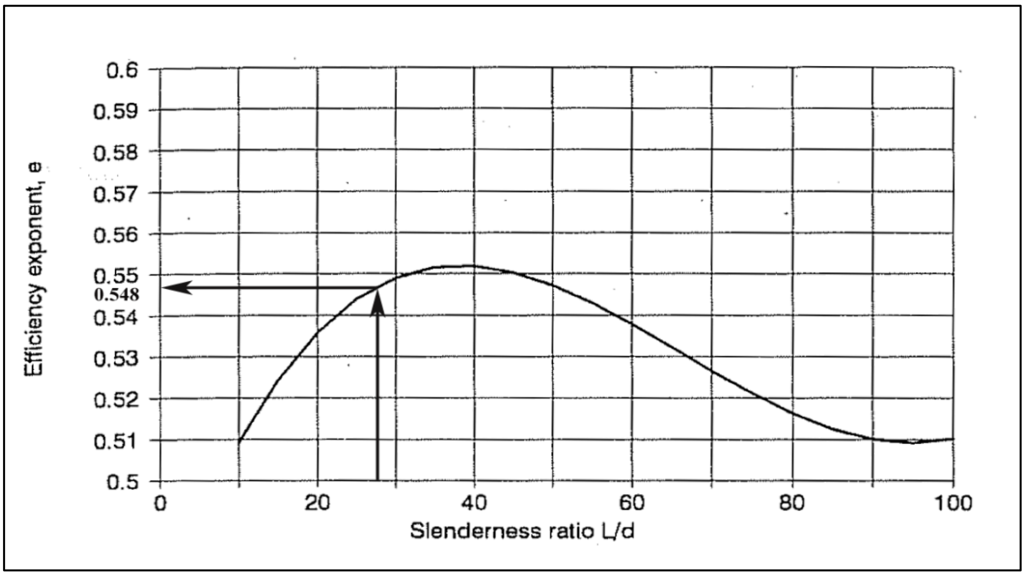

Figure B1 Efficiency exponent for pile group stiffness (after Randolph, 1994)

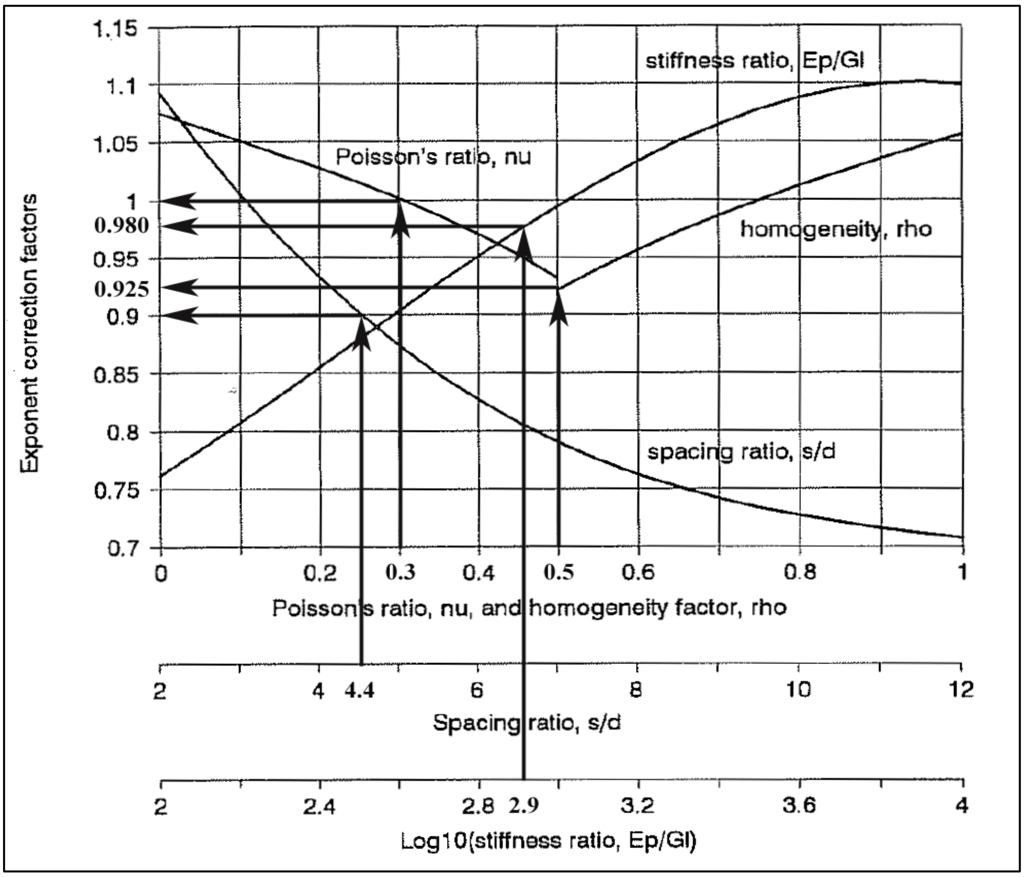

Figure B2 Exponent correction factors (after Randolph, 1994)

$e = 0.548 * 0.98 * 0.90 * 0.925 * 1.0$
$e = 0.45$

$K_p = k_p * n^{1-e}$

$K_p = 1037.4 * 126^{1-0.45}$

$K_p = 14830$ MN/m

Pile group stiffness : K_p = 14830 MN/m

Randolph Method (Randolph, 1994)

Load Sharing Ratio between Piles and Raft

$$\frac{P_r}{P_p} = \frac{0.2}{1 - 0.8\left(\frac{K_r}{K_p}\right)} \frac{K_r}{K_p} = \frac{0.20}{1 - 0.80\left(\frac{4110}{14830}\right)} * \frac{4110}{14830} = 0.07 = \alpha$$

$$\frac{P_p}{P_t} = \frac{1}{1+\alpha} = \frac{1}{1+0.07} = 0.93 \text{ (93\% of total load carried by piles)}$$

Settlement of the Foundation (Elastic)

Stiffness of piled raft : $K_{pr} = \dfrac{1 - 0.6\left(\frac{K_r}{K_p}\right)}{1 - 0.64\left(\frac{K_r}{K_p}\right)} K_p$

$$K_{pr} = \frac{1 - 0.60\left(\frac{4110}{14830}\right)}{1 - 0.64\left(\frac{4110}{14830}\right)} * 14830 = 15030 \text{ MN/m}$$

Weight of the structure : P $\cong$ 551 MN

Elastic settlement of the system : $s = \dfrac{P}{K_{pr}} = \dfrac{551 MN}{15030 MN/m} = 36.7$ mm

Poulos-Davis-Randolph Method (Poulos, 2001)

Ultimate Vertical Load Capacity of Pile Group

Single Pile Axial Load Capacity

Pile type : Post grouted bored pile

Pile diameter : D = 1.2 m.

Pile length : l = 34.5 m.

Pile starting depth = 5.3 m.

$K_s / K_0 = 1$

$\alpha = 0.80$

SP-SM Layer (5.30 - 10.5 m)

$\sigma_v'{}_{@5.3} = 1*18 + 4.3*8 = 52.4$ kN/m^2

$\sigma_v'{}_{@10.5} = 1*18 + 9.5*8 = 94$ kN/m^2

$\sigma_v'{}_{avg.} = \dfrac{52.4 + 94}{2} = 73.2$ kN/m^2

$\phi'_{sp} = \frac{2}{3}\phi' = 20.3°$

$K_0 = 1 - \sin\phi' = 1 - \sin 30.5 = 0.49$

$q_s = K_s * \sigma_v'{}_{avg.} * \tan\phi'_{sp}$

$q_s = 0.49 * 73.2 * \tan 20.3 = 13.2$ kN/m^2

$A_s = \pi * D * h = \pi * 1.2 * (10.5 - 5.30) = 19.60$ m^2

$Q_s = q_s * A_s = 13.2 * 19.60 = 260$ kN

CH Layer (10.5 - 20 m)

$q_s = \alpha * c_u$

$q_s = 0.80 * 52 = 41.6$ kN/m^2

$A_s = \pi * D * h = \pi * 1.2 * (20 - 10.5) = 35.8$ m^2

$Q_s = q_s * A_s = 41.6 * 35.8 = 1490$ kN

CL Layer (20 - 32 m)

$q_s = \alpha * c_u$

$q_s = 0.80 * 45 = 36$ kN/m^2

$A_s = \pi * D * h = \pi * 1.2 * (32 - 20) = 45.2$ m^2

$Q_s = q_s * A_s = 36 * 45.2 = 1625$ kN

SC Layer (32 - 39.8 m)

$q_s = \alpha * c_u$

$q_s = 0.80 * 65 = 52 \text{ kN/m}^2$

$A_s = \pi * D * h = \pi * 1.2 * (39.8 - 32) = 29.4 \text{ m}^2$

$Q_s = q_s * A_s = 52 * 29.4 = 1530 \text{ kN}$

$q_b = N_q{}^* * \sigma_v{}'_{@\,pile-tip}$

$\sigma_v{}'_{@\,pile-tip} = 1*18 + 4.3*8 + 5.2*8 + 9.5*9 + 12*10 + 7.8*10 = 377.5 \text{ kN/m}^2$

Pile slenderness ratio : 34.50/1.2 = 28.75

$\text{N}_q{}^* = 40$ (from Berezantsev's method -see Figure B3-)

$q_b = 40 * 377.5 = 15100 \text{ kN/m}^2$

$Q_b = A_b * q_b$

$A_b = \dfrac{\pi D^2}{4} = \dfrac{\pi * 1.2^2}{4} = 1.13 \text{ m}^2$

$Q_b = 1.13 * 15100 = 17065 \text{ kN}$

(Base resistance value will not be reduced because of post-grout operation)

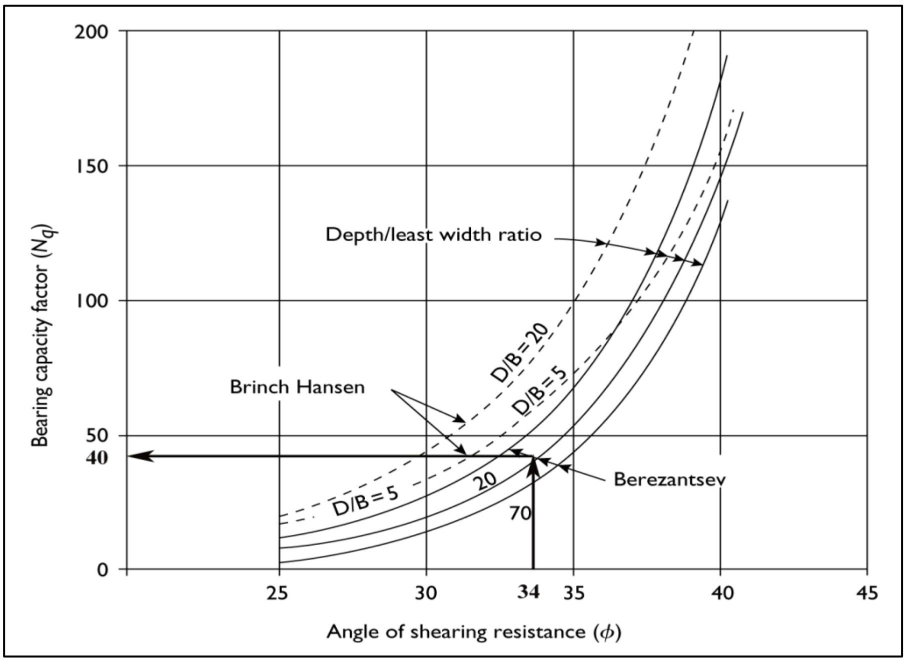

Figure B3 Obtaining bearing capacity factor ($N_q{}^*$) with Berezantsev's Method (after Tomlinson & Woodward, 2008)

$Q_p = Q_b + \sum Q_s$

$Q_p = 17065 + (260 + 1490 + 1625 + 1530)$

$Q_p = 21970 \text{ kN}$

Raft's Bearing Capacity (Only Raft)

Raft's bearing capacity is determined by calculating the stress that causes the 50 mm (which is generally accepted as limit settlement value for rafts) of elastic raft settlement.

$$\rho = \frac{\mu_0 * \mu_1 * q * B}{E}$$

where;

ρ = Elastic settlement of the raft

q = Applied vertical stress

B = Width of raft

E = Elasticity modulus of soil

μ_0, μ_1 = Correction factors depend on L/B, H/B and D/B (see Figure B4)

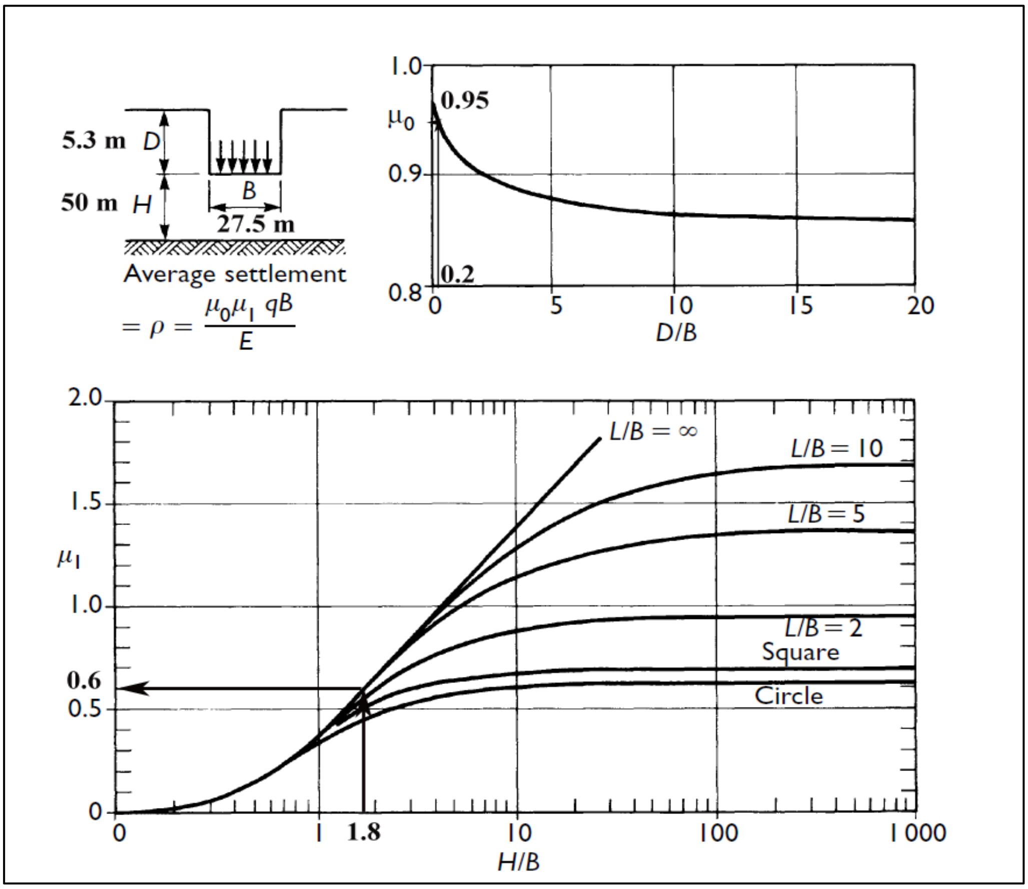

Figure B4 Obtaining elastic raft settlement correction factors, μ_1, μ_2 (after Tomlinson & Woodward, 2008)

μ_0 and μ_1 are determined as 0.95 and 0.60, respectively.

$$\rho = \frac{\mu_0 * \mu_1 * q * B}{E}$$

$$0.05 = \frac{0.95 * 0.60 * q * 27.50}{45850}$$

$q = 146.25$ kN/m^2

Axial Load Capacity of Raft: Q_r

$Q_r = q * A_r = 146.25 * (27.50 * 109.1) = 438.8$ MN

Load Sharing Ratio between Piles and Raft

Pile-raft interaction factor : $\alpha_{rp} = 1 - \dfrac{\ln(r_c / r_0)}{\zeta}$

$$r_c = \frac{\text{Area of raft}}{\text{Number of piles}} = \frac{3000.25}{126} = 23.81 \text{ m}$$

$\zeta = 3.892$ (from pile stiffness calculations)

$$\alpha_{rp} = 1 - \frac{\ln(23.81 / 0.6)}{3.892} = 0.054$$

$$\frac{P_r}{P_r + P_p} = X = \frac{K_r\left(1 - \alpha_{rp}\right)}{K_p + \left(1 - 2\alpha_{rp}\right)K_r} = \frac{4110 * (1 - 0.054)}{14830 + (1 - 2 * 0.054) * 4110} = 0.21$$

$1 - X = 0.79$ (79 % of total load carried by piles)

Settlement of the Foundation (Elastic)

$$K_{pr} = \frac{K_p + \left(1 - 2\alpha_{rp}\right)K_r}{1 - \alpha_{rp}{}^2\left(\dfrac{K_r}{K_p}\right)} = \frac{14830 + \left(1 - 2 * 0.054\right) * 4110}{1 - 0.054^2 * \left(\dfrac{4110}{14830}\right)} = 18515 \text{ MN/m}$$

Pile group's bearing capacity : P_{up}

$P_{up} = Q_p * n = 21970 * 126 = 2768.3$ MN

$$P_1 = \frac{P_{up}}{1 - X} = \frac{2768.3}{1 - 0.21} = 3505 \text{ MN}$$

$P = 551$ MN < P_1 =3505 MN

Elastic settlement of the system : $s = \dfrac{P}{K_{pr}} = \dfrac{551 \text{ MN}}{18515 \text{ MN/m}} = 29.8$ mm

Modified Version of Poulos-Davis-Randolph Method (Poulos, 2000)

Load Sharing Ratio between Piles and Raft

Vertical load at "Point A" : $\mathrm{V}_A = \dfrac{V_{pu}}{\beta_p}$

V_{pu} :Ultimate vertical load capacity (equal to P_{up} from previous section)

$V_{pu} = P_{up} = 2768.3$ MN

β_p is assumed as 0.85 for first approximation.

$$V_A = \frac{V_{pu}}{\beta_p} = \frac{2768.3}{0.85} = 3256.8 \text{ MN}$$

V_p and V_r : Load carried by piles and raft, respectively

$V_p = 0.85 * 551 = 468.4$ MN

$\mathrm{V}_r = (1 - 0.85) * 551 = 82.6$ MN

V_{pu} and V_{ru} : Ultimate load capacity of piles and raft, respectively

$V_{pu} = 2768.3$ MN

$V_{ru} = 438.8$ MN

K_{pi} and K_{ri} = Initial stiffnesses of pile group and raft

$K_{pi} = 14830$ MN/m

$K_{ri} = 4110$ MN/m

R_{fp} and R_{fr} =Hyperbolic factor for pile group and raft

$R_{fp} = 0.50$ and $\mathrm{R}_{fr} = 0.75$ (Poulos, 2000)

$$K_p = K_{pi}\left(1 - R_{fp}\frac{V_p}{V_{pu}}\right) = 14830 * \left(1 - 0.50 * \frac{468.4}{2768.3}\right) = 13575.4 \text{ MN/m}$$

$$K_r = K_{ri}\left(1 - R_{fr}\frac{V_r}{V_{ru}}\right) = 4110 * \left(1 - 0.75 * \frac{82.6}{438.8}\right) = 3529.7 \text{ MN/m}$$

$$a = \frac{0.2}{1-0.8(K_r / K_p)}\left(\frac{K_r}{K_p}\right) = \frac{0.20}{1-0.80(3529.7/13575.4)} * \left(\frac{3529.7}{13575.4}\right) = 0.066$$

$$\beta_{p,calculated} = \frac{1}{1+\alpha} = \frac{1}{1+0.066} = 0.94$$

$$\beta_{p,calculated} \neq \beta_{p,assumed}$$

New assumed $\beta_p = 0.94$

$$V_p = 0.94 * 551 = 517.9 \text{ MN}$$

$$\mathrm{V}_r = (1-0.94) * 551 = 33.1 \text{ MN}$$

$$K_p = K_{pi}\left(1 - R_{fp}\frac{V_p}{V_{pu}}\right) = 14830 * \left(1 - 0.50 * \frac{517.9}{2768.3}\right) = 13442.8 \text{ MN/m}$$

$$K_r = K_{ri}\left(1 - R_{fr}\frac{V_r}{V_{ru}}\right) = 4110 * \left(1 - 0.75 * \frac{33.1}{438.8}\right) = 3877.5 \text{ MN/m}$$

$$a = \frac{0.2}{1-0.8(K_r / K_p)}\left(\frac{K_r}{K_p}\right) = \frac{0.20}{1-0.80(3877.5/13442.8)} * \left(\frac{3877.5}{13442.9}\right) = 0.075$$

$$\beta_{p,calculated} = \frac{1}{1+\alpha} = \frac{1}{1+0.075} = 0.93$$

$$\beta_{p,calculated} \neq \beta_{p,assumed}$$

New assumed $\beta_p = 0.93$

$$V_p = 0.93 * 551 = 512.4 \text{ MN}$$

$$\mathrm{V}_r = (1-0.93) * 551 = 38.6 \text{ MN}$$

$$K_p = K_{pi}\left(1 - R_{fp}\frac{V_p}{V_{pu}}\right) = 14830 * \left(1 - 0.50 * \frac{512.4}{2768.3}\right) = 13457.5 \text{ MN/m}$$

$$K_r = K_{ri}\left(1 - R_{fr}\frac{V_r}{V_{ru}}\right) = 4110 * \left(1 - 0.75 * \frac{38.6}{438.8}\right) = 3838.8 \text{ MN/m}$$

$$a = \frac{0.2}{1-0.8(K_r / K_p)}\left(\frac{K_r}{K_p}\right) = \frac{0.20}{1-0.80(3838.8/13457.5)} * \left(\frac{3838.8}{13457.5}\right) = 0.074$$

$$\beta_{p,calculated} = \frac{1}{1+\alpha} = \frac{1}{1+0.074} = 0.93$$

$\beta_{p,calculated} \cong \beta_{p,assumed} = 0.93$ (93% of total load carried by piles)

Settlement of the Foundation (Elastic)

$$X = \frac{1-0.60\left(\dfrac{K_r}{K_p}\right)}{1-0.64\left(\dfrac{K_r}{K_p}\right)} = \frac{1-0.60*\left(\dfrac{3838.8}{13457.5}\right)}{1-0.64*\left(\dfrac{3838.8}{13457.5}\right)} = 1.014$$

$V = 551$ MN < $V_A = 3256.8$ MN

$$S = \frac{V}{XK_{pi}\left(1-\dfrac{R_{fp}\beta_p V}{V_{pu}}\right)} = \frac{551}{1.01*14830*\left(1-\dfrac{0.5*0.93*551}{2768.3}\right)} = 40.5 \text{ mm}$$

Elastic settlement of the system : S = 40.5 mm

CHAPTER C

Materials Properties Used in PLAXIS 3D Analysis

Table C1 Soil Properties

Identification		**PY1MC-Fiil**	**PY2MC-Silty Sand (Imp)**	**PY3MC-Soft Clay (Imp)**	**PY4MC-Medium Stiff Clay**	**PY5MC-Dense G.Sand**
Identification number		1	2	3	4	5
Drainage type		Drained	Undrained (A)	Undrained (A)	Undrained (A)	Drained
γ_{unsat}	kN/m^3	18.00	18.00	18.00	20.00	20.00
γ_{sat}	kN/m^3	20.00	20.00	20.00	21.00	21.00
Dilatancy cut-off		No	No	No	No	No
e_{init}		0.5000	0.5000	0.5000	0.5000	0.5000
e_{min}		0.000	0.000	0.000	0.000	0.000
e_{max}		999.0	999.0	999.0	999.0	999.0
Rayleigh α		0.000	0.000	0.000	0.000	0.000
Rayleigh β		0.000	0.000	0.000	0.000	0.000
E	kN/m^2	50.00E3	45.85E3	38.40E3	60.00E3	150.0E3
ν (nu)		0.3000	0.3000	0.3000	0.3000	0.3000
G	kN/m^2	19.23E3	17.63E3	14.77E3	23076	57692

Table C1 Soil properties (Continued)

Identification		**PY1MC-Fiil**	**PY2MC-Silty Sand (Imp)**	**PY3MC-Soft Clay (Imp)**	**PY4MC-Medium Stiff Clay**	**PY5MC-Dense G.Sand**
E_{oed}	kN/m^2	67.31E3	61.72E3	51.69E3	33.65E3	134.6E3
E_{inc}	$kN/m^2/m$	0.000	0.000	0.000	1000	3000
c_{ref}	kN/m^2	35.00	23.60	52.00	45.00	15.00
c_{inc}	$kN/m^2/m$	0.000	0.000	0.000	5.0	0.000
φ (phi)	°	30.00	30.50	2.500	5.000	34.00
ψ (psi)	°	0.000	0.5000	0.000	0.000	4.000
z_{ref}	m	0.000	0.000	0.000	0.000	0.000
Tension cut-off		Yes	Yes	Yes	Yes	Yes
Tensile strength	kN/m^2	0.000	0.000	0.000	0.000	0.000
Undrained behaviour		Standard	Standard	Standard	Standard	Standard
Skempton-B		0.9783	0.9783	0.9783	0.9783	0.9783
ν_u		0.4950	0.4950	0.4950	0.4950	0.4950

Table C1 Soil properties (Continued)

Identification		PY1MC-Fiil	PY2MC-Silty Sand (Imp)	PY3MC-Soft Clay (Imp)	PY4MC-Medium Stiff Clay	PY5MC-Dense G.Sand
$K_{w,ref}$ / n	kN/m^2	1.875E6	1.719E6	1.440E6	937.5E3	3.750E6
$C_{v,ref}$	m^2/day	0.000	744.4	775.3	834.5	0.000
Strength		Manual	Manual	Manual	Manual	Manual
R_{inter}		0.6000	0.6700	0.8000	0.8000	0.8000
δ_{inter}		0.000	0.000	0.000	0.000	0.000
K_0 determination		Automatic	Automatic	Manual	Manual	Automatic
$K_{0,x} = K_{0,y}$		Yes	Yes	No	Yes	Yes
$K_{0,x}$		0.5000	0.4925	0.5500	0.5500	0.4408
$K_{0,y}$		0.5000	0.4925	0.9564	0.5500	0.4408
k_x	m/day	0.6000	0.1206	0.1500	0.2480	0.1206
k_y	m/day	0.6000	0.1206	0.1500	0.2480	0.1206
k_z	m/day	0.6000	0.1206	0.1500	0.2480	0.1206

Table C2 Plate properties

Identification		**PY_Raft**	**PY_Wall**
Identification number		1	2
Comments			
Colour			
d	m	2.200	0.2000
γ	kN/m^3	0.01000	0.01000
Linear		Yes	Yes
Isotropic		Yes	Yes
E_1	kN/m^2	30.00E6	30.00E6
E_2	kN/m^2	30.00E6	30.00E6
ν_{12}		0.2000	0.2000
G_{12}	kN/m^2	12.50E6	12.50E6
G_{13}	kN/m^2	12.50E6	12.50E6
G_{23}	kN/m^2	12.50E6	12.50E6

Table C3 Embedded pile properties

Identification		**PY_D1.2**
Identification number		1
E	kN/m^2	30.00E6
γ	kN/m^3	4.000
Pile type		Predefined
Predefined pile type		Massive circular pile
Diameter	m	1.200
A	m^2	1.131
I_3	m^4	0.1018
I_2	m^4	0.1018
Skin resistance		Layer dependent
$T_{top, max}$	kN/m	0.000

Table C3 Embedded pile properties (Continued)

Identification		**PY_D1.2**
$T_{bot, max}$	kN/m	0.000
T_{max}	kN/m	100.0E3
F_{max}	kN	17.41E3